Dissertation zur Erlangung des Grades Doktor der Naturwissenschaften

- Dr. rer. nat. -

am Fachbereich Human- und Gesundheitswissenschaften

der Universität Bremen

Using Multimodal MRI Techniques to Derive a Biomarker for Tracking the Pathological Changes Occurring at Different Stages of Cognitive Decline in Parkinson's Disease in a Cross-Sectional Study Design

Vorgelegt von:

Emel Erdogdu, M.Sc.

Bremen, den 20 Juni 2017

Institut für Psychologie & Kognitionsforschung

Gutachter

Prof. Dr. Canan Başar-Eroğlu

Institute for Psychology & Cognition Research. Human and Health Sciences, University of Bremen, Bremen, Germany.

Prof. Dr. Tamer Demiralp (MD)

Department of Physiology. Istanbul Faculty of Medicine, Istanbul University, Istanbul, Turkey.

This study was realized in collaboration of the institutions listed below.

In cooperation with:

This study was supported by the Yearly Doctorate Stipend of the DAAD (German Academic Exchange Service) over the whole time-period of two years that this study lasted.

DAAD
Deutscher Akademischer Austausch Dienst
German Academic Exchange Service

DEDICATION

This work is dedicated to all those sixty lovely patients participating in this study and the future patients that will hopefully benefit from our findings.

I would like to express my gratitude to the DAAD (German Academic Exchange Service) for the awarded Yearly Doctorate Stipend helping me to realize my research project.

SUMMARY

Cognitive symptoms are common in Parkinson disease (PD) and range from mild cognitive impairment (PD-MCI) to dementia (PDD). It is not fully understood, whether PD-MCI and PDD are consecutive events and evolve into each other or whether they display two different entities. The high conversion rate from PD-MCI to PDD points to a progressive pattern, while different cognitive profiles seems to be related with higher conversion risk to PDD. Clinical diagnostic criteria have been developed in order to diagnose PD-MCI and PDD, but there is an important need for the development of a reliable biomarker that can give valuable information about the underlying pathological changes and that can discriminate between patients without cognitive symptoms (PD-N), PD-MCI and PDD. This biomarker should further be able to track the disease progression and thereby help to identify those patients with high dementia risk.

The aim of this study was to derive a multi-modal magnetic resonance imaging (MRI)-based biomarker for the reliable discrimination of PD patients at different stages of cognitive decline and to identify pathologic patterns related with increased dementia risk, as no reliable biomarkers are available at this time. We collected the resting-state functional MRI (rs-fMRI), diffusion tensor imaging (DTI), perfusion (Arterial Spin Labeling, ASL) and MR spectroscopic imaging (MRSI) data together with neuropsychological data from 20 PD-N, 20 PD-MCI and 20 PDD patients followed at the Neurology Department of Istanbul Faculty of Medicine.

We evaluated the rs-fMRI data using binary logistic regression analysis and identified the combination of resting-state networks (RSNs) that yield discriminative power based on the expression scores of the RSNs among the groups. We identified five RSNs, that were successful in discriminating between PDD and the other PD groups. The two modulatory default mode network (DMN) and salience network (SN) were significantly stronger expressed in the PDD group compared to PD-N, although the increase evolved from PD-N through PD-MCI to PDD. On the other hand, the frontostriatal network (FSN), posterior-temporal network (PTN) and limbic network that are related with executive, visuo-spatial and memory dysfunction, were significantly lower expressed in the PDD group.

The DMN and SN are known to be functionally related in a way that the SN regulates the activation and deactivation of the DMN and the central executive network (CEN) in the presence or absence of salient stimuli, and that may be an indicator for an altered switching mechanism of these RSNs in PDD patients, which is different from altered activation pattern

that have been described for other types of dementia cases. The voxel-wise analysis of the RSNs revealed complementary results pointing to pathological changes in major hubs of the SN (insula), limbic network (thalamus and hippocampus) and FSN (caudate/putamen).

We further were able to show significant global white matter (WM) degeneration in the PDD group using DTI measurements, stemming from pathological changes in various WM tracts that relate to RSN alterations observed in PDD. Additionally, we found pattern of hypoperfusion (ASL) and metabolic changes (MRSI) mainly in structures that supported the findings of the rs-fMRI and DTI measurements. The significant findings from the single MRI modalities showed significant correlation with various clinical and neuropsychological variables among the patient groups.

In the end, we tested a discriminative model using the significant parameters of the rs-fMRI, DTI and ASL data by feeding them stepwise into a discriminant analysis that revealed a combination of rs-fMRI and DTI findings to be most successful in discriminating the PDD from the PD-N with 100% sensitivity and PDD from PD-MCI cases with 83.3% sensitivity.

We were able to show progressive neuro-pathological changes at different stages of cognitive decline that, after validation, could be used as biomarker for PDD and, due to the easy application of MRI measurements, could be established as diagnostic tool and follow-up of the PD patients with the aim to generate individual treatment and identification of patients with dementia risk.

ZUSAMMENFASSUNG

Kognitive Störungen sind häufig auftretende Symptome in Morbus Parkinson (PD) und können von milden kognitiven Störungen (PD-MCI) bis hin zur Demenz (PDD) reichen. Es ist derzeit noch nicht völlig erforscht, ob es sich bei PD-MCI und PDD um aufeinander folgende Ereignisse handelt, bei denen PD-MCI sich zu PDD entwickelt, oder aber es sich um zwei unabhängige Formen kognitiver Störungen handelt. Die hohe Rate von PD-MCI Patienten, die im Verlauf der Krankheit eine Demenz entwickelt, deutet auf einen progressiven Verlauf hin, wobei die Ausprägung von verschiedenen kognitiven Defiziten mit erhöhtem Demenzrisiko in Verbindung gebracht wird.

Obwohl Kriterien zur klinischen Diagnostik von PD-MCI und PDD entwickelt wurden, besteht der Bedarf an der Definition eines verlässlichen Biomarkers, welcher wertvolle Informationen nicht nur über die pathophysiologischen Vorgänge liefern kann, sondern gleichzeitig auch zwischen kognitiv normalen PD Patienten (PD-N), PD-MCI und PDD unterscheiden kann. Solch ein Biomarker sollte zudem über die Eigenschaften verfügen das Fortschreiten der Krankheit verfolgen zu können und damit auch die frühe Identifikation von Patienten mit erhöhtem Demenzrisiko zu ermöglichen.

Ziel dieser Studie was es, mit Hilfe multi-modaler MRT Methoden einen Biomarker zur verlässlichen Unterscheidung von PD Patienten mit unterschiedlichen Graden an kognitiver Beeinträchtigung zu entwickeln und die pathologischen Muster, die mit erhöhtem Demenzrisiko in Verbindung stehen, zu identifizieren, da bisher noch kein verlässlicher Biomarker für PDD beschrieben wurde. Wir haben die Daten der funktionalen MRT Aufnahmen während des Ruhezustandes (resting-state) (rs-fMRI), die Diffusions-Tensor-Bildgebungs Aufnahmen (DTI), die MR-Perfusionsbildgebungs Aufnahmen (ASL) und die MR-Spektroskopischen Bildgebungs (MRSI) Aufnahmen von 20 PD-N, 20 PD-MCI und 20 PDD Patienten, die an der Neurologischen Abteilung der medizinischen Fakultät der Universität Istanbul betreut werden, untersucht.

Die rs-fMRI Daten werteten wir mittels der “binary logistic regression / Binären logistischen Regressions” Methode aus und identifizierten die Kombination an Ruhezustands Netzwerken (resting-state networks, RSNs) im Gehirn der Patienten, die aufgrund des Grades ihrer Ausprägung im Vergleich mit den anderen Patintengruppen die höchste Unterscheidungsstärke zeigten. Dabei identifizierten wir fünf Netzwerke, die über signifikante Unterscheidungsstärke zwischen den Patientengruppen verfügten. Die zwei modulatorischen

Netzwerke, das „default mode network / Standartmodus Netzwerk“ (DMN) und das „salience network“ (SN), waren in der PDD Gruppe signifikant stärker ausgeprägt als in den nicht-dementen Patienten, obwohl anzumerken ist, dass der Anstieg fließend von PD-N über PD-MCI nach PDD verlief. Dem gegenüber, waren das frontostriatale Netzwerk (FSN), das posterior-temporale Netzwerk (PTN) und das limbische Netzwerk, welche wiederum mit exekutiven, Gedächtnis und visuell-räumlichen Störungen in Verbindung stehen, in der PDD Gruppe signifikant schwächer ausgeprägt als in den anderen Patientengruppen.

Das DMN und das SN sind auf eine Weise funktional miteinander verbunden, in der das SN die Aktivität des DMN und des „zentralen exekutiven Netzwerkes / central executive network“ (CEN) in An- und Abwesenheit von hervorstechenden Stimuli reguliert. Das könnte ein Hinweis auf die Störung dieses Umschalte-Mechanismus in PDD Patienten sein, wobei andere Muster der Dysregulation dieser gleichen Netzwerke zuvor für andere Formen der Demenz beschrieben wurden. Die Voxel-basierte Analyse der RSNs erbrachte komplementäre Ergebnisse und diese deuten darauf hin, dass es zu pathologisch Veränderungen in Hauptzentren des SNs (Insula), dem limbischen Netzwerkes (Thalamus und Hippocampus) und dem FSNs (Caudat Nucleus/Putamen) in PDD Patienten kommt.

Darüber hinaus war es uns möglich die Degeneration in weiten Teilen der weißen Substanz bei PDD Patienten nachzuweisen, die auf pathologischen Veränderungen in verschiednen Trakten der weißen Substanz beruhen und die wiederum mit den zuvor identifizierten RSNs in Verbindung stehen. Ergänzend lieferten die ASL und MRSI Methoden Ergebnisse über reduzierte Durchblutungsmuster und veränderte Metabolitkonzentrationen in Strukturen des Gehirns, die in grossen Teilen mit den Ergebnissen der identifizierten RSNs und den strukturellen Veränderungen in den Trakten der weißen Substanz übereinstimmten. Die signifikanten Ergebnisse der einzelnen MRT Modalitäten waren korreliert mit vielen der klinischen und neuropsychologischen Variablen über die gesamte Patientengruppe.

In einem letzten Schritt prüften wir die Diskriminationsstärke der kombinierten signifikanten rs-fMRI, DTI und ASL Variablen, indem diese schrittweise in eine Diskriminanzanalyse gegeben wurden und das erhaltene Model, aus einer Kombination von RSNs und DTI Variablen, verfügte über 100% Sensitivität in der Unterscheidung von PDD und PD-N und 83.3% Sensitivität zwischen PDD und PD-MCI Patienten.

Es war uns möglich progressive neuropathologische Veränderungen während unterschiedlicher kognitiver Stadien in PD mittels multi-modaler MRT Aufnahmen zu

identifizieren und sind der Auffassung, dass diese Veränderungen, nach Validation in einer größeren Studiengruppe, als möglicher Biomarker für PDD genutzt und aufgrund der einfachen Handhabung der MRT Messungen auch als diagnostisches Mittel im Klinik-Alltag eingesezt werden kann. Die Nutzung multi-modaler MRT Aufnahmen zur Diagnose und Kontrolle des Krankheitsverlaufs ermöglicht die frühzeitge Identifikation von PD Patienten mit erhöhtem Demenzrisiko und schafft somit die Grundlage für die optimale Behandlung mit dem Ziel der Verlangsamung der kognitiven Symptome und trägt somit zum wesentlichen Erhalt der Lebensqualität der Patienten bei.

ACKNOWLEDGEMENTS

I would like to express my sincere gratitude to my advisor Prof. Dr. Canan Başar-Eroğlu at the University of Bremen, for her continuous support and guidance through my research, giving me the opportunity to plan this dissertation abroad and for her enormous help with the stipend arrangements.

I would like to thank my second advisor Prof. Dr. Tamer Demiralp MD at the University of Istanbul for the great opportunity to be part of the cooperative Parkinson's disease project with the Boğaziçi University and offering me to conduct my dissertation at the Hulusi Behçet Life Sciences Research Laboratory at the Istanbul University and Istanbul Faculty of Medicine in connection with this project. I am especially thankful for his continuous motivation and support of my research, his immense knowledge and his incomparable guidance and helping me through the writing of this thesis. I consider myself very lucky, having such great advisors and teachers to learn from.

I want to thank Prof. Dr. Hakan Gürvit MD, for his precious comments and advices on the neuropsychologic assessment and MRI data interpretation.

My special thank goes to Assoc. Prof. Dr. Başar Bilgiç MD, who not only dedicatedly helped during patient recruitment and always found the time to clinically evaluate our patient's MRI data but also was so patient with all our worries and questions about the patient profiles and always gave wonderful advice.

I further want to thank Prof. Dr. Haşmet Hanağası MD, for his enormous help with the patient selection and fruitful comments on this study.

I specially want to thank Dr. Zeynep Tüfekçioğlu MD, for her unlimited and selflessly help in the clinical evaluation of the patients and who always found the time for us, even if that meant she had to postpone or skip her break.

In short, I am very thankful to all the members of the Neurology Department at the Istanbul Faculty of Medicine for their full trust in me for working with their patients despite some language issues from my side.

I want to thank Asstist. Prof. Dr. Esin Öztürk-Işık from the Boğaziçi University for her passionate engagement in the planning of the main project, her knowledge for the set-up of a huge part of the scanning protocols and the help in analyses of the ASL and MRSI data.

I am especially thankful to doctoral student Ani Kıçik, who went with me through the whole project, the sometimes-chaotic days in the clinic, the patient recruitment and who was

an indispensable help during the neuropsychological testing's of the patients and the whole project.

I also want to thank psychologist Seda Büker from Istanbul University for her help and teaching of the neuropsychological testing's and the Ph.D. students Dilek Betül Arslan and Sevim Cengiz from the Boğaziçi University for their incomparable engagement in the analysis of the ASL and MRSI data, which I couldn't have succeed without them.

One of my special thank goes to Dr. Çiğdem Yıldız-Ulaşoğlu who was so important to me because of her selfless help in giving me fruitful advice and guidance for the evaluation of the neuropsychological tests and the statistics despite her own huge workload.

I also would like to thank Asstist. Prof. Dr. Ali Bayram for his huge support in the data analyses and of course I want to thank doctoral student Elif Kurt who taught me how to perform the MRI recording, much of the data analyses and for the unforgettable funny lab moments.

Last but not least, I want to thank my parents Sylvia and Adnan for their infinite believe in me, their spiritual support and always motivating me to continue with what I do, although that meant we had to live in spatially distance from each other.

Of course, I also want to thank all my friends for always pushing me, believing in me and helping me through this journey, especially Ali Ozan Dörtgül who faced a snowstorm to surprise me with a comfortable chair just to make sure I will successfully write this thesis!
Thank you.

CONTENTS

LIST OF TABLES

LIST OF FIGURES

ABBREVIATIONS

1H-MRSI: Proton MR Spectroscopic Imaging

3D: Three Dimensional

AAT: Arterial Arrival Times

AC: Anatomical Connectivity

ACE-R: Addenbrooke's Cognitive Examination - Revised

AC-PC: Anterior-Posterior Commissure

AD: Alzheimer's disease

AD: Axial Diffusivity

AES: Apathy Evaluation Scale

ALIC: Anterior Limb of the Internal Capsule

ANOVA: Analysis of Variance

Ant.: Anterior

ASL: Arterial Spin Labeling

ATR: Anterior Thalamic Radiation,

BAI: Beck Anxiety Inventory

BET: Brain Extraction Tool

BG: basal ganglia

BOLD: Blood Oxygenation Level Dependent signal

bvFTD: Behavioral Variant of the Fronto-Temporal Dementia

C.: Cortex

CBD: Cortico-basal degeneration

CBF: Cerebral Blood Flow

Cho: Choline

cing.: Cingulate

CN: Cerebellar network

COMT: Catechol-O-Methyltransferase gene

con.: congruent

Corr.Coef.: Correlation Coefficient

Cr: Creatine

CSF: Cerebrospinal Fluid

CST: Corticospinal Tract

DA: Dopamine

DAN: Dorsal Attention Network

DBS: Deep Brain Stimulation

df: Degrees of Freedom

DLB: Dementia with Lewy Bodies

DL-PFC: Dorso-Lateral Pre-Frontal Cortex

DMN: Default Mode Network

dMRI: Diffusion MRI

DTI: Diffusion Tensor Imaging

EC: Eddy Currents

EPI: Echo Planar Imaging

Eq.: Equation

F: F-Value

FA: Fractional Anisotropy

FC: Functional Connectivity

FDG-PET: 18F-fluorodeoxyglucose PET

FDT: FMRIB's Diffusion Toolbox

FWE: Family-Wise Error

FFE: Fast Field Echo

FFEPI: Fast Field Echo Planar Imaging

FLAIR: Fluid Attenuated Inversion Recovery

FLIRT: FMRIB's Linear Image Registration Tool

fMRI: Functional MRI

FMRIB58: High-resolution average Image of 58 good quality FA images

FNIRT: FMRIB's Non-Linear Image Registration Tool

Forc.: Forceps

FOV: Field of view

FPN: Frontoparietal Network

FSL: FMRIB Software Library

FSLstats: FMRIB Software Library Statistics

FSN: Frontostriatal Network

FWHM: Full-Width at Half-Maximum

GABA: gamma-aminobutyric acid

GDS: Geriatric Depression Scale

GIFT: Group ICA fMRI Toolbox

Glx: Glutamine/Glutamate complex

GM: Gray Matter

GPe: Globus Pallidus Externa

GPi: Globus Pallidus Interna

Gyr.: Gyrus

HC: Hippocampus

HS: Healthy Subject

IC: Independent Components

ICA: Independent Component Analysis

ICN: Intrinsic Connectivity Networks

IFOF: Inferior Fronto-Occipital Fasciculus

ILF: Inferior Longitudinal Fasciculus

inc.: incongruent

Inf. Temp. Gyr: Inferior Temporal Gyrus (ITG)

JHU-ICBM: Johns Hopkins University-International Consortium of Brain Mapping

JOLO: Benton Judgment of Line Orientation test

L: Left

Lat.vis: lateral Visual Network

LB: Lewy Bodies

L-Dopa: Levodopa, L-3.4-dihydroxyphenylalanine

LN/Lim.Nw.: Limbic Network

LN: Lewy neurites

M: Mean

M0: Mean Magnetization

MAPT: Microtubule-Associated Protein Tau gene

maxprob.: Maximum Probabilistic

MCI: Mild Cognitive Impairment

MD: Mean Diffusivity

MDS: Movement Disorder Society

Med.vis: Medial Visual Network

mI: Myo-Inositol

Mid. Front. Gyr.: Middle Frontal Gyrus (MFG)

Mid. Temp. Gyr.: Middle Temporal Gyrus (MTG)

Min: Minute

mm: Millimeter

MMSE: Mini Mental State Examination

MNI-152: Montreal Neurological Institute - 152 subjects average Image

MOCA: Montreal-Cognitive Assessment

MRI: Magnetic Resonance Imaging

MRSI: Magnetic Resonance Spectroscopic Imaging

ms: millisecond

MSA: multiple system atrophy

n: Number

NAA: N-acetylaspartate

NAAG: N-acetylaspartylglutamate

NPT: Neuropsychological test

NS: Non-Significant

NW: Network

p: p-Value, Statistical Significance

Para.HC: Parahippocampal Network

PCA: Principal Component Analysis

PCC: Posterior Cingulate Cortex

PD: Parkinson's disease

PDD: Dementia in Parkinson's disease

PD-MCI: Mild Cognitive Impairment in Parkinson's disease

PD-N: Parkinson's Disease without cognitive symptoms

PD-nd.: PD-non-demented

PET: Positron Emission Tomography

Post.: Posterior

PRESS: Point-RESolved Spectroscopy

PS: Parkinsonian Syndrome

PSP: Progressive Supranuclear Palsy

PTN: Posterior-Temporal Network

R: Right

R^2: Coefficient of Determination

RD: Radial Diffusivity

ROI: Region of Interest

rs-fMRI: Resting-State Functional MRI

RSN: Resting State Networks

s: second

sd: Standard Deviation

SDMT: Symbol Digit Modalities Test

SENSE: Sensitivity encoding

SLF: Superior Longitudinal Fasciculus

SLF-T: Superior Longitudinal Fasciculus Temporal

SM: Somato-Motor Network

SN: Salience Network

SNpc: Substantia Nigra pars compacta

SNpr. Substantia Nigra pars reticulata

SPECT: Single Photon Emission Computed Tomography

SPM: Statistical Parametric Mapping

SPSS: Statistical Package for the Social Sciences

STN: Subthalamic Nucleus

Sup. Front. Gyr.: Superior Frontal Gyrus (SFG)

Sup. Temp. Gyr.: Superior Temporal Gyrus (STG)

Task-fMRI: Task-Based Functional MRI

TE: Echo-time

Temp. Fus. C.: Temporal Fusiform Cortex (TFC)

Temp. Occ. Fus. C.: Temporal Occipital Fusiform Cortex (TOFC)

TH: tyrosin hydroxylase

Thal.: Thalamus

thr.: Threshold

TI: Inversion Time

TO: Temporo-occipital

TR: Time of Repetition

UPDRS: Unified Parkinson's disease Rating Scale

WCST: Wisconsin Card Sorting Test

WM: White Matter

WMH: White Matter Hyperintensities

Y-BOCS: Yale-Brown Obsessive Compulsive Scale

$\lambda 1$: primary eigenvalue

$\lambda 2$: secondary eigenvalue

$\lambda 3$: tertiary eigenvalues

χ^2: Chi-Squared Statistics

1 INTRODUCTION

"Some have regarded its characteristic symptoms as distinct and different diseases, and others have given its name to diseases differing essentially from it; whilst the unhappy sufferer has considered it as an evil, from the domination of which he had no prospect of escape."- James Parkinson (1817)

This statement is taken from James Parkinson's "An assay of the shaking palsy" (1817), in which he is the first to describe the symptoms of the second most prevalent neurodegenerative disease of our time after Alzheimer's disease (AD) and that was later named after him: Parkinson's disease (PD).

Besides the dominant motor symptoms of Parkinson's disease, non-motor symptoms are increasingly recognized as part of PD and do not only cover features such as mood disorders, psychosis, sleep disturbances and autonomic dysfunction, but also mild to severe cognitive dysfunction. Studies showed, that mild cognitive impairment in Parkinson's disease (PD-MCI) is frequent (20-50%) and may represent the earliest stage of cognitive decline in PD (Goldman and Litvan 2011). It was further shown, that during the course of the disease up to 80% of the PD cases developed dementia symptoms (Aarsland et al. 2003; Hely et al. 2008), hence PD-MCI might be a major risk factor for the development of dementia in PD (PDD) (Goldman and Litvan 2011). Yet, the neuropathological counterparts of the cognitive dysfunctions and the conditions for the possible expression of PD-MCI and transition to PDD are unknown.

Recently, the diagnosis of PD-MCI and PDD solely relies on the judgement of the clinicians, but reliable biological markers are needed for a clear diagnosis of PD-MCI and PDD, as it allows to identify PD patients with high dementia risk and offer individual treatment for those patients. As Magnetic Resonance Imaging (MRI) techniques are yet to be established as means for diagnosis and follow-up of cognitive decline in PD, the investigation of the cognitive dysfunctions in PD and the definition of a discriminative biomarker for PDD using multi-modal MRI measurements build the subject of this thesis.

The definition of PD, the neurological basis of the motor symptoms in PD, the neuropathology and the cognitive deficits in PD will be briefly discussed in the following.

1.1 Parkinson`s Disease

Above all, PD is a hypokinetic movement disorder defined by its characteristic motor symptoms of bradykinesia/akinesia, tremor at rest, rigidity, postural instability and gait impairment (UK Parkinson's Disease Society Brain Bank clinical diagnostic criteria; Gibb and Lees, 1988; Hughes et al., 1992; Watts and Koller, 2004, p.233) most likely based on the degeneration of dopaminergic neurons in the substantia nigra, a part of the basal ganglia (BG). PD is known to affect men twice as much as women (Watts and Koller, 2004) and age is one of the most prominent risk factors for PD. In 50% of the cases the disease onset lays between 50-60 years, and in 30% of the cases the disease starts after 60 years, while almost 10 % of the PD patients are under 40 years (Thümler, 2002). It is estimated that around 6-7 million people around the world are affected by PD, with a prevalence rate of 0.5-1% in population of industrial countries over 60 years of age, going up to 1-4% of the population at higher ages and with an incidence rate between 8-18 per 100,000 persons a year (de Lau and Breteler, 2006; Pringsheim et al. 2014). Higher prevalence rates in Northern Europe and Northern America have been noticed compared to lowest prevalence rates in Southern Europe, Asia and Africa (Watts and Koller, 2004; Pringsheim et al. 2014).

1.1.1 Types of PD

With its unknown etiology (Watts and Koller, 2004, p.223), the idiopathic PD represents approximately 75-90% of the cases (de Lau and Breteler, 2006), is the most frequent type of all Parkinsonian Syndromes (PS) and covers among the akinetic-rigid type, the equivalent type, the tremor-predominant type of PD and also cases of mono-symptomatic resting tremor. Other than for general PS diagnosis, the diagnosis of PD requires at least two out of three characteristic symptoms, namely bradykinesia, tremor or rigidity. Additionally, the unilateral onset of symptoms and positive L-Dopa response are helpful criteria in the diagnosis of PD (Hughes et al. 1992). As postural instability is common in all forms of PS, it is not included in the main criteria for PD (Watts and Koller, 2004, p.233). However, final PD diagnosis can only be made after the patient’s death and brain dissection.

The secondary form represents another group of PS and is mainly caused by drug intake, head trauma (Taylor et al., 1999), toxins like methanol, carbon monoxide and pesticides (Rajput et al., 1986; Tanner et al 1990) or by metabolic or vascular reasons such as encephalitis (Ogata et al., 1997).

The third group of PS is known as Parkinsonism-plus syndrome and covers besides multiple system atrophy (MSA), progressive supranuclear palsy (PSP), corticobasal degeneration (CBD) and dementia with Lewy bodies (DLB). DLB represents a form of dementia with similar features to Alzheimer‘s disease and should not be mistaken for PD dementia (PDD), which will be described later. Finally, PS may also occur as the result of hereditary neurodegenerative diseases.

For the sake of simplicity, the abbreviation PD will be used for idiopathic PD in this study.

1.1.2 Clinical manifestations of PD

One of the cardinal features present in most of the patients is the resting tremor. The tremor at rest is defined by involuntary rhythmic muscle contraction and relaxation, especially occurring in parts of the limbs such as fingers, hands, arms, and legs. However, eyes, face, head and trunk can also be affected. Intentional movement of the affected body parts can interrupt the tremor, and it disappears during sleep, while stress, excitement or situations with higher cognitive load can lead to an increase of the tremor (Watts and Koller, 2004, p.235).

Bradykinesia and akinesia are early appearing symptoms in PD as well and describe the slowing or loss of spontaneous movements, the impairment of automatic movements and delayed motor initiation (start hesitation) as well as monotonic (dysphonia) and cluttered speech (dysarthria), writing disorders (micrographia) and mask-like face.

As another cardinal feature of PD, rigidity describes the increased muscle tone leading to increased resistance of flexors and extensors resulting in inflected posture of the extremities and head. Postural instability and gait disturbances are common manifestations in the later phase of the disease.

Typical for PD is the rule of asymmetric onset of the motor symptoms, which often become bilateral during the course of the disease and can be described using the Hoehn & Yahr Scale (Hoehn and Yahr, 1967).

1.1.3 Possible causes of PD

Although the etiology of the idiopathic PD is still unknown, it is speculated that the interplay of genetic predisposition, environmental factors and/or disorders of the mitochondrial

oxidative metabolism may lead to the main pathological findings in PD (Watts and Koller, 2004).

What we already know is, that the degeneration of dopamine (DA) producing cells in the pigmented region of the substantia nigra pars compacta (SNpc) leads to a neurobiochemical imbalance and the degeneration of the nigrostriatal pathways, thereby causing the motor symptoms in idiopathic PD.

PD is a slowly progressing disease and the motor signs usually become obvious only after the degeneration of about 80 % of the DA producing cells in the SNpc (Watts and Koller, 2004).

As the tyrosin hydroxylase (TH) is highly specific for the cells in the SNpc and catalyzes the conversion of L-Tyrosin to L-Dopa, TH plays an essential and rate-limiting role for the DA synthesis and DA concentration in the related brain regions (Watts and Koller, 2004)

Main steps of DA synthesis are:

$$\text{L-Tyrosin} \xrightarrow{Tyrosin\ Hydroxylase} \text{L-Dopa (L-3,4-dihydroxyphenylalanine)} \xrightarrow{DOPA-decarboxylase} DA.$$

1.1.4 Neuropathology of PD

1.1.4.1 Pathophysiology of basal ganglia in PD

As the dysfunction of the basal ganglia is thought to be the main cause of the motor symptoms in idiopathic PD, the pathophysiology of the BG in PD will be discussed shortly in the following.

The basal ganglia are part of the motor system located in the telencephalon of the human brain. They are composed of structures such as the striatum (putamen and caudate nucleus), the pallidum (globus pallidus interna (GPi) and externa (GPe)), the substantia nigra (SN pars reticulata and SN pars compacta) and the subthalamic nucleus (STN). The various structures of the BG are subdivided into several functional territories such as oculomotor, skeletomotor, associative and limbic divisions depending on their physiological properties and cortical and thalamic connections (Watts and Koller, 2004; Alexander et al., 1990) that form parallel organized loops reentering the cortical areas (Watts and Koller, 2004). By large, they are involved in the processing and the control of the planned actions or movement sequences and modulate planned actions of cortical areas by modulating thalamic input to the cortex (Watts and Koller, 2004). The different nuclei of the BG are heavily interconnected, but less connections exist among the discrete functional loops.

The majority of the BG neurons possess GABA (gamma-aminobutyric acid) as the main transmitter and thus have inhibitory effects on target neurons. Striatal neurons inhibit the discharge of neurons of the SN pars reticulata (SNpr) which in turn leads via disinhibition to an activation or increase of firing rates of the postsynaptic cells of the SN such as those in the thalamus. Different striatal neurons carry DA receptors (D1, D2,) thus DA release of the SNpc acts excitatory on GABAergic striatal neurons bearing D1-receptors and inhibitory on those bearing D2-receptors (Kandel et al., 2000).

The BG are characterized by two different pathways. In the direct pathway, the striatum which receives transient excitatory inputs from the cortex and SNpc, sends direct GABAergic efferents to the GPi/SNpr, which send tonic inhibitory GABAergic output to the thalamus. Hence, with the increased activity in the direct pathway the disinhibited thalamus, which has glutamatergic excitatory projections to the cortex, increases the excitability of the cortex (Figure 1-1). The other large part of information leaves the BG by the indirect pathway. The indirect pathway takes its origin from the GABAergic neurons of the striatum that receive inhibitory input from SNpc through D2 receptors and project to GPe. In two arms of the indirect pathway the GABAergic GPe neurons either send efferents to the GABAergic GPi cells or to the neurons of the subthalamic nucleus, which receive a strong excitatory input from the cortex and send excitatory glutamatergic efferents to the GPi. Both arms of the indirect pathway oppose the disinhibitory effect of the direct pathway and lead to decreased thalamo-cortical activations (Figure 1-1) (Kandel et al., 2000, Watts and Koller, 2004).

The dopamine signal of the SNpc triggers the different processing pathways in the BG by differential activation of the D1 or D2 receptors on the striatal neurons and modulates the response of the thalamic nuclei, which in turn indirectly affect cortical motor activities. The BG are involved during learning and/or adaptation of tasks, and in the initiation and execution of movements via feedback loops to the cortex, but the exact role of the BG during this process still needs further clarification (Watts and Koller, 2004).

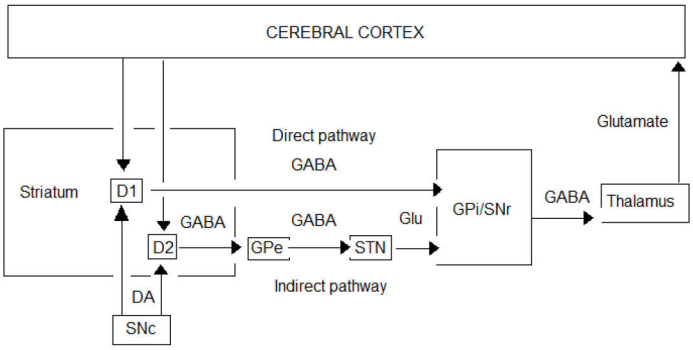

Figure 1-1: Simplified diagram of the two pathways of basal ganglia circuit.
SNc: SN pars compacta, SNr: SN pars reticulate, STN: Subthalamic nucleus.

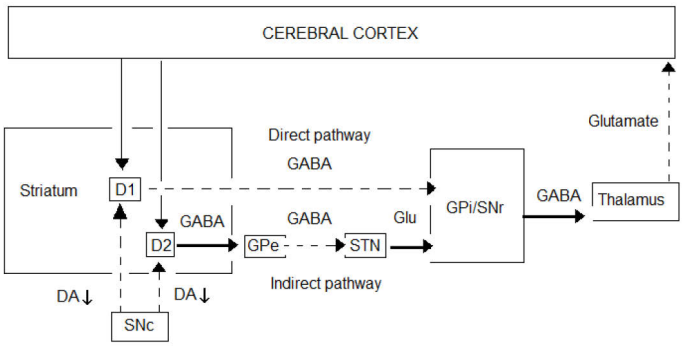

Figure 1-2: Simplified diagram of the two pathways of basal ganglia circuit as it is thought to be disturbed in Parkinson`s Disease. Dashed lines display the DA depletion based activation imbalance of the two pathways. *SNc: SN pars compacta, SNr: SN pars reticulate, STN: Subthalamic nucleus.*

Most of the common described movement disorders are due to a disruption of the activation balance of the direct and indirect pathways in the BG (Watts and Koller, 2004). Hyperkinetic disorders are thought to be based on the shift of the activation balance towards the direct pathway leading to reduced inhibitory BG output to the thalamus. In contrast to hyperkinetic diseases such as Chorea, Ballismus and Dystonia, Parkinson's disease is a typical hypokinetic movement disorder (Watts and Koller, 2004). Hypokinetic diseases may arise from a stronger activation of the indirect pathway leading to an increase of the inhibitory BG output to the thalamus and thereby leading to increased inhibition of the thalamo-cortical neurons. In PD, the degeneration of the nigrostriatal pathway due to the degeneration of DA producing cells in the SNpc is thought to lead to differential changes in the striatopallidal projections resulting in increased inhibitory BG output to the thalamus (Figure 1-2).

Although, several drug therapies are available against the motor symptoms of PD in order to enhance the patient's daily living conditions, for example by means of the substitution treatment with L-Dopa, not many therapy options exist against the second group of symptoms, namely the cognitive and behavioral impairments.

1.1.4.2 Synucleinopathies

Besides the pallor of the SNpc, histological studies revealed the presence of Lewy Bodies (LB) and Lewy neurites (LN) in different regions of the brain in PD (Braak et al. 2003; Chung et al. 2001; Dickson 2012; Forno 1996; Hughes et al. 1992; McCann et al. 2014). LBs are eosinophilic cytoplasmatic inclusions mostly composed of aggregated alpha-synuclein, ubiquitin and other proteins and were first described by Friedrich H. Lewy in the 1910s. The abnormal accumulation of alpha-synuclein in neurons, nerve fibers or glial cells is one main characteristic of the so-called alpha-synucleinopathies (McCann et al. 2014). Other members of the alpha-synucleinopathies are dementia with Lewy Bodies (DLB) and Multiple System Atrophy (MSA). Braak and colleagues (2003) were able to show that the distribution of the LB pathology related with PD seems to evolve from brainstem towards limbic areas, forebrain and the cortex and that these phases can be staged from 1-6 (Braak et al. 2002; Braak et al. 2003; Lin and Wu 2015).

1.2 Cognitive symptoms in PD

A spectrum of cognitive dysfunctions, ranging from mild cognitive impairment (MCI) to dementia have been described in PD (Litvan et al. 2012). Mild cognitive impairment in Parkinson's disease (PD-MCI) has been increasingly recognized as a distinct entity in PD, and studies suggest that PD-MCI may represent the earliest stage of cognitive decline and might be a main risk factor for developing dementia in PD (PDD) (Goldman and Litvan, 2011). Hence, PD-MCI may represent an intermediate state between normal cognition (PD-N) and PDD (Goldman and Litvan, 2011). PD-MCI appears to be common even at the time of PD diagnosis and prior to initiation of dopaminergic therapy (Muslimovic et al., 2005; Litvan et al. 2011). Litvan and colleagues (2011) report that about 26.7% of non-demented PD patients have PD-MCI and that PD-MCI predicts the development of dementia, which can occur in up to 80% of PD patients over the long term (Aarsland et al. 2003; Litvan et al. 2012).

1.2.1 Clinical definition and diagnosis of PD-MCI

Several criteria for the definition of MCI were proposed by Petersen et al. (2004, 2006 and 2009), the National Institute on Aging and the Alzheimer's Association MCI criteria committee (Albert et al., 2011) and the DSM-5 Neurocognitive Disorders Work Group (Jeste et al., 2010; Ganguli et al., 2011). MCI is mainly characterized by subjective cognitive complaint and evidence of cognitive abnormalities unusual for age but with no/only minimal effect on daily function (Petersen et al., 2004).

In order to characterize MCI associated with PD and identify possible predictors for the conversion to dementia, the Movement Disorder Society (MDS) Task Force proposed criteria for PD-MCI that include the characterization of the clinical syndrome and methods for PD-MCI diagnosis (Litvan et al., 2012). The criteria were developed comparable to the PDD criteria earlier proposed by Dubois et al. (2007) and Emre et al. (2007), and offer a two-level assessment scheme for the diagnosis of PD-MCI (Litvan et al., 2012).

Level I (abbreviated assessment) criteria allow for the diagnosis of PD-MCI based on the validation of global cognitive abilities and/or the use of only a limited battery of neuropsychological tests. That means, in order to be diagnosed as PD-MCI, the patient has to show impairment on minimum two tests when (a) less than two tests within each of the five cognitive domains are carried out or (b) when less than five cognitive domains are tested (Litvan et al., 2012). Complementary, the Level II (comprehensive assessment) criteria allow for the additional sub-typing of PD-MCI using comprehensive neuropsychological tests including at least two tests for each of the five cognitive domains (attention and working memory, executive functions, language, memory, and visuospatial functions). Impaired performance on at least two tests, representing either one single cognitive domain or in different cognitive domains are required for PD-MCI diagnosis according Level II criteria (Litvan et al., 2012).

Regarding the affected cognitive domain, subtypes of PD-MCI have been formulated. There is a huge heterogeneity among these sub-types and while according to Litvan et al. (2011) and Yarnall et al. (2013) the non-amnestic single-domain type seems to be the most common subtype, others report about frequent multiple domain impairment with predominant deficits in executive function, memory, and visuospatial function (Goldman et al. 2013; Lawrence, Gasson, and Loftus 2016). Another subtype is the amnestic domain subtype.

Memory, executive functions and visuo-spatial functions are often reported to be affected in PD-MCI patients (Janvin et al., 2006; Watson et al., 2010; Litvan et al., 2012) with manifested symptoms such as multi-tasking and planning difficulties, slowing of information processing speed, attention and concentration difficulties, memory impairments and word-finding difficulties (Goldman and Litvan, 2011).

1.2.1.1 Executive dysfunction

Performance deficits of non-demented PD patients in tasks related with executive functions have been reported. Among these tasks were tests examining divided attention (trail making test B), response inhibition (Stroop test), working memory (Digit Span Reverse) and mental flexibility (Wisconsin Card Sorting Test) (Bohnen et al., 2006, de Frias et al., 2007, Fama et al., 2000, Grace et al., 2005, Janvin et al., 2006, Lima et al., 2008, Muslimovic et al., 2008, Siegert et al., 2008, Watson et al., 2010). Dysfunction of the prefrontal cortex may cause the performance deficits in the executive domain, as the pre-frontal cortex allows the subject to pay attention to one event and exclude others and to switch among them (Watson et al., 2010).

1.2.1.2 Visuo-spatial dysfunction

On the other hand, visuo-spatial deficits have been reported to develop throughout the course of the disease. Visuo-spatial functions cover pattern recognition (facial recognition), constructional abilities (figure drawing), color recognition (color naming) and spatial analysis (ability to identify multiple objects in a visual field) which are necessary for the processing of visual information (Watson et al., 2010). Dysfunction of parietal areas including the parietal, occipital and temporal lobes have been associated with deficits in visual-spatial skill (Watson et al., 2010). A widely used neuropsychological tool for the investigation of visuo-spatial abilities of patients is the Benton Judgment of Line Orientation test (JOLO) (Benton et al., 1978). Beyond poor performance in the JOLO (Janvin et al., 2006, Martin et al., 2009, Muslimovic et al., 2007, Uc et al., 2006), facial recognition and form-discrimination (Pereira et al., 2009) and block construction (Goldman et al., 1998, Uc et al., 2006) abilities have been reported to be disturbed in PD patients even without dementia symptoms. Gullet and co-workers (2013) demonstrated right parietal, occipital as well as bilateral frontal activation in the JOLO test during functional MRI, and PD is known to adversely affect these pathways.

1.2.2 Clinical definition and diagnosis of PDD

Dementia is common in PD, and the systematic review of Aarsland et al. 2005 showed a 24-31% prevalence of PDD in PD. PDD represents 3-4 % of all dementia cases in the population. Dementia incidence is 6 times higher in PD compared to normal population (Emre et al., 2007) and in the 10-year follow-up study of Williams-Gray et al. (2013) the authors report about a dementia incidence rate of 54.7 per 1000 person over the years.

PDD is characterized by a gradually intensifying cognitive loss affecting domains of attention, executive and visuospatial functions as well as memory, with relatively preserved core language functions, while a dysexecutive profile seems do dominate the cognitive characteristics (Emre et al. 2007).

The MDS Task Force proposed criteria for the clinical diagnosis of dementia in PD, and one of the core features for PDD is the previous diagnosis of idiopathic PD and the onset of dementia symptoms after established PD (Emre et al., 2007). Furthermore, dysfunction in more than one of four cognitive domains (attention, executive function, memory and visuo-spatial function) must be present and severe enough to affect daily living activities independent from motor dysfunction. The presence of at least one behavioral feature such as personality change, apathy, hallucination or delusion support the PDD diagnosis (Emre et al., 2007).

PDD and Dementia with Lewy Bodies (DLB) are both Lewy Body Dementias, share clinical and pathological features and therefore should not be confused. PDD and DLB are mostly differentiated by their time-course, such that PDD is diagnosed when dementia symptoms follow well established PD motor symptoms, while DLB is characterized by dementia symptoms appearing prior to the onset of motor symptoms or developing within one year after the motor symptoms. This discrimination is also known as the 1-year rule.

1.2.3 Proposed risk factors of PDD

Known risk factors for the development of PDD beyond PD-MCI (Goldman and Litvan, 2011; Galtier, Nieto, Lorenzo, & Barroso, 2016) are old age at disease onset, long disease duration, the severity and symmetry of motor symptoms, the dominant axial symptoms, autonomic symptoms appearing at an early stage and the early development of confusions and hallucinations (Emre et al., 2007; Hanagasi, Tufekcioglu, & Emre, 2017). The poor response to

dopaminergic treatment, excessive day-time sleepiness and REM sleep behavior disorder are also associated with higher dementia risk in PD (Hanagasi, Tufekcioglu, & Emre, 2017). The non-tremor phenotype, low performance in the semantic verbal fluency test and difficulties in copying the intersecting pentagon figures are also related with higher dementia risk (Williams-Gray et al., 2007 and 2009).

However, there are controversial results regarding different cognitive profiles and their dementia risks, such that Dubois et al. (2007), Emre et al. (2007) and Hanagasi et al. (2017) report about PDD risk associated with frontal-striatal dysfunction, while Williams-Gray et al. (2007 and 2009) found association between dementia risk and more posterior cortically based and visuo-spatial dysfunction, suggesting there might be distinct cognitive syndromes with different PDD prognosis (Litvan et al. 2012). Anyway, PDD is characterized by a dysexecutive cognitive profile displaying impairment in planning, abstract thinking and mental flexibility as a result of deficits in attention and visuo-spatial functions and moderately impaired episodic memory, while the core language functions are relatively preserved (Emre et al., 2007; Hanagasi, Tufekcioglu, & Emre, 2017). Impaired attention may not only affect daily living but also influence the patient's abilities in the other cognitive domains, hence poor memory or executive test performance may rely on attentional deficits. The dysexecutive profile in PDD is commonly accompanied by behavioral symptoms such as apathy and psychosis.

1.3 Need for a reliable discriminative biomarker for cognitive decline in PD

Although diagnostic criteria for cognitive decline have been developed in the recent years (Litvan et al., 2012; Emre et al., 2007), the diagnosis of PD-MCI or PDD is still only based on the judgment of a clinician, and there are no reliable biomarkers for the identification of patients with high dementia risk. Besides the Unified Parkinson's Disease Rating Scale (UPDRS), which is one of the most common tools to scale the Parkinson's disease status in clinical environment by interview and clinical observation, neuropsychological tests (NPTs) such as the Mini Mental State Examination (MMSE), Montreal-Cognitive Assessment (MOCA) and Addenbrooke's Cognitive Examination - Revised (ACE-R) have been established as sensitive and specific cognitive screening instruments for early cognitive dysfunction by covering cognitive domains such as orientation/attention, memory, verbal fluency, language and visuo-spatial abilities (Mioshi et al., 2006). But, the diagnosis according to these criteria

happens to be a result of arbitrary stated standard deviations of neuropsychological test scores which don't allow for a reliable biomarker for the different stages of cognitive decline in PD. Additionally, a study on the normalization of ACE-R for Turkish population showed that the scores are more robust and discriminative for the higher-educated people, while their correlation with detailed neuropsychological test results decreases with decreasing educational years (Uysal Cantürk, 2013), which emphasizes the importance to develop a biology-based reliable and easily applicable marker for the evaluation of patient's cognitive state. On the other hand, as PD-MCI and PDD cover a heterogeneous spectrum of cognitive dysfunctions, it is not well understood, whether these cognitive conditions display different severity states during disease progression or they may represent different pathological patterns. As the high conversion rate from PD-MCI to PDD (Litvan et al., 2011 and 2012) may point to a continuous course of the same patho-physiological background, it is important to identify the clinical and pathological characteristics of the cognitive impairment in PD and identify their pattern predictive for the conversion from PD-MCI to PDD.

Frontostriatal executive dysfunction and dementia in PD have been reported as cognitive correlates of sequentially occurring pathological changes, namely Lewy body deposition in the nigrostriatal system during the early stages of the disease followed by pathological changes within the cortex occurring in later stages of the disease (Braak et al., 2002). These findings led to the assumption that executive dysfunction evolves into dementia and thus has been described as key feature in PDD (Dubois and Pillon, 1996; Emre et al., 2007). However, Williams-Gray and co-workers (2007 and 2009) described two types of cognitive dysfunction in the early stages of the disease, which differ in terms of their prognosis by performing a longitudinal investigation of Parkinson's disease patients. They showed that frontostriatal executive deficits were common in early disease stages, but did not appear to evolve into dementia over 3.5 years of follow-up, whereas the more posterior cortex-based deficits did (Williams-Gray et al., 2007).

In addition, they also mentioned a genetic impact on the cognitive deficits, such as the involvement of functional polymorphism in the catechol-O-methyltransferase gene (COMT, Val158Met) onto performance and frontal activation in executive tasks, while the inverted genomic region containing the microtubule-associated protein tau gene (MAPT, H1 haplotype) was strongly associated with dementia risk over 3.5 years in the follow-up (Goris et al., 2007; Williams-Gray et al., 2009).

Because different sub-types with significantly different prognoses seem to be correlated with neurobiological changes in various anatomic structures and molecular mechanisms, it gets important to follow the underlying neuropathological changes along the progression of the disease leading to the cognitive deficits with methods that have anatomical localization capability in line with their sensitivity to changes in neural activations and metabolic and molecular changes in the brain tissue. Therefore, the combined use of a set of MRI-based neuroimaging modalities that reflect such changes with a high spatial resolution seems to be a plausible approach for deriving a reliable biomarker for the various subtypes of cognitive impairments in PD patients.

Identifying a progressive pathological pattern related to the cognitive decline would not only help to identify those PD patients at high risk of progressive cognitive decline and developing dementia, but also those who may benefit from early clinical interventions at a pre-dementia state (Litvan et al., 2012). Early interventions are especially important for the patients in order to maintain the patient's life quality and delaying the worsening of the impairments.

Some structural, functional and metabolic MRI studies attempt to describe specific markers for cognitive decline in PD and PD-MCI and for their transition towards PDD. But no consistent reliable MRI-based biomarker for PD-MCI nor PDD have been described so far. A brief overview about the recent literature addressing these questions will be given in the following sections.

1.4 Literature Review of MRI Related Findings of Cognitive Decline in PD

The MRI research describing cognitive decline in PD can be generally classified as studies based on functional, structural, metabolic and perfusion imaging techniques. Most of the MRI studies investigated changes related with PD-MCI, while there are a limited number of studies investigating PDD. The majority of the PDD related MRI studies have been volumetric studies using the voxel-based morphometry method for the quantification of brain atrophy. However, these studies lack detailed information about the functional changes leading to PDD.

Some of the most important MR-based findings for cognitive decline in PD and the basics of these techniques are presented in the following.

1.4.1 Functional MRI

Functional MRI (fMRI) studies generally rely on the blood oxygenation level dependent (BOLD) signal, which is based on the different magnetic effects of oxy- and deoxy-hemoglobin on the dephasing period of the resonating proton spins in the tissue. As deoxy-hemoglobin increases the speed of the dephasing, its increased level in the capillaries and vessels around neuronal populations of increased activity leads to a faster decrease of the MRI signal, while the relative increase of the oxy-hemoglobin in a region produces the opposite effect. This contrast produces the BOLD signal as a measure of the hemodynamic changes due to neurovascular coupling in brain tissue: The increased metabolic activity of the neural populations leading to increasing oxygen consumption initially creates a small decrease in the MRI signal, the initial dip, which is replaced by a large increase due to the vascular response, hence increase in oxy-hemoglobin, peaking around 8 s after the increase of the neural activity lasting almost 20 s to return to the initial level.

Functional MRI works can be generally separated into task-based functional MRI (task-fMRI) and resting state functional MRI (rs-fMRI) studies.

In the task-fMRI technique, activation maps are estimated, based on BOLD signal changes in the brain of a person performing a given task in contrast to a baseline condition. In contrast, rs-fMRI is based on measurement of low-frequency 'intrinsic' fluctuations in MRI signals while the brain is at rest (Fox and Raichle, 2007; Smith et al., 2012).

The functional brain connectivity is defined in terms of the covariance of BOLD fluctuations received from various locations of the brain (Biswal et al., 1995). While they can be computed based on activation areas in task-fMRI data, the presence of intrinsic BOLD fluctuations during 'rest' also allows to estimate temporal correlations or coherences among various brain areas in rs-fMRI data. Brain regions showing coherent fluctuations in rs-fMRI constitute the resting state networks (RSNs).

While seed-based functional connectivity analyses build a hypothesis-driven framework, a blind separation method based on the spatial or temporal independence of decomposed components of a compound data based solely on a mathematical constraint, the Independent Component Analysis (ICA), also provided similar, reproducible RSN patterns from rs-fMRI data. One very important property of this approach is that it is a data-driven approach, which does not rely on or require any hypothesis-based initial seed regions, which makes it prone to any subjective decisions about the nodes of an RSN.

Notably, the spatial topography of the RSNs resemble brain regions that are active during a variety of cognitive, motor and sensory tasks in task-fMRI studies (Smyser et al., 2013). While most of the RSNs are task-positive, increasing their intrinsic connectivity during specific tasks, the default mode network (DMN) shows increased intrinsic connectivity during rest (Raichle 2015).

Baggio et al. (2014) investigated the functional connectivity of the resting state networks in PD, PD-MCI and healthy subjects and found reduced long range connectivity and higher local inter-connectivity for PD-MCI. In another study of Baggio et al. (2015), the authors found reduced connectivity between the dorsal attention network (DAN) and right fronto-insular areas, while there was increased connectivity of the DMN with the medial and lateral occipital-parietal areas. The data further revealed reduced within-DAN, within-DMN and DAN-FPN (dorsal attention network-frontoparietal network) connectivity, as well as loss of normal DAN-DMN anticorrelation in PD-MCI patients (Baggio et al., 2015).
Amboni et al. (2015) in contrast showed lower DMN connections in both PD and PD-MCI, while PD-MCI additionally showed decreased bilateral prefrontal cortex connections in FPN. In a combined rs-fMRI and SPECT study by Lebedev and colleagues (2014) the resting state fMRI correlates of cognitive impairment in PD and the impact of dopamine deficiency on these networks were investigated and better executive performance was associated with increased dorsal fronto-parietal cortical processing and inhibited subcortical and primary sensory involvement, while better memory performance correlated with increased prefronto-limbic processing (Lebedev et al., 2014).

Decreased connectivity in the medial and middle orbitofrontal cortex and the occipital lobe, but increased connectivity in the superior parietal cortex, posterior cingulate gyrus, supramarginal gyrus and supplementary motor area were detected for PD patients compared to controls (Goettlich et al., 2013) as well as decreased functional connectivity of the right medial temporal lobe and bilateral inferior parietal cortex within the DMN in PD compared to healthy subjects (HS) (Tessitore et al., 2012). Furthermore, Rektorova (2012) showed decreased connectivity in right frontal gyrus and bilateral inferior occipital gyrus in PDD compared with PD and controls.

Corticostriatal functional connectivity was disrupted in PDD compared to PD and healthy subjects in a study by Seibert et al. (2012), especially between the prefrontal cortex and caudate.

In short, there are varying results reported on the DMN connectivity patterns, one of the mostly investigated RSNs in cognitive disorders, while the task-positive networks have been reported in general to reduce their functional connectivity with decreasing cognitive performance.
There are also several task-based fMRI studies on PD, PD-MCI and PDD, however, they will not be introduced here in detail as they are out of the scope of the present study.

1.4.2 Structural MRI

1.4.2.1 Diffusion Tensor Imaging - DTI

Diffusion tensor imaging (DTI) is an MRI technique enabling to produce neural tract images based on the measurement of the restricted diffusion of water in tissue (Mukherjee et al., 2008). The DTI related measurements are the fractional anisotropy (FA), mean diffusivity (MD), radial diffusivity (RD) and axial diffusivity (AD). Changes in these measurements can relate to biological changes in the neural tissue. FA is used as a measure of microstructural integrity and density of the neuronal tracts, and decreases with axonal loss and demyelination as the diffusion of water in the intercellular space would decrease the anisotropy of diffusion (Feldman et al, 2010). The degree of displacement of the water molecules in the neurons is characterized by the MD given in micrometers per millisecond (μm/ms) and is an inverse marker for cell-membrane density (Feldman et al, 2010). MD increases along demyelination processes and neural degeneration. RD on the other hand also increases together with demyelination and changes in axonal diameters. Lastly, the AD represents the direction of diffusion that is parallel to the white matter (WM) tract and decreases with axonal injury but is also known to increase during maturation (Feldman et al., 2010).

Chen et al. (2015) investigated the anatomical and functional changes related to PDD in a combined DTI and fMRI study and found that PDD is associated with reduced functional connectivity between the right posterior cingulate cortex (PCC) and medial temporal lobe as well as microstructural damage of the left hippocampus. Agosta et al. (2014) found

abnormalities in the anterior and superior corona radiata, genu and body of corpus callosum, anterior inferior fronto-occipital, uncinate and superior longitudinal fascicules of PD-MCI patients compared with PD and healthy controls. Deng et al. (2012) additionally detected changes in the left frontal/right temporal white matter and bilateral anterior cingulum bundles of PD-MCI patients by comparison with controls. Melzer et al. (2013) aimed to characterize the different cognitive states in PD and identified decreased factional anisotropy (FA) and increased mean diffusivity (MD) levels in PD-MCI and PDD compared to controls. Significantly lower FA values in PDD patients in many major tracts compared to control subjects as well as significantly lower FA values at the prefrontal white matter and the genu of the corpus callosum as compared to PD patients have been described by Kamagata et al. (2013). Furthermore, there was a significant correlation between the Mini-Mental State Examination (MMSE) scores and the FA values of the prefrontal white matter and the genu of the corpus callosum in patients with PD from which they conclude a relationship between cognitive impairment and alteration of the prefrontal white matter and genu of the corpus callosum (Kamagata et al., 2013). Lee (2010) compared DTI data of PDD and Lewy body dementia (LBD) patients and found lower diffusivity in posterior temporal, posterior cingulate and visual association fibers of PDD patients. Hattori et al. (2012) detected a widespread lower fractional anisotropy (FA) in superior longitudinal fascicule, anterior limb of the internal capsule, and inferior longitudinal fascicule of PDD patients, by comparison with controls and further suggest that white matter damage underlies cognitive impairment in PD, and cognitive impairment in PD progresses with functional alteration (hypoperfusion) followed by structural alterations in which white matter alteration precedes gray matter atrophy.

1.4.2.2 Anatomical changes – Atrophy and White Matter Hyperintensities

Morales et al. (2013) found different cerebral white matter values and volumes of the lateral ventricles and hippocampi for the PD-cognitively intact, PD-MCI and PDD groups and defined these as the most predictive neuroanatomical findings to distinguish between these groups. The hippocampal volume and white matter hyperintensity as a major factor predicting the development of mild cognitive impairment and dementia in PD has also been described by Kandiah et al. (2014).

Furthermore, Rektorova et al. (2014) reported that gray matter changes in PDD involve areas associated with Alzheimer-like pathology while fronto-parietal abnormalities are possibly an

early marker of PD cognitive decline and mentioned these findings are consistent with a non-linear cognitive progression in PD. These findings are supported by an earlier study of Mak et al. (2013) who found that domain specific cognitive impairment in mild PD is associated with distinct areas of gray matter atrophy and that these regions of atrophy are early in the disease course and may serve as a biomarker for dementia in PD.

In a study by Compta et al. (2013) thinner superior-frontal/anterior cingulate and precentral regions were found to be baseline predictors for PDD.

In a combined (18F-fluorodeoxyglucose, FDG) positron emission tomography (PET) and MRI study from Gonzales-Redendo and colleagues (2014) investigating the extension and topographical distribution of hypometabolism and atrophy in the different cognitive states of PD they found hypometabolism exceeded atrophy in the angular gyrus, occipital, orbital and anterior frontal lobes in PD-MCI and that in patients with dementia, the hypometabolic areas observed in PD-MCI were replaced by areas of atrophy, which were surrounded by extensive zones of hypometabolism. They conclude that there is a gradient of severity in cortical changes associated with the development of cognitive impairment in Parkinson's disease in which hypometabolism and atrophy represent consecutive stages of the same process in most of the cortical regions affected (Gonzales-Redendo et al., 2014).

In a study by Lee and colleagues (2013) PD-MCI patients were prospectively followed-up for a minimum of 2 years, and showed that atrophy in the frontostriatal areas and cholinergic structures, as well as frontal lobe associated cognitive performance, may act as predictors of dementia in PD-MCI patients, suggesting distinctive patterns of cognitive profiles and a neuroanatomical basis for progressive PD-MCI (Lee et al., 2013). Shin et al. (2012) demonstrated that the burden of white matter hyperintensities (WMH) within cholinergic pathways was significantly higher in patients with PDD relative to other groups, and that cholinergic WMH was significantly correlated with a decline in frontal executive function and attention. Sunwoo and colleagues (2014) were able to reproduce the findings of Shin et al. (2012) as PD and PD-MCI patients were prospectively followed-up for 2 years and demonstrated that the WMH burden is a significant predictor of conversion from PD-MCI to PD dementia and its relation to ongoing decline in frontal-lobe-based cognitive performance. Based on the structural MRI findings, the neuroimaging data provides a relatively high sensitivity as well as specificity for cognitive impairment and prediction of dementia compared with neuropsychological test (NPT) scores.

1.4.3 Metabolic Neuroimaging Techniques and Magnetic Resonance Spectroscopic Imaging (MRSI)

Diverse neuroimaging modalities can investigate the metabolic changes in the brain and have been quantified for the different cognitive conditions in PD (Duncan et al., 2013). Hypometabolism, amyloid-load and dopaminergic as well as cholinergic dysfunctions are the most described metabolic findings for cognitively impaired PD patients.

Thus, PD-MCI related hypometabolism in posterior and prefrontal cortical areas were described in several studies (Lyoo et al., 2010; Silbert and Kaye 2010; Bohnen et al., 2011). For both, PD-MCI and early stage PDD, increasing amyloid load in posterior cortical areas were identified (Hilker et al., 2005, Bohnen et al., 2006; Pappata et al., 2011), and widespread dopaminergic and cholinergic dysfunctions have been reported (Wolk et al., 2009; Silbert and Kaye 2010). When compared to cognitively unimpaired PD patients Positron Emission Tomography (PET) studies show the presence of parietal, temporal and occipital hypoperfusion in PD-MCI (Nobili et al., 2009). Hypometabolism was shown in prefrontal and parietal areas in PD-MCI (Huang et al., 2008), and in bilateral posterior parietal lobe and right occipital lobe in PD-MCI by comparison with controls (Nobili et al., 2011). Studies using Single Photon Emission Computed Tomography (SPECT) technique revealed low cerebral blood flow (CBF) values, as well as minor and diffuse hypoperfusion focus in frontal and temporoparietal lobes in PDD (Derejko et al., 2001).

1.4.3.1 Magnetic Resonance Spectroscopic Imaging – MRSI

Proton MR spectroscopic imaging (1H-MRSI) is a noninvasive, ionizing radiation free MRI technique that provides information about the metabolic changes in the brain. Similar to MRI, MRSI uses signals from the hydrogen proton, but it uses the signal to determine the relative concentrations of the target brain metabolites in a specific brain volume (Castillo et al., 1996). The technique is based on the principle that protons in different molecular structures resonate in different frequencies due to chemical shifts, depending on the magnetic field generated in the opposing direction to the magnetic field created by the electron cloud around protons.

There are four important metabolites reflecting the neurodegenerative processes, the N-acetylaspartate (NAA), choline (Cho), glutamine/glutamate complex (Glx) and myo-inositol (mI) (Nie et al., 2013; Pagonabarraga et al., 2013). While the NAA is thought to represent a neural marker and mI a glial marker indicating demyelination, Cho is a marker for both

neurons and glia cells. Creatine (Cr) on the other hand is used as reference value, as it is known to be more stable in the tissue.

Pagonabarraga et al. (2012) investigated the 1H-MRSI features of PD, PD-MCI and PDD in comparison to controls and found decreased N-acetylaspartate (NAA) concentrations in the right dorso-lateral pre-frontal cortex (DL-PFC) in PD-MCI compared with PD patients correlated with frontal subcortical tasks, while the NAA concentrations in the left hippocampus were decreased in PDD compared to PD-MCI and correlated with confrontation naming. As the presence of NAA and choline point to a neurodegenerative process in the first line, the authors' findings support that executive impairment is related to dorsolateral prefrontal dysfunction from the early stages, while progression to dementia is linked to the additional impairment of temporal lobe structures (Pagonabarraga et al., 2012). Complementing this findings Nie and colleagues (2013) found decreased NAA/Cr ratios at the occipital lobe and increased choline/Cr ratios at posterior cingulate related to PD-MCI and conclude that metabolite changes in these structures occur in the early cognitive impairment phase of PD patients, hence can be used as marker for the detection of PD-MCI (Nie et al., 2013). Griffith et al. (2008) observed a decrease in NAA, NAA/Cr, and Glutamate/Cr primarily in posterior cingulate gyrus for PDD compared to PD and controls, while Summerfield et al. (2002) obtained a lower NAA/Cr in the occipital lobe in PDD, compared to PD. A lower NAA/Cr at posterior cingulate gyrus was also observed in PD-MCI patients in a study conducted by Camicioli et al. (2004).

1.4.4 Arterial Spin Labeling – ASL as Method to Measure Brain Perfusion

The benefit of the arterial spin labeling (ASL) MR imaging technique is that it allows to calculate the cerebral blood flow without the use of any radioactive or contrast agents like it is necessary in PET and SPECT (Detre et al., 1994). In ASL, the arterial blood water is magnetically labeled just below the region of interest (closer to the heart) by applying a 180-degree radiofrequency inversion pulse. The result of this pulse is the inversion of the net magnetization of the blood water and consequently the MR signal as well as image intensity. The image taken during this time-window will provide an estimate of the blood flow in the region of interest (ROI) (http://fmri.research.umich.edu/research/main_topics/asl.php).

Only a few studies using ASL for the investigation of the cognitive impairment in PD exist. Melzer et al. (2011) attempted to describe a PD related perfusion network by using the ASL technique and found hypoperfusion in precuneus, cuneus and middle frontal gyrus in PDD. Kamagata et al. (2011) detected hypoperfusion in the posterior cortex in PD and PDD patients using ASL perfusion MRI. Both studies mention the possible application of ASL technique as a tracking tool for the disease progression due to the non-invasive and safe method (Melzer et al., 2011). Prolonged overall arterial arrival times (AAT) and neuropsychological test score (MOCA) correlated regional CBF values were found for PD patients compared to controls (Al-Bachari et al., 2014). Fernandez-Seara et al. (2015) used the ASL technique to investigate the resting state of PD patients and detected increased connectivity of the subthalamic nucleus and cognitive and motor areas.

Although these studies give promising insight about the changes related with cognitive decline in PD, they are partially controversial and lack the formulation of a reliable biomarker for the development of PDD. Many studies are insufficient regarding study-size, follow-up and the compared groups (PD/PD-MCI, PD/PDD, PD-MCI/PDD, lack of HS). But most importantly, there are only few studies trying to combine the different imaging modalities.

1.5 AIM OF THE STUDY

The aim of this study is to track the progression of the neuropathological changes related to cognitive impairment in PD patients by using multimodal magnetic resonance imaging (MRI) techniques in a cross-sectional study design. Based on measurements of PD patients at different stages of the cognitive decline, we attempt to describe a discriminant biomarker for PDD. Intending to do so, the combined functional, structural, metabolic and perfusion neuroimaging modalities of PD-N (PD without cognitive symptoms), PD-MCI and PDD patients will be evaluated in combination with the clinical profile and neuropsychological test scores.

1.5.1 Integration of the brains functional connectivity derived from rs-fMRI and structural connectivity derived from Diffusion Tensor Imaging

The resting-state functional MRI (rs-fMRI) and Diffusion Tensor Imaging (DTI) data from all study groups will be obtained and integrated in order to investigate the large-scale functional connectivities of the brain related to cognitive decline in PD.

The cumulated knowledge on neuroimaging findings suggests that correlates of behavioral changes are better reflected in connectivity patterns of the brain than anatomic or functional changes occurring at specific local portions of the neural tissue. The temporal correlations of hemodynamic signals obtained with rs-fMRI allow the visualization of a series of functionally meaningful connectivities in the brain, namely the intrinsic connectivity networks (ICNs) or resting-state networks (RSNs). The independence from any task condition makes this type of functional measurements easier to apply in clinical settings. The integration of these functional connectivity (FC) results with anatomical connectivity (AC) patterns derived from Diffusion Tensor Imaging measurements will decrease the variability and increase their sensitivity, because any functional connectivity needs to reside on anatomical connections between brain areas.

1.5.2 Integration of MR Spectroscopic Imaging Data

Magnetic Resonance Spectroscopic Imaging (MRSI) will be performed and allows for the non-invasively measurement of NAA+NAAG, Cho, Glx and mI metabolite concentrations in the brain tissue. The MRSI data will focus on these substances specifically in the frontal parietal areas, which seem to be responsible for the executive and visuo-spatial impairments. According to a group of previous studies deficits in the parietal areas point to a more malign development of cognitive decline in PD (Williams-Gray et al.2009; Rektorova et al. 2012; Moustafa et al., 2013; Jellinger2013; Winder-Rhodes et al.,2014; Nombela et al., 2014). Based on the positive findings in the literature, the MRSI approach within this multimodal MRI study will contribute important findings related to the prediction of developing dementia in PD.

1.5.3 Integration of Brain Perfusion data

Brain perfusion will be investigated by means of Arterial Spin Labeling measurements, which may indirectly reflect the areas where the neurodegenerative process has started and may represent reduced metabolic activity in areas with tau abnormalities, which has been already

accepted as a reliable FDG-PET marker for the follow-up of PD and AD (Musiek et al., 2012, Huang et al., 2008; Nobili et al., 2011; Garraux et al., 2013; Gonzales-Redondo et al., 2014).
It is not clear whether the hypoperfusion measured with ASL appears to occur before or after the neuronal changes measured with other MRI techniques. Nonetheless, ALS is a non-invasive technique and will be used to measure perfusion in this multimodal MRI study.

1.5.4 Benefits of the cross-sectional study design

Because a longitudinal study design needs a long-lasting work with some other complexities such as the compliance of the initial patient group to repeated measurements along the years, a cross-sectional study design on patients at various stages of the disease was preferred for this study. By this design, we intend to describe a set of neuroimaging features that show a progressive gradual change among PD patients without any cognitive decline (PD-N), patients diagnosed as PD-MCI and PDD. This cross-sectional study design will enable to re-create the longitudinal neuropathological progression. Identifying a progressive pathological pattern based on cross-sectional multimodal investigations would allow characterizing a multimodal MRI-based biomarker for the risk of cognitive impairment and by this way the discrimination of the PD patients with increased risk to convert to PDD.

1.6 MAIN HYPOTHESES

1. The main working hypothesis is that a set of derived multimodal MRI parameters will be able to provide novel information about the mechanisms underlying the pathogenesis and progression of the cognitive decline in PD to PDD.
2. We hypothesize that a multimodal neuroimaging-based biomarker will be capable to track the gradual change of cognitive decline in PD, which will be verified by its correlation with the clinical/neuropsychological evaluation of the PD population. Within this framework, we assume that a parsimonious set of derived multimodal neuroimaging parameters will suffice to describe the progression of the cognitive decline.
3. We assume that in addition to functional and diffusion MRI measurements, MRSI and ASL techniques will provide additional sensitive spectroscopic and perfusional findings that will correlate with the cognitive dysfunction in PD.
4. In case we will be able to define significant pathological differences between the different cognitive states of the patients, we mostly expect them to be related to reduced functional

connectivity in the RSNs by measures of fMRI, decreased connectivity and FA values of the WM tracts by the use of DTI/dMRI measurements, reduced NAA values using MRSI and reduced perfusion by ASL measurements, each increasing in severity along the severity of the cognitive decline.

5. As an additional output of the study, the correlations of the investigated neuroimaging parameters with the change of neuropsychological test (NPT) scores related with specific cognitive domains will allow us to describe neuroimaging counterparts of specific neuropsychological tests, which might shed light on the design of future neuroimaging studies on cognition in general.

While for other neurodegenerative diseases such as Alzheimer's disease (AD) MRI techniques have already been well established as substantial tool for the diagnosis and follow up of the disease, the application and use of MRI techniques in PD are yet to be established. The evaluation of multimodal structural, functional and metabolic MRI data collected from PD patients at different stages of cognitive impairment will provide important information about the pathological basis these cognitive impairments rely on and give insight about the essential pathological changes predicting the progression to dementia in PD. The investigation of multimodal data will provide a more detailed and complete picture about the PD pathogenesis than only single modalities can. Furthermore, multimodal MRI-based measures will allow the use of totally non-invasive and task-independent data offering a clinical set-up that could easily be applied in future follow-ups and as diagnostic tool for clinicians. Additionally, multimodal MRI will plausibly provide more sensitive results than NPT scores alone and will be less biased by the motivational level of the patients in the NPTs. To our knowledge such a cross-sectional multimodal MRI study design investigating the pathological progression related with cognitive decline in PD and PDD has not been performed before.

2 METHODS

2.1 Subjects

Sixty idiopathic PD patients participated in this study (PD-N= 20, PD-MCI=20, PDD=20). Patients followed at the Department of Neurology and Movement Disorders of Istanbul Faculty of Medicine diagnosed with idiopathic PD by a neurologist according to the UK - Parkinson's Disease Society Brain Bank Criteria were included in the study. Shortly, the basic criteria were the presence of bradykinesia/akinesia and at least one of the other cardinal features of PD such as rigidity, tremor at rest and the absence of atypical features or secondary causes of the disease (Gibb and Lees, 1988, Hughes et al., 1992). While initially the patients were recruited taking into consideration comparable age, educational level, duration of disease and medication in each group, 4 PD-N, 2 PD-MCI and 2 PDD patients were excluded from the study to reduce the difference of the main age among the 3 groups (Table 3-1). The study is approved by the Ethics-Committee of the Istanbul Medical Faculty of Medicine in accordance with the Principles of the Declaration of Helsinki, and all subjects gave written permission for their participation in this study and the measurements.

As the aim of the study is to investigate the neuroimaging markers of the cognitive decline within the Parkinson's disease and to define a discriminant biomarker for the identification of PDD patients, the PD-N group has been considered as the reference group.

2.2 Clinical examination

2.2.1 Unified Parkinson's disease Rating Scale

In order to ascertain the disease status, the patients were examined by a neurologist using the Unified Parkinson's disease Rating Scale (UPDRS), before the neuropsychological tests and MR measurements were carried out. The UPDRS is one of the most common tools to scale the Parkinson's disease status in clinical environment by interviewing and clinical observation, and covers among others the evaluation of the patients mental and mood state, the self-evaluation of daily life, scoring of the motor abilities (UPDRS part III) and staging of the disease severity (Hoehn & Yahr scale, Hoehn & Yahr 1967).

2.3 Criteria for the Diagnosis of PD-MCI

All subjects underwent a comprehensive neuropsychological test battery and were diagnosed as PD-MCI according to the Level I criteria (Litvan et al., 2012). For this, a cut-off score of ≤83 of the ACE-R examination (Addenbrook's Cognitive Examination Revised) was used, as 83 points in the ACE-R showed 80% specificity and 52% sensitivity for PD-MCI in an earlier study on the global screening of the Turkish PD population (Uysal Cantürk, 2013).

2.4 Criteria for the Diagnosis of PDD

The Clinical Diagnostic Criteria for Dementia Associated with Parkinson's Disease (Emre et al., 2007) were used for PDD diagnosis. The PDD patients had to show impairment in at least two cognitive domains and in contrast to the PD-MCI group, the deficits in the PDD patients have to be severe enough to affect the daily life such as hygiene, outside activity and social interactions. These are independent from the motor deficits (Emre et al., 2007).

2.5 Exclusion criteria

All participants of this study were tested for signs of major depression. Subjects with scores >16 of 30 in the Geriatric Depression Scale (GDS) were excluded. Antidepressant treatment in the PD groups was tolerated as long as the GDS score was ≤ 16. Subjects with history of other significant psychiatric or neurological diseases were excluded. Subjects with severe tremor or dyskinesia and other conditions prohibiting participation in the MR measurements such as deep brain stimulation (DBS), coronary stent implant, old prosthetics or teeth implants, when not MR-compatible, were not included. Additionally, subjects with anticholinergic drug treatment were excluded due to possible interaction with the brain activity. Because psychotic symptoms are common in PD dementia, antipsychotic drug treatment was partly accepted in the PDD group. All subjects had minimum educational level of 5 years (primary school) except a single PDD case.

Subjects with severe pathological MRI findings due to tumor, anoxic brain damage, stroke, lacunae, other neurological or developmental disorder, white-matter hyperintensities (WMH) > 3 according the Fazekas scale in a clinically oriented anatomical MR sequence (FLAIR) were excluded. Finally, subjects with head motion > ±3mm translation and rotation in the rs-fMRI and diffusion MRI measurements were excluded.

2.6 Medication

The patient groups were medicinally balanced mainly regarding the treatment with L-Dopa, dopamine agonists and inhibitors of dopamine decomposition pathway but varied regarding other drug treatments, such as anti-dementia drugs and blood-pressure or pain-killers.

2.6.1 Dementia drug treatment in PDD

Against the cognitive symptoms of dementia, most of the (12) PDD patients were treated with the Exelon® Patch. The active substance of Exelon is rivastigmine which acts as an acetylcholine esterase inhibitor and leads to an increase of acetylcholine in the brain, and thereby helps in reducing the dementia symptoms of the patients. One patient was treated with Aricept (active substance is donepezil), which also is an acetylcholine esterase inhibitor.

2.7 Neuropsychological examination

All study participants (PD-N, PD-MCI and PDD) underwent a wide battery of neuropsychological examinations.

2.7.1 Global neuropsychological tests

The ACE-R, MMSE and MOCA were used for the global neuropsychological evaluation of the subjects.

2.7.1.1 Addenbrooke's Cognitive Examination- Revised (ACE-R)

As a sensitive and specific cognitive screening instrument for early cognitive dysfunction, the ACE-R has been established as a reliable test over the last decades. The ACE-R covers five cognitive domains such as orientation/attention, memory, verbal fluency, language and visuo-spatial abilities (Mioshi et al., 2006). The patients performed the Turkish version of the ACE-R, and the administration usually lasted between 15-20 minutes. The maximal score of the test is 100 points. Based on the previous results of Uysal Cantürk (2013) at the Istanbul Faculty of Medicine, the patients were diagnosed as PD-MCI when they obtained ≤ 83 in the ACE-R. However, the other test scores, the UPDRS evaluation and the patients subjective complaints were considered for the final diagnosis in case the ACE-R performance left subjective doubts about the diagnosis.

2.7.1.2 Mini Mental State Examination (MMSE)

The MMSE was originally introduced by Folstein et al. in 1975, and is because of its easy and fast administration used in clinical environment in order to obtain an overview about the patient's cognitive status and the progression of the cognitive decline, although it is criticized by its lack of sensitivity for the detection of cognitive impairment. In this study, the MMSE scores were obtained from within the ACE-R test.

2.7.1.3 The Montreal Cognitive Assessment (MOCA)

The MOCA was introduced by Nasreddine et al. (2005), and is such as the ACE-R and the MMSE a quickly applicable cognitive screening instrument. For the Turkish population, a cut-off score of ≤ 21/30 is suggested for dementia, however this diagnosis was made by the clinicians.

2.7.2 Tests investigating the executive functions

As the executive functions seem to be strongly affected in PD-MCI, the domains of executive function were explicitly tested using the Stroop, Wisconsin Card Sorting Test and Symbol Digit Modalities Test (SDMT). Additionally, we evaluated sub-scores of the ACE-R test such as verbal fluency (phonemic fluency=k letter, semantic fluency=animal naming) and clock drawing scores to further score the patients executive abilities. The dysfunction of these domains may rely on the dysfunction of the prefrontal cortex, as it allows the subject to pay attention to one event and exclude others and to switch among them (Watson et al., 2010).

2.7.2.1 Stroop Test

Previous studies reported about low performance of PD and PD-MCI patients in the standard Stroop test, showing longer reaction times and higher error rates compared to healthy controls (Bohnen et al., 2006, Lima et al., 2008). The word-color Stroop task, in which participants are either asked to read the written word (red, blue, green, yellow) or to name the ink color of the written word, is the most common test in order to demonstrate the Stroop effect. The interference effect becomes obvious when the written color and its ink color are incongruent. The interference effect for color naming in incongruent conditions is bigger than for word reading showing that healthy subjects are more trained to automatically read a word and that one has to put more effort/attention to inhibit the automatic word reading in order

to name the ink color of the written word. The Stroop task is considered to measure not only selective attention but cognitive flexibility and processing speed, and is therefore a common test to evaluate the executive functions of subjects and patients.

In this study, the word-color Stroop test was performed in Turkish language. The patients had normal or corrected to normal vision, and color blindness was excluded. First the patients had (1) to name the color of some rows of squares, (2) to read the name of the written words ("red" ("kırmızı" in Turkish), "blue" ("mavi" in Turkish) and "green" ("yeşil" in Turkish)) and (3) to name the ink color of the written words (Figure 2-1). Each time the seconds to complete the task, the number of spontaneous corrections and the mistakes were counted. The time difference between the word reading and ink naming (Stroop effect) was calculated.

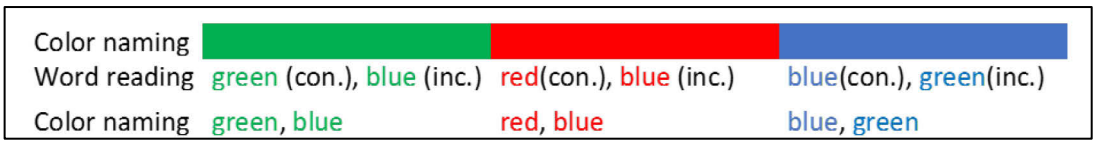

Figure 2-1: Stroop test in which the patients have to name the color of colored squares, read the written words and name the color of the written words. con.: congruent, inc.: incongruent

2.7.2.2 Symbol Digit Modalities Test – SDMT

The SDMT (Smith 1968 and 1982) is an easy applicable tool to test short term memory, visual scanning and attention. It is a simple substitution task in which the subjects have to fill boxes below the symbols with numbers between 1-9 regarding a symbol reference key (Figure 2-2). After 10 training boxes, the test starts and the participants have to fill as much boxes a possible within 90 seconds. The written responses were collected in this study, although in some patients with severe hand tremor the average of both the written and spoken responses where used.

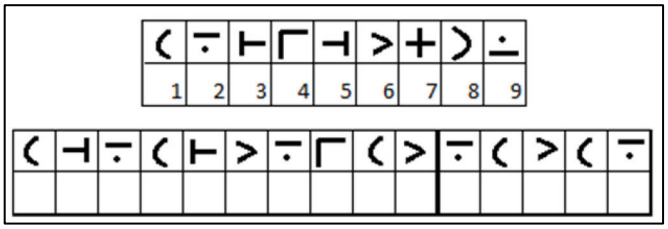

Figure 2-2: The key and the first line of the SDMT including 9 training fields.

2.7.2.3 Wisconsin card sorting test - WCST

In order to test for domains of the executive functions (frontal lobe function) in the study groups the WCST was used. The WCST (Berg, 1948) is a widely-used tool to evaluate the subject's ability to deduce concepts and strategy, and to shift the strategy in response to concept changes (Eling et al., 2008). Hereby the WCST also covers domains such as mental flexibility, short term memory and attention.

In the test, the subject has to find a shared characteristic of a central appearing card and one of the four steady cards displayed below this card based on the feedback of the examiner (correct, wrong) (Figure 2-3). The shared characteristic can either be the color, shape or number of items on the card. One category contains 10 correct answers in a row, after that the rule changes without announcement. In this study, a minimum of 128 cards/maximum 6 categories were used. The test was conducted computer-based, and the subjects gave verbal response to the examiner, who in turn manually gave the answer into the keyboard. The number of categories, percentage of perseverative error response and total number of errors have been evaluated.

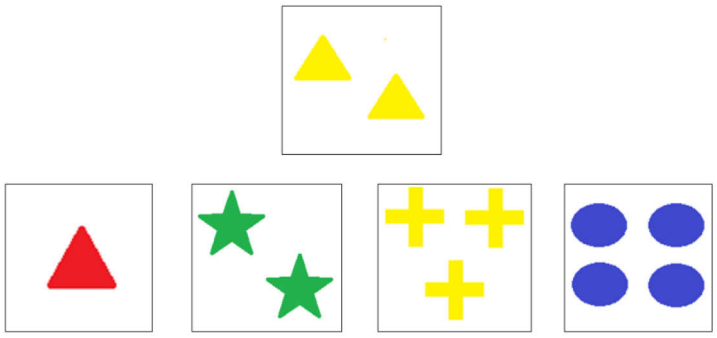

Figure 2-3: Example figure for the WCST.

2.7.2.4 ACE-R sub-tests for executive functions

2.7.2.5 Verbal fluency test

Verbal functioning can be quickly assessed using the verbal fluency test, which can be divided into phonemic and semantic word fluency. While the performance in the phonemic word fluency seems to strongly depend on frontal function, semantic fluency performance may stronger rely on the function of temporal areas (Baldo et al., 2006). Worse semantic fluency has been reported as a risk factor for PDD.

Letter/Phonemic fluency

In the k-letter task the subjects had to name as many words as possible starting with “k” as the first letter in 60 seconds. The subjects were instructed not to use proper nouns such as names or cities (e.g. Kemal/Klaus, Kastamonu/Köln). Perseverations, unreal words and proper nouns were noted but not counted in the end. The responses for each 15 s were separately recorded on the control paper. By this way it was possible to see whether the subjects gave steady responses or had higher performance at the beginning or at the end of the test.

Category/Semantic fluency

In a second task the participants were asked to name as many animals as possible within 60 s independent of the starting letter. The responses were noted in the same way as in the phonemic fluency task.

2.7.2.6 Clock-drawing test

The clock-drawing test actually represents parts of both of the executive and visuo-spatial functions. In this test, the subjects were asked to freely draw a clock out of their memory and set the time to 11:10. Subjects were required to draw a closed circle, put all numbers in the right place and indicate the time with the hands in the correct length in order to obtain full points (5pt.). While drawing, the examiner gained information about the subjects planning skills, visuo-spatial construction abilities and abstract thinking. Rotation, missing numbers, wrong placement and inability to show the time provide different information about the subject’s cognitive state.

2.7.3 Tests investigating the visuo-spatial function

Studies showed that besides the executive dysfunction, the presence and degree of the visuo-spatial dysfunction seem to be crucial for the development of PD-MCI and PDD. Therefore, the subject’s visuo-spatial abilities were tested with the Benton Judgement of Line Orientation test, the Navon test and sub-parts of the ACE-R test such as the pentagon and cube copying and clock-drawing.

2.7.3.1 Benton Judgment of Line Orientation Test

A widely used neuropsychological tool for the investigation of visuo-spatial abilities of patients is the Benton Judgment of Line Orientation test (JOLO). In the test, patients have to match two lines with different orientation with two lines of a target array composed of 11 lines arranged in even steps from 0 to 180º (Figure 2-4). The target array is placed below the two lines. In total, 30 pairs of lines have to be matched with the target array. Both of the two lines have to be identified correctly in order to get 1 point. The patients had normal or corrected to normal vision.

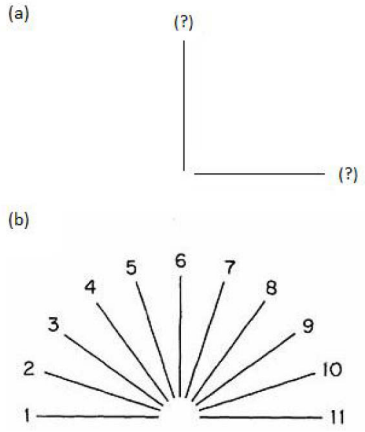

Figure 2-4: Example arrangement of the Benton Judgment of Line Orientation test. Patients have to match the lines on page (a) with the corresponding lines on page (b).

2.7.3.2 Navon

In order to control for simultanagnosia in any of the participants the Navon figure test (Navon 1977) was used. In this test four letters (H, T, L, F) were composed out of different (incongruent) small letters (E, R, K, C) (Figure 2-5). The subjects had to identify the little letters (local feature) and the big letter (global feature) without the borders to get full points. People with simultanagnosia would only identify the local features of the letter but not the global features. The identification of only local letter equals 0 points, the detection of the global letters with the help of the outer linings equals 1 point and the detection of both local and global letters without the help of the outer lines results in the maximum point of 2.

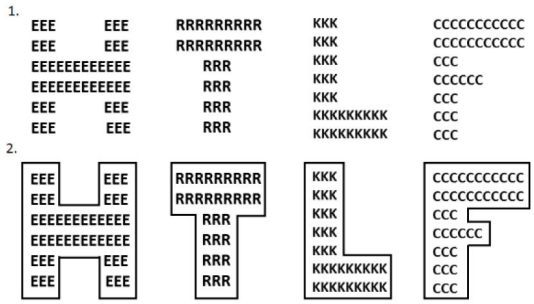

Figure 2-5: The Navon test.

2.7.3.3 Pentagon and cube copying

Patients were asked to copy the two overlapping 5-edged pentagon figures (max. points 1) and the 3D cube figure (max. points 2) (Figure 2-6). The figure had to resemble the cube illusion and consist out of 12 lines.

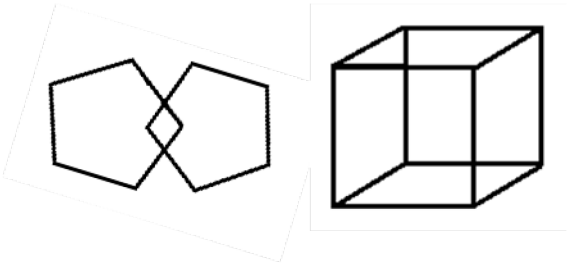

Figure 2-6: The Pentagon and Cube figure copy test.

2.8 Psychiatric assessment

In order to assess the participant's mental status, the patients were interviewed with the geriatric depression scale (GDS), the Beck Anxiety Inventory (BAI, Beck et al., 1988), the Yale-Brown Obsessive Compulsive Scale (Y-BOCS, Goodman et al., 1989) and the Apathy Evaluation Scale (AES, Marin et al., 1991).

2.9 Statistical Analysis of the Neuropsychological Test Scores

The scores of the neuropsychological tests were compared among the patient groups by using one-way Analysis of Variance (ANOVA) method in the SPSS statistics software (IBM SPSS Statistics for Windows, Version 21.0. Armonk, NY: IBM Corp).

2.10 MR Imaging

The structural, functional, diffusion, metabolic and perfusion MR imaging was performed with a 3T whole-body Phillips MRI scanner (Philips Achieva TX, Enschede, Holland) equipped with a 32-channel SENSE head-coil. High-resolution anatomic MR image, resting-state functional MR (rs-fMRI) images, diffusion MR (DTI) images, MRSI data and ASL-based perfusion images were recorded in one session that lasted about 48 minutes in total. Exceptionally, measurements were suspended or paused in case the patients could not tolerate the long session, were scared or due to technical problems, and were then completed at a later time-point maximally within one week. The recording parameters for each modality were selected as explained in the following sub-headings.

2.10.1 T1 weighted and FLAIR data acquisition

Two anatomic images were obtained by using (1) a T1-weighted fast field echo sequence (FFE) (TR=8.3ms, TE=3.8ms, FOV=250x250 mm, number of slices=180, voxel size=1x1x1mm^3, total scan duration=5:55min) and (2) two instances of a T2-weighted fluid attenuated inversion recovery (FLAIR) sequence (TR=4800ms, TE=259ms, TI=1650ms, FOV=250x250 mm, number of slices=60, voxel size=1.11x1.11x3mm^3, total scan duration=0:53min). Both scans covered the whole brain.

2.10.2 Resting-state fMRI data acquisition

The resting-state fMRI data were acquired using the fast field echo planar imaging (FFEPI) sequence with the following parameters: TR=2000ms, TE=30ms, FOV=224x240 mm, number of slices=36, voxel size=2x2x4mm^3, total scan duration=7:30min. In addition to the first 10 dummy recordings, 214 consecutive time points were sampled yielding 7704 images in total.

2.10.3 Diffusion tensor imaging data acquisition

The diffusion tensor imaging (DTI) data were recorded using 32 gradient directions: TR=10538ms, TE=86ms, FOV=240×240 mm, number of slices=90, voxel size=2x2x2mm^3, b=1000 s/mm2, total scan duration=07:15min.

2.10.4 T2 weighted image acquisition

In order to facilitate the co-registration of perfusion and structural images, a single shot gradient-EPI scan covering the whole head was acquired: TR=10243ms, TE=80ms, FOV=240x240 mm, number of slices=90, voxel size=2x2x2mm^3, total scan duration=1:42min.

2.10.5 Arterial spin labeling data acquisition

ASL images were acquired using a multi-slice single-shot gradient-EPI sequence. The following parameters were used: TR=250ms, TE=16ms, FOV=240x240mm^2, matrix size=80x80, number of slices=6, slice thickness=6 mm, slice gap=2 mm, flip angle=40°, Sensitivity encoding (SENSE) 1.2, label thickness=130 mm, label gap=20 mm, label delay=300ms, number of dynamics=48, total scan duration=4:08min.

Due to the limited slice number, ASL MR images were acquired in three separate scans. In each single scan, 6 slices were obtained. The FOV in the first session was placed bordering the superior part of the cortex close to the skull and the FOVs in the second and third ASL-scans each were placed next to the lower border of the previous scan. Thereby, almost the whole brain was covered without any gap.

During a single ASL-MRI scanning session each of the 6 slices was acquired at 8 different phases (time points) using distinct inversion times (TIs) that are 250ms apart and each consecutive slice was acquired 32ms later in time than the previous. This means, the first phase of the first slice was acquired at 300ms and the last (8th) phase at 2050ms, while the sixth slice's first phase was acquired at 459ms and the last phase at 2209ms. The signal to noise ratio was increased by repeating the measurements 30 times in each scan. By this way, 1440 images were obtained for each of the Control and Tag Images (total 2880 images).

2.10.6 MRSI data acquisition

The multi-slice 3-dimensional 1H-MRSI images were acquired using the Point-RESolved Spectroscopy (PRESS) sequence with a short echo time and the following parameters: TR=1000ms, TE= 52ms, 1024 points, FOV=140x140 mm, number of slices=3, voxel size: 10x10x12 mm^3, slice-thickness=12 mm, total scan duration=323 s.

In the same way as for the ALS imaging, the MRSI images were acquired in two separate scans. In each scan 3 slices were obtained. The maximum number of voxels per slice was 196 (14x14),

but may vary according to the adjustment for each subject's brain size. The MRSI Images where acquired from (1) the fronto-parietal areas and (2) the parieto-occipital areas.

2.10.7 Scan alignment

The alignment of the FOV in the T1 weighted and rs-fMRI imaging was slightly more inclined than the anterior-posterior commissure (AC-PC) plane. T2 weighted, FLAIR, DTI, ASL and MR spectroscopy imaging were performed in straight axial orientation (x:0, y:0, z:0).

2.11 MRI DATA ANALYSES

2.11.1 Analysis of the Resting-state fMRI data

2.11.1.1 Pre-Processing of the fMRI data

Statistical Parametric Mapping (SPM8) software (http://www.fil.ion.ucl.ac.uk) in MATLAB 7.9.0 (The MathWorks, Inc., Natick, MA) was used to preprocess the fMRI data. Pre-processing consisted of the following steps:

1- The fMRI images were spatially realigned to the first volume to correct the bias due to head movements.
2- The high resolution anatomical T1-image was co-registered to the mean fMRI image.
3- T1 image was segmented using the SPM8 segmentation tool, and a transformation matrix to the Montreal Neurological Institute 152 (MNI-152) standard space was obtained.
4- This matrix was used in the normalization of all fMRI images to MNI-152 standard space.
5- After spatial normalization, the fMRI images were spatially smoothed by an isotropic Gaussian filter with a full-width at half-maximum (FWHM) of 8 mm to increase the signal-to-noise-ratio.

2.11.1.2 Group Independent Component Analysis of the rs-fMRI Data

After the pre-processing steps, the resting-state functional connectivity networks were obtained by applying the Independent Component Analysis (ICA), which is a method used to blindly reveal the implicit components, corresponding to discrete sources, in compound signals (Hyvärinen and Oja, 2000). Various neuronal networks in the brain can be determined by applying the ICA method to the rs-fMRI data either based on spatial or temporal

independence among the decomposed components (Smith et al., 2012). Spatial independence is the more preferred approach in fMRI literature, which decomposes the 4-dimensional (3 spatial dimensions + time) rs-fMRI data into such components that are maximally independent from each other in space, while, on the other hand, the BOLD time series are the same for all voxels that belong to each spatial component, with different weighting factors for each voxel. This data-driven approach has the significant advantage over seed-based functional connectivity estimation techniques in terms of using the whole-brain BOLD data without imposing any prior hypothesis about the spatial characteristics of the resting-state networks.

Group independent component analysis (Calhoun et al., 2009), an extension of the traditional ICA (McKeown et al., 1998), was applied to fMRI data by using the Group ICA fMRI Toolbox (GIFT) (Calhoun et al., 2001) (http://icatb.sourceforge.net/). The GIFT software provides consistent resting state networks across multiple subjects and sessions.

Prior to ICA analysis, principal component analysis (PCA) was used to reduce data. The number of ICA components was set to 30 and the INFOMAX ICA algorithm was used, while the ICASSO analysis was used for ICA algorithm reliability determination. The independent components of single subjects were reconstructed using dual regression (spatial-temporal regression) method. In the first step of reconstruction, the aggregate component spatial maps were used as basic functions and projected onto each subject's original data resulting in the subject's component time-course. In the next step, the obtained time-course was used as basic function and projected onto the subject's original data resulting in the component spatial map for that subject (Rachakonda et al., 2007, Calhoun et al., 2009). As we used the intensity normalization during the pre-processing step of the data (at each voxel the time-series was scaled to a have a mean of 100), the aggregate components display arbitrary units, while the subjects' reconstructed data display the percent signal change.

ICA components were visualized using xjView toolbox (http://www.alivelearn.net/xjview), and ICAs corresponding to typical artifacts were excluded from further analysis. The remaining 16 components were assigned to specific RSN patterns as described in the related literature (Raichle 2011). Comparisons of the RSNs among the patient groups were carried out by two methods: (1) Binary logistic regression analysis of the expression scores for each network representing the similarity of the general pattern of the subject RSN to the overall RSN pattern

computed from the whole group of subjects, and (2) voxel-wise t-statistics carried out for each RSN between pairs of patient groups.

2.11.1.3 Logistic regression analyzes of the GIFT components

In order to illustrate the individual level of the RSN expression, the expression scores of the components in each subject were obtained by calculating the dot product of the subject's and group aggregate spatial maps, which yielded a scalar value that represents the similarity of each of the subject's RSNs to the global RSN pattern obtained from the whole group. The expression scores were fed into the forward stepwise conditional binary logistic regression analysis in SPSS software (21.0. Armonk, NY: IBM), and the combination of the ICs/RSNs that together best discriminate PDD from PD-MCI or PD-N patients and also PDD from the both of the other PD groups together (PD-non-demented) were identified.

Using the dot product in the logistic regression analysis allowed us to quantify the weight of each network in each subject's raw fMRI data in terms of an expression score for each RSN and testing the power of these scores in classifying the patients into correct groups without the need to define certain threshold values. Additionally, the quantification of each network expression in each subject with a single scalar value also allowed us to easily calculate correlation coefficients between the RSN expressions and various neuropsychological test scores.

2.11.1.4 Voxel-based comparison for functional connectivity

Additional to the binary logistic regression analysis, we performed whole-brain voxel-wise comparisons for the 16 RSNs in order to investigate the difference in functional connectivity between the patient groups. One- and two-sample t-tests were conducted on the back-reconstructed subject data using SPM stats implemented in GIFT toolbox (Ma et al., 2007, Calhoun et al., 2009).

In order to run the comparisons within the specific spatial extent of each network, an explicit mask of each network was created based on a one-sample t-test carried out on the reconstructed network maps of all subjects. Only voxels with a t value above 3 were included in the explicit mask. By this way, a common solution space was created for each network before the group comparisons are carried out by two sample t-tests with family-wise error (FWE) correction. The clusters obtained with an uncorrected height-threshold of $p < 0.001$

were compared between pairs of patient groups and clusters with cluster-level FWE-corrected $p < 0.05$ are reported.

2.11.2 Analysis of the Diffusion Tensor Imaging (DTI) Data

2.11.2.1 Processing of the DTI data

Preprocessing procedures for DTI analyses were carried out with FSL software (FMRIB Software Library v5.0, Oxford, UK) (Smith, 2004). Brain extraction for B0 images was performed using BET tool in FSL (Jenkinson et al., 2005). B0- and T2-weighted images were co-registered using the linear image registration tool of FSL (FLIRT) (Jenkinson and Smith, 2001; Jenkinson et al., 2002), and binary skull-free B0 masks were used to extract the brain from the co-registered T2 images. For the correction of susceptibility induced distortions, the brain extracted B0 and T2 images were fed together into the "Topup" tool of FSL (Andersson, 2003). The principle behind the Topup procedure is to estimate the susceptibility off-resonance field by using two (or more) acquisitions with different acquisition parameters such that the field distortions are different. Topup estimates the field, which when applied to the two images will maximize their similarity.

The two unwarped images output by the Topup tool were averaged and thresholded to obtain a binary mask to input to the "Eddy" tool of FSL (Jasper et al., 2016) in addition to the estimated off-resonance field image and diffusion weighted images in all diffusion directions. In addition to the susceptibility-induced distortions there are two more sources of artifacts in diffusion weighted images: eddy currents (EC) as a result of rapid switching of the diffusion weighting gradients and movements of the subject's head during the quite long diffusion protocol. Eddy tool corrects these three types of imaging artifacts and returns motion parameters, which can later be used to evaluate the significance of the differences of movement artifacts among the experimental groups. In the present study, the groups did not show any significant difference regarding motion parameters.

After visual inspection of the performed motion and deformation correction, we ran DTIfit in FDT (FMRIB's Diffusion Toolbox), a part of FSL (Behrens et al., 2003), for fitting the diffusion tensor model at each voxel. By this way, we obtained fractional anisotropy (FA) and mean diffusivity (MD) maps as well as the maps of the primary ($\lambda 1$), secondary ($\lambda 2$) and tertiary ($\lambda 3$) eigenvalues and corresponding unit eigenvectors. Main diffusion parameters are explained in the following formulae:

$$\mathrm{FA} = \sqrt{\frac{1}{2}} \times \frac{\sqrt{(\lambda_1 - \lambda_2)^2 + (\lambda_2 - \lambda_3)^2 + (\lambda_3 - \lambda_1)^2}}{\sqrt{\lambda_1^2 + \lambda_2^2 + \lambda_3^2}} \qquad \text{Eq. 1}$$

$$\mathrm{MD} = \frac{\lambda 1 + \lambda 2 + \lambda 3}{3} \qquad \text{Eq. 2}$$

$$\mathrm{AD} = \lambda 1 \qquad \text{Eq. 3}$$

$$RD = \frac{\lambda 2 + \lambda 3}{2} \qquad \text{Eq. 4}$$

As many patients, especially PDD patients, showed large ventricles and signs of atrophy, we chose the non-linear registration tool of FSL (FNIRT) (Andersson et al., 2007) for the registration of the subject FA maps to the 1x1x1mm^3 FMRIB58 FA template, which is in the same space as the MNI-152 standard image. We visually inspected the non-linear registration results of all subjects and identified 11 subjects with unsuccessful registration. For those patients, we performed another registration option as follows: the subjects were non-linearly registered to each other and the most representative subject, which displayed the least average difference from the rest of the subjects, was automatically chosen as the target. The chosen target image itself was then linearly affine registered to MNI-152 1x1x1 mm^3 standard space. After this step, each subject's FA image is nonlinearly transformed to the target and then affine transformed to the MNI-152 space. This type of registration is especially useful when working with WM images of patient groups, in which the large-scale changes of the brain anatomy complicates a reliable registration of each subject's image directly to the standard space. After controlling for correct registration, the same registration to the standard space was repeated for the MD and RD maps of each subject by using the subject's transformation matrix computed based on her/his FA map as described above.

2.11.2.2 Region of Interest (ROI) based analysis of the DTI parameters

For data analysis, the FA maps of all patients were averaged and voxels with intensity <0.2 in the obtained mean image were excluded in order to create a gray matter (GM) and cerebrospinal fluid (CSF) free study specific white-matter mask, as the FA values of GM and

CSF regions are usually below this value. The mask was binarized and multiplied with the Johns Hopkins University-International Consortium of Brain Mapping (JHU-ICBM) atlas containing 20 predefined white-matter tracts, in order to adapt these ROIs to our patient group. The included tracts were: anterior thalamic radiation L+R, corticospinal tract L+R, cingulum cingulate gyrus L+R, cingulum hippocampus L+R, forceps major, forceps minor, inferior fronto occipital fasciculus L+R, inferior longitudinal fasciculus L+R, superior longitudinal fasciculus L+R, uncinate fasciculus L+R, superior longitudinal fasciculus temporal part L+R.

The ROI-based analysis was carried out using the FSLstats tool. The atlas masked with the group-specific white-matter mask and the subjects' FA maps were fed into the FSLstats. The mean ± standard deviation of each subject's voxels within each ROIs were calculated and this process was repeated for MD, AD and RD values.

2.11.2.3 Statistical analysis of DTI data

For comparisons of the PD-N, PD-MCI and PDD groups one-way ANOVAs were first performed for FA values of each of the 20 ROIs with Bonferroni adjusted alpha ($p < 0.05/20=0.0025$). For the ROIs, that showed statistically significant FA differences among the 3 groups, further one-way ANOVAs were carried out for MD, AD and RD values with the same adjusted alpha ($p < 0.0025$) and post-hoc two-sample t-tests between pairs of patient groups (PDD vs PD-N, PDD vs PD-MCI and PD-MCI vs PD-N) corrected with a Bonferroni adjusted alpha for the number of pair-wise comparisons x number of significant results in the initial ANOVA of FA values.

2.11.3 Analysis of the Arterial Spin Labeling (ASL) based perfusion data

2.11.3.1 Processing of the ASL data

ASL-perfusion data were pre-processed and analyzed using a recently developed MATLAB-based program by Arslan and Öztürk-Işık (2016a and b). In order to calculate the cerebral blood flow (CBF) maps, the mean magnetization (M0) for each pixel of the control image (not labeled) was estimated by fitting multiple inversion time (Ti) data to the longitudinal relaxation equation. The perfusion image was calculated by subtracting the labeled from unlabeled ASL-MR images (deltaM). Together with the M0 and deltaM, the cerebral blood flow was estimated using the general kinetic model (Buxon et al., 1998).

Brain extraction was performed for the T2-weighted images using BET in FSL. The skull-free T2-weighted images were registered to the MNI-152 2x2x2 mm^3 brain standard space. As the non-registered T2 and CBF maps were initially in the same plane, the same transformation was also applied to the CBF maps during the linear registration process.

2.11.3.2 ROI-based analysis for ASL Data

We used a ROI-based approach for the analysis of difference in regional cerebral blood flow among the patient groups. Therefore, 70 (35 lateralized) predefined ROIs were extracted from the Harvard Cortical Structural Atlas (ROI size: max-prob-thr 0, $2mm^2$), and the mean intensity of the voxel within the ROIs was calculated.

2.11.4 Analysis of the Magnetic Resonance Spectroscopic Imaging (MRSI) Data

2.11.4.1 Pre-processing of the MRSI data

The MRSI data are expressed by the peak intensities and ratios of the seven prominent resonances of NAA at 2.0 ppm (parts per million), creatine (Cr) at 3.0 ppm, choline (Cho) at 3.2 ppm, glutamine/glutamate complex (Glx) at 2.3 ppm, GABA at 2.4 ppm, myo-inositol (mI) at 3.5 ppm and lactate + lipid at 1.3 ppm.

The quantification of total NAA (tNAA) and N-acetylaspartylglutamate (NAAG), total choline (tCho), myo-inositol (mI), total creatine (tCr), and glutamate/glutamine complex (Glx) of each voxel was performed using the LCModel (Provencher 2001), and the tCr values were used for the normalization of the metabolites. During the calculations of the LCmodel analyses, the metabolite concentrations exceeding %30 of the automatically estimated standard deviation of that specific metabolite resulted in exclusion of that value. These steps lead to three outputs providing an estimated spectrum, the calculated residual noise spectrum and the required baseline spectra for the fitting. Adapting a recently developed software by Cengiz and Öztürk-Işık (2016a and b) working in MATLAB environment, $1H^+$ MR spectroscopic peak parameter maps were created for each slice and overlaid on the single subject T2 weighted images. The overlaid parameter maps were fed into another script (Cengiz and Öztürk-Işık, 2016a and b), resulting in the linear registration (FLIRT) of the parameter maps to the MNI-152 standard brain in FSL.

2.11.4.2 ROI-based analyses for MRSI data

We used a ROI-based approach for the evaluation of MRSI data. As slice-size and slice number was limited for MRSI data, the number of ROIs was also limited. We chose 54 ROIs from the Harvard-Oxford Cortical Structural Atlas, the MNI Structural Atlas and the Harvard-Oxford Subcortical Structural Atlas that were covered by the restricted recording area. Independent samples t-test were performed for each of the NAA+NAAG/Cr, Cho/Cr, Glx/Cr and mI/Cr metabolite ratios of the voxel within the ROIs and compared for PDD vs PD-non-demented groups (PD-N and PD-MCI together).

2.11.5 Analysis of the Correlations between the MRI and clinical/neuropsychological variables

In order to associate the cognitive dysfunctions and motor symptoms of the PD patients with the functional, structural and perfusional MRI variables, one-tailed non-parametric (Spearman's) bivariate correlation analyses were carried out for the variables of each of these modalities that revealed significant differences among the three patient groups and the clinical and neuropsychological data collected from the 52 PD patients.

For Bonferroni correction, the clinical/neuropsychological variables were grouped into categories and based on the numbers of parameter in each category the alpha was adjusted: clinical data ($p < 0.05/5 = 0.01$; UPDRS-total, UPDRS-III, UPDRS-cognitive score, Hoehn & Yahr, GDS), global neuropsychological tests ($p < 0.05/7 = 0.0071$; MOCA, ACE-R total and from the ACE-R derived: semantic fluency, phonemic fluency, pentagon copying, cube copying, clock drawing,) and specific neuropsychological tests ($p < 0.05/7 = 0.0071$; Stroop-mistakes and Stroop-effect, SDMT-total and SDMT-correct, WCST-category and WCST-error, JOLO).

2.11.6 Testing the Performance of Multimodal MRI Variables for the Discrimination of the PDD Patients by Discriminant Analysis

The variables of the rs-fMRI, DTI and ASL modalities that when tested in a single modality resulted in significant differences between the PD patient groups were fed stepwise into a discriminant analysis in order to test the efficiency of a multimodal MRI based classification of PD cases into PDD and one of the PD-N or PD-MCI subgroups. This is carried out by testing the

performance of a discriminant function on PD-N & PDD groups or PD-MCI & PDD groups by stepwise entering the variables from rs-fMRI, DTI and ASL modalities for the classification of the cases to one of the two groups with leave-one-out cross-validation. For this purpose, the significant expression scores of the RSNs, mean values of the FA, MD, RD and AD in the DTI ROIs and mean CBF values obtained from the ROIs of the ASL measurements that resulted in significant group differences in variance analyses among the three groups are included in a stepwise manner in the discriminant analysis and the sensitivity and specificity of the resulting discriminant functions in dissociating the PDD patients from PD-N or PD-MCI groups are reported.

3 RESULTS

3.1 Demographic data

Initially, we collected the data of 60 PD patients (PD-N=20, PD-MCI=20, PDD=20). Because the patient groups differed significantly regarding age, and age is known to be a major risk factor for PDD, we created age matched patient groups for the final data analysis. The final data set was composed of 16 PD-N, 18 PD-MCI and 18 PDD patients (Table 3-1), which according to the one-way ANOVA test did not show any significant difference regarding age (p = 0.121), but displayed a significant difference between PD-N and PDD groups regarding years of education (p = 0.024), while PD-N vs PD-MCI and PD-MCI vs PDD comparisons revealed no significant differences in terms of educational years (Table 3-2). As education is expected mainly to play a role in terms of cognitive symptoms and the PD-MCI and PDD groups were almost identical regarding education, we did not reduce the amount of data further to equalize the education among PD-N and PDD groups.

Table 3-1: Definition of the final patient groups and their respective mean age and education in years

Initial group (n=60)	**PD-N** ***M*** ± ***sd***	**PD-MCI** ***M*** ± ***sd***	**PDD** ***M*** ± ***sd***	***ANOVA*** ***F***	***p***
Age	65.65 ± 6.9 (56 – 81)	70.25 ± 5.1 (63 – 79)	72.55 ± 5.5 (63 – 85)	*F (2,57)* = 7.102	0.002
Education	9.65 ± 4.2	8.05 ± 4.2	6.7 ± 4.0	*F (2,57)* = 2.580	0.085
Female, Male	9, 11	3, 17	7, 13	-	-
Age matched (n=52)	**PD-N**	**PD-MCI**	**PDD**	***F***	***p***
Age	67.8 ± 5.9 (59 – 81)	69.3 ± 4.5 (63 – 77)	71.3 ± 4.3 (63 – 78)	*F (2,49)* = 2.21	0.121
Education	10.81 ± 3.8	8.06 ± 4.3	6.89 ± 4.2	*F (2,49)* = 4.00	0.025
Female, Male	7, 9	3, 15	5, 13	-	-

Remarks: p < 0.05

Table 3-2: Bonferroni corrected (3 groups) multiple comparison results for age and education after age matching (n=52)

	PD-N vs PD-MCI	**PD-N vs PDD**	**PD-MCI vs PDD**
	p	*p*	*p*
Age	1.000	0.126	0.682
Education	0.171	0.024	1.000

Remarks: p < 0.05

3.2 Clinical characteristics of the patient groups

The statistical comparison of the clinical characteristics revealed significantly longer disease duration (*overall: p* = 0.003) for the PDD group (10.8 ± 7.7 yrs.) compared to PD-N (4.9 ± 2.9 yrs.) (*p* = 0.005) and PD-MCI (5.8 ± 3.2 yrs.) (*p* = 0.018) but not between PD-N and PD-MCI (*p* = 1.0). All three patient groups differed significantly from each other in the total score of the UPDRS (*p* < 0.001). Post-hoc tests showed higher UPDRS score for PDD group compared to the PD-N (*p* < 0.001) and for PDD vs PD-MCI groups (*p* < 0.001). UPDRS part III also differed significantly among the three patient groups (*p* < 0.001) with higher scores for PDD vs PD-N (*p* < 0.001) and PDD vs PD-MCI (*p* = 0.004). Motor dysfunction as indicated by the Hoehn & Yahr scale also showed a significant overall group effect (*p* < 0.001), which stemmed from significantly more severe motor symptoms of the PDD group compared to PD-N (*p* < 0.001) and PD-MCI (*p* < 0.001) groups. The cognitive status reflected by UPDRS cognitive scores significantly differed among the patient groups (*p* < 0.001), where PDD patients obtained significantly higher scores when compared to PD-N (*p* < 0.001) and PD-MCI groups (*p* < 0.001) (Table 3-3, Table 3-4).

Table 3-3: Clinical characteristics of the final patient groups and one-way ANOVA

	PD-N n=16	**PD-MCI** n=18	**PDD** n=18	***One-way ANOVA***	
	M* ± *sd	***M* ± *sd***	***M* ± *sd***	***F***	***p***
Disease Duration (yrs.) [a)]	4.88 ± 2.87	5.83 ± 3.2	10.78 ± 7.67	*F* (2,49) = 6.61	0.003
UPDRS total [b)]	40.19 ± 12.76	56.72 ± 22.6	103.72 ± 38.65	*F* (2,49) = 25.244	0.000
UPDRS Part III [b)]	23.06 ± 8.59	33.67 ± 13.34	51.83 ± 22.56	*F* (2,49) = 13.917	0.000
UPDRS Cognitive Score [b)]	0.94 ± 0.99	1.39 1.04	3.61 ± 0.61	*F* (2,49) = 44.35	0.000
Hoehn & Yahr [a)]	1.69 ± 0.6	1.89 ± 0.47	3 ± 1.09	*F* (2,49) = 14.640	0.000

Remark: [a)]: p < 0.05; [b)]: adjusted alpha p < 0.05/3= 0.017.

Table 3-4: Post-Hoc - Bonferroni corrected (3 groups) multiple comparison results

	PD-N vs PD-MCI	**PD vs PDD**	**PD-MCI vs PDD**
	p	*p*	*p*
Disease Duration (yrs.) [a)]	1.000	0.005	0.018
UPDRS total [b)]	0.253	0.000	0.000
UPDRS Part III [b)]	0.186	0.004	0.000
UPDRS Cognitive Score [b)]	0.449	0.000	0.000
Hoehn & Yahr [a)]	1.000	0.000	0.000

Remark: [a)]: p < 0.05; [b)]: adjusted alpha p < 0.05/3 = 0.017.

3.3 Psychiatric/Psychological tests

The patient groups were tested for signs of major depression (exclusion criteria), anxiety, apathy and obsessive-compulsive behavior using the Geriatric depression scale (GDS), Beck Anxiety Inventory (BAI), Yale-Brown Obsessive Compulsive Scale (Y-BOCS), and Apathy Evaluation Scale (AES). The mean scores were statistically compared among the patient groups using one-way ANOVA and Bonferroni corrected independent t - test ($p < 0.05$) in the post-hoc test. The groups differed significantly in the GDS ($p= 0.002$) stemming from higher scores of the PDD compared to PD-N ($p = 0.005$) and PD-MCI ($p = 0.005$). Importantly, the groups did not show signs of major depression, as we used a cut-off of > 16 as an exclusion criterion. The groups further differed significantly regarding apathy symptoms ($p = 0.022$), stemming from stronger apathy signs in the PDD patients compared to the PD-N group ($p = 0.034$) (Table 3-5). There were no significant differences regarding signs of anxiety or obsessive-compulsive behavior.

Table 3-5: Summary of the psychiatric evaluation of the patient groups

					One-way ANOVA		**Post-hoc**	
Test	**Group**	***n***	***M***	***sd***	***F***	***p***	***Contrast***	***p***
GDS	PD-N	16	5.31	3.701	F (2,48) = 7.349	0.002	PD-N vs PD-MCI:	1.0
	PD-MCI	18	5.33	3.236			PD-N vs PDD:	0.006
	PDD	17	10.00	5.160			PD-MCI vs PDD:	0.005
AES	PD-N	12	61.92	2.906	F (2,41) = 4.189	0.022	PD-N vs PD-MCI:	1.0
	PD-MCI	16	60.19	5.683			PD-N vs PDD:	0.034
	PDD	16	53.81	11.680			PD-MCI vs PDD:	0.089
BAI	PD-N	12	5.50	4.739	F (2,40) = 2.797	0.073	-	
	PD-MCI	16	6.13	4.815				
	PDD	15	9.93	6.464				
Y-BOCS	PD-N	12	1.58	4.274	F (2,40) = 0.966	0.389	-	
	PD-MCI	16	0.25	0.775				
	PDD	15	0.93	1.792				

Remarks: p < 0.05; Geriatric depression scale (GDS), Beck Anxiety Inventory (BAI), Yale-Brown Obsessive Compulsive Scale (Y-BOCS), Apathy Evaluation Scale (AES).

3.4 Drug treatment of the patient groups

The respective drug treatment of the three patient groups is displayed in the Table 3-6. While the usage of anti-parkinsonian drugs was quite balanced across the patient groups regarding their active substances, the PDD group mostly differed from the PD-N and PD-MCI in the treatment against cognitive symptoms (acetylcholinesterase inhibitors) and the usage of anti-psychotic drugs (quetiapine, clozapine).

Table 3-6: PD-related and neuropsychiatric drugs used in the patient groups

Drug-type	Active substance	PD-N	PD-MCI	PDD
Acetylcholinesterase inhibitors (Dementia symptoms)	Rivastigmine, donepezil	0	0	12
Antidepressants	Citalopram, escitalopram, sertraline, venlafaxine	6	5	8
Antipsychotics	Seroquel (quetiapine), Lithium, Leponex (clozapine)	0	0	7
Monoamine oxidase (MAO)-B inhibitors	Nervogil and Azilect (rasagiline)	8	12	3
L-amino acid decarboxylase / DOPA decarboxylase inhibitor	Madopar (benserazide)	4	10	12
L-Dopa (levodopa)	Madopar - HBS (benserazide + L-Dopa (L-3.4-dihydroxyphenylalanine))	1	3	3
	Stalevo (entacapone/ L-Dopa/ carbidopa (lodosyn))	8	4	4
	Sinemet (carbidopa, L-Dopa)	1	2	1
	Total L-Dopa	10	9	8
Catechol-O -methyl transferase inhibitor	Comtan (entacapone)	1	2	0
Dopamine - Agonists	Pexola (pramipexol)	4	7	3
	Trivastal (piribedil)	1	1	1
	Apo-go (apomorphine)	0	0	2
	Requip (ropinirole)	2	0	0
	Total DA-Agonist	7	8	6
NMDA-blocker (indirect DA-agonist)	PK-Merz (amantadine)	4	5	2
Anti-cholinergic	Sormodren (bornaprin)	1	0	0

Remarks: Displayed in number of patients.

3.5 Neuropsychological data

All patients underwent a comprehensive neuropsychological investigation, and the PD-MCI diagnosis was based on the level I criteria (see introduction and methods).

All patients completed the ACE-R test (including verbal fluency, pentagon copying, cube copying, clock drawing) and MMSE test. One PDD patient did not finish primary school, thus a special version of the MMSE was applied. That particular patient still completed ACE-R test, but not the JOLO, Stroop, SDMT, Navon and WCST. Beyond this subject, several tests couldn't be administered to some patient's due to severe cognitive deficits.

Precisely, six additional PDD patients were not able to perform the Stroop, 11 PDD patients were not able to complete the WCST, 2 PDD patients could not finish the MOCA and 9 PDD patients did not understand the SDMT during the training part of the SDMT. Six PDD patients did not succeed in the training part of the JOLO, thus did not finish the test.

The MOCA was not applied to 1 PDD, 4 PD-N and 3 PD-MCI patients, and Navon was not administered to 3 PDD, 4 PD-N and 3 PD-MCI cases. Hence, various subsets of patient groups were statistically compared for the respective tests.

All NPTs were statistically evaluated using the one-way ANOVA test (Table 3-7). For significant tests the Bonferroni corrected multiple comparison results were inspected and a significance level of either $p < 0.05$ (independent tests such as ACE-R) or the Bonferroni adjusted alpha (dependent tests, e.g. different values for WCST) were reported (Table 3-8). The initial alpha ($p < 0.05$) was adjusted for the number of variables in dependent tests, according Bonferroni method (e.g. WCST: $p < 0.05/3 = 0.017$).

3.5.1 Global tests

The patient groups differed significantly between each other according the ACE-R (overall: $p < 0.001$) with lower scores for PD-MCI vs PD-N ($p = 0.013$), PDD vs PD-N ($p < 0.001$) and for PDD vs PD-MCI ($p < 0.001$) (Table 3-7 and Table 3-8).

While the PD-N and PD-MCI did not differ significantly for the MMSE ($p = 0.936$), the PDD scored significantly worse compared to PD-N ($p < 0.001$) and to PD-MCI ($p < 0.001$).

Additionally, the groups differed for the MOCA test performance ($p < 0.001$), with PD-MCI being worse than PD-N ($p = 0.039$) and PDD being worse than PD-N ($p < 0.001$) and PD-MCI ($p < 0.001$).

3.5.2 Test for visuo-spatial functions

3.5.2.1 Benton Judgement of Line Orientation Test - JOLO

The patient groups differed significantly in the JOLO test ($p < 0.001$) stemming from a significantly worse performance of the PDD compared to PD-N ($p < 0.001$). The PDD vs PD-MCI ($p = 0.092$) and PD-MCI vs PD-N ($p = 0.052$) comparison were not significant (Table 3-8).

3.5.2.2 Figure copying

In the pentagon copying test (overall: $p < 0.001$) the PDD scored significantly less compared to PD-N ($p < 0.001$) and PD-MCI ($p < 0.001$), but PD-N and PD-MCI did not show any difference ($p = 1.0$). The PDD also showed significantly lower abilities in the cube copying compared to PD-N ($p < 0.001$) and PD-MCI ($p = 0.035$), but the PD-MCI and PD-N did not differ significantly from each other ($p = 0.0157$) (Table 3-8).

3.5.2.3 Navon

Two PDD patients showed signs of simultanagnosia, but the patient groups did not differ significantly regarding their performance in the Navon test ($p = 0.166$).

3.5.2.4 Clock drawing

In the clock drawing tests ($p < 0.001$) the PDD group showed significantly lower abilities compared to PD-N ($p < 0.001$) and PD-MCI ($p < 0.001$), while there was no significant difference between PD-N and PD-MCI ($p = 0.873$) (Table 3-8).

3.5.3 Tests for executive functions

3.5.3.1 Stroop

In the Stroop test, the patient groups differed significantly regarding the number of mistakes ($p < 0.001$) and the time difference ($p = 0.016$) but not regarding the amount of spontaneous corrections ($p = 0.543$) (Table 3-7). The PDD made significantly more mistakes than the PD-N ($p < 0.001$) and PD-MCI ($p < 0.001$) but the overall Stroop effect did not survive the Bonferroni corrected group comparison and using Bonferroni adjusted alpha ($p < 0.017$) (PD-MCI vs PD-N: $p = 0.055$, PDD vs PD-N: $p = 0.030$, PDD vs PD-MCI: $p = 1.0$) (Table 3-8).

3.5.3.2 Wisconsin Card Sorting Test - WCST

The three groups did not differ for the % of perseverative errors in the WCST (p = 0.147) but showed significant difference for both, the number of categories and number total errors ($p < 0.001$) (Table 3-7). While, the PD-MCI and PDD did not differ significantly regarding their performance in the number of completed categories (p = 0.669) and the total number of errors (p = 0.826), the PD-MCI and PDD completed significantly less categories compared to PD-N (PD-MCI vs PD-N: p = 0.002, PDD vs PD-N: p = 0.001). The PDD and PD-MCI also made significantly more errors in the WCST than PD-N (PD-MCI vs PD-N: p =0.003, PDD vs PD-N: p = 0.002) (Table 3-8).

3.5.3.3 Verbal fluency

The PD-N were significantly better in phonemic fluency when compared to PD-MCI (p = 0.017) and PDD ($p < 0.001$) but there was no difference for PD-MCI vs PDD (p = 0.101) (Table 3-8).
PDD showed worse performance in the semantic fluency test compared to PD-N ($p < 0.001$) and PD-MCI ($p < 0.001$), while PD-N compared to PD-MCI did not show any significant difference (p = 0.414) (Table 3-8).

3.5.3.4 SDMT

The overall statistical comparison of the SDMT scores demonstrated significant difference between the study groups regarding the total number of answers ($p < 0.001$) and the number of correct answers ($p < 0.001$). While there was no difference between PDD and PD-MCI ($p > 0.025$), the PD-MCI showed significantly worse performance than the PD-N group (number of answers*:* $p < 0.001$, correct answers: $p < 0.001$) and PDD was also significantly worse than PD-N (number of answers*:* $p < 0.001$, correct answers: $p < 0.001$) (Table 3-8).

Table 3-7: The mean and standard deviation for all conducted neuropsychological tests and one-way ANOVA results

	PD-N n=16	**PD-MCI n=18**	**PDD n=18**	***One-way ANOVA***	
	M* ± *sd	***M* ± *sd***	***M* ± *sd***	***F***	***p***
ACE-R (100) [a)]	88.63 ± 3.56	77.28 ± 5.39	56.5 ± 17.59	*F* (2,49) = 37.57	0.000
MMSE (30) [a)]	29.19 ± 0.83	28.17 ± 1.54	21.72 ± 4.62	*F* (2,49) = 33.88	0.000
Phonemic fluency (7) [a)]	5.0 ± 1.1	3.56 ±1.29	2.5 ±1.82	*F* (2,49) = 12.64	0.000
Semantic fluency (7) [a)]	5.44 ± 1.41	4.67 ± 1.37	2.17 ±1.66	*F* (2,49) = 22.93	0.000
Pentagon copy (1) [a)]	0.94 ± 0.25	0.83 ± 0.38	0.11 ± 0.32	*F* (2,49) = 33.32	0.000
Cube copy (2) [a)]	1.69 ± 0.60	1.17 ± 0.86	0.5 ± 0.79	*F* (2,49) = 10.41	0.000
Clock Drawing (5) [a)]	4.56 ± 0.81	4.11 ± 1.02	1.83 ± 1.65	*F* (2,49) = 24.66	0.000
	n=12	**n=15**	**n=14**		
MOCA (30) [a)]	25.25 ± 1.96	21.73 ± 2.76	14.14 ± 4,89	*F* (2,38) = 35.24	0.000
	n=16	**n=18**	**n=11**		
JOLO (30) [a)]	24.19 ± 3.71	19.33 ± 6.04	14.46 ± 7.33	*F* (2,42) = 9.64	0.000
	n=12	**n=15**	**n=14**		
Navon (2) [a)]	1.83 ± 0.39	1.93 ± 0.26	1.57 ± 0.76	*F* (2,38) = 1.89	0.166
Stroop [b)]	**n=16**	**n=18**	**n=11**		
Mistakes	0.38 ± 1.03	1.61 ± 3.05	24.55 ± 18.92	*F* (2,42) = 25.78	0.000
Spontan. correction	3 ± 3.62	4.44 ± 3.91	3.91 ± 3.86	*F* (2,42) = 0.62	0.543
Time diff. in s	59.19 ± 15.36	92.94 ± 43.51	101.46 ± 56.35	*F* (2,42) = 4.54	0.016
WCST [b)]	**n=16**	**n=18**	**n=6**		
Categories	4.38 ± 1.96	2.28 ± 1.27	1.33 ± 1.51	*F* (2,37) = 10.77	0.000
Perseverative error %	20.86 ± 10.19	28.73 ± 10.75	29.43 ± 20.92	*F (2,37)* = 2.02	0.147
Error	42.31 ± 21 89	64.39 ± 15.04	73.67 ± 11.45	*F* (2,37) = 9.65	0.000
SDMT [c)]	**n=16**	**n=18**	**n=8**		
Total	31.19 ± 10.34	16.89 ± 7.08	13 ± 6.72	*F* (2,39) = 17.32	0.000
Correct	30.63 ± 10.53	15.11 ± 7.79	11.25 ± 6.52	*F* (2,39) = 18.54	0.000

Remark: [a)] $p < 0.05$, [b)] $p < 0.05/3 = 0.017$, [c)] $p < 0.05/2 = 0.025$.

Table 3-8: Bonferroni corrected (3 groups) multiple comparison results

	PD-N vs PD-MCI	**PD-N vs PDD**	**PD-MCI vs PDD**
	p	***p***	***p***
ACE-R [a)]	0.013	0.000	0.000
MMSE [a)]	0.936	0.000	0.000
Semantic fluency [a)]	0.414	0.000	0.000
Phonemic fluency [a)]	0.017	0.000	0.101
Pentagon copy [a)]	1.0	0.000	0.000
Cube copy [a)]	0.157	0.000	0.035
Clock Drawing [a)]	0.873	0.000	0.000
MOCA [a)]	0.039	0.000	0.000
JOLO [a)]	0.052	0.000	0.092
Navon [a)]	1.0	0.608	0.197
Stroop [b)]			
Mistakes	1.0	0.000	0.000
Spontaneous correction	0.823	1.000	1.00
Time diff. in s	0.055	0.030	1.0
WCST [b)]			
Categories	0.002	0.001	0.669
Perseverative error %	0.219	0.474	1.00
Error	0.003	0.002	0.826
SDMT [c)]			
Total	0.000	0.000	0.853
Correct	0.000	0.000	0.918

Remark: [a)] $p < 0.05$, [b)] $p < 0.05/3 = 0.017$, [c)] $p < 0.05/2 = 0.025$.

3.6 MR-DATA

3.6.1 Group Independent Component Analysis of the rs-fMRI Data

30 independent components (IC) were obtained using the group independent component analysis. After visual inspection and artifact rejection 16 ICs that best resembled the well-established RSNs in the literature were chosen for further analysis: somato-motor network (3 sub-components: SM1, L-SM2 and R-SM2), visual network (2 components: medial and lateral visual cortices), posterior- temporal network (PTN), salience network (SN), limbic network (LN), left and right fronto-parietal networks (L-FPN and R-FPN), dorsal attention network (DAN), parahippocampal network, thalamus, frontostriatal network (FSN), cerebellar network (CN) and the default mode network (DMN) (Figure 3-1).

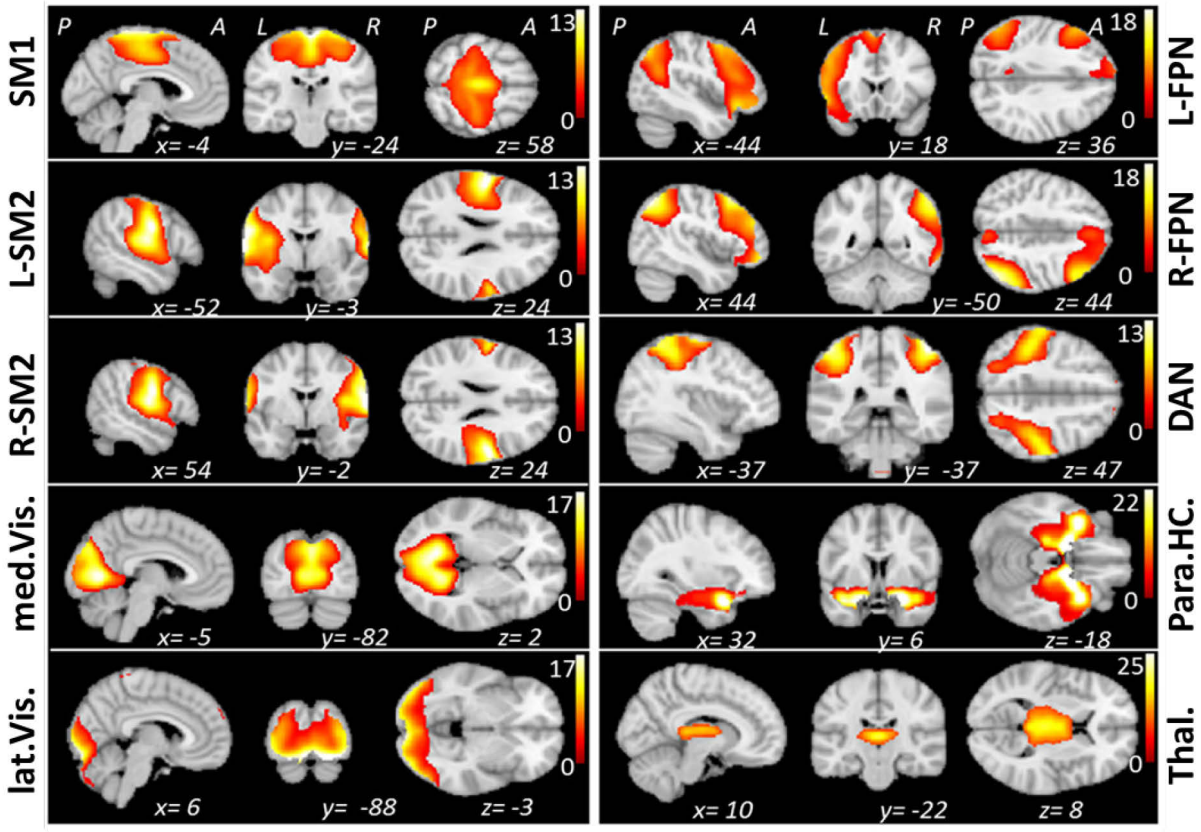

Figure 3 -1: Identified ICs as output of the Group Independent Component Analysis. Figure continues on next page.

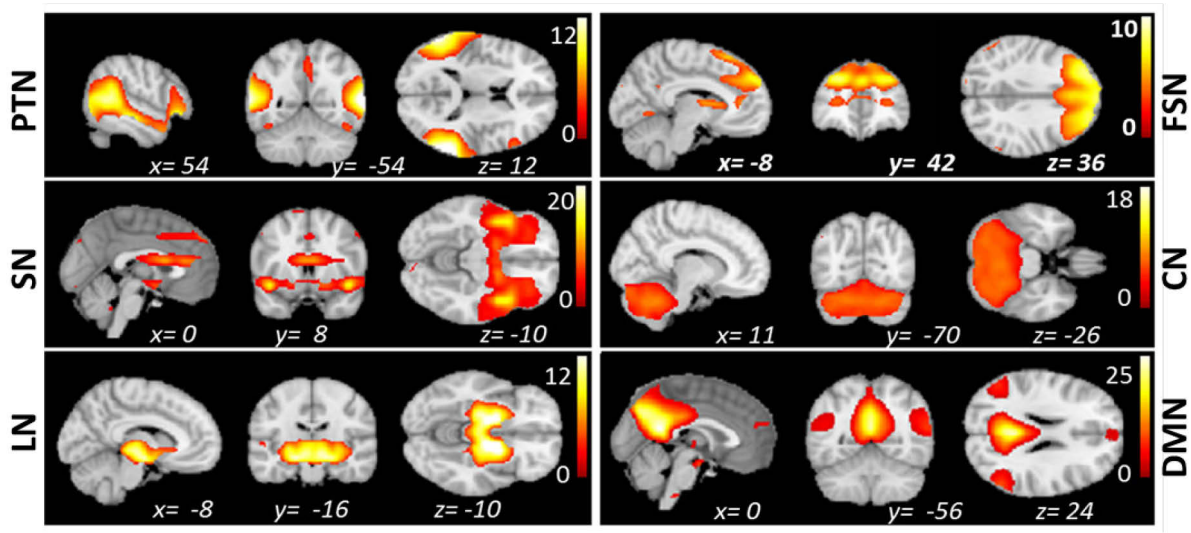

Figure 3-1: Identified ICs as output of the Group Independent Component Analysis. The RSNs are displayed overlaid on the average MNI-152 T1 weighted brain extracted standard template (average anatomic image of 152 person) and the respective MNI coordinates are shown under each picture. The color coding represents the relative contribution of each voxel to the specific independent component. The following RSNs are displayed: PTN: Posterior-temporal network, SN: Salience network, LN: limbic network, DMN: Default mode network, CN: Cerebellar network, FSN: Frontostriatal network, FPN: Frontoparietal network, med.Vis. and lat.Vis.: medial and lateral visual network, SM1 and SM2: Somato-motor networks, DAN: Dorsal attention network, parahippocampal network and thalamus.

3.6.1.1 LOGISTIC REGRESSION ANALYSIS for NETWORK EXPRESSION

The expression scores of the 16 RSNs in each subject were obtained by calculating the dot product of the subject's and mean group spatial maps, and fed into the forward stepwise conditional binary logistic regression analysis in order to identify the combination of the RSNs that based on their expression level best discriminated PDD from other PD patients. For this purpose, the following pairs of groups were separately analyzed with binary logistic regression: PD-N vs PDD, PD-MCI vs PDD, PD-non-demented (PD-N+PD-MCI) vs PDD and PD-N vs PD-MCI.

In order to visualize the relative weights of the discriminative RSNs in each patient group, the means of the subjects back-reconstructed images are displayed in Figure 3-2, Figure 3-3 and Figure 3-4 for each component that significantly contributed to the logistic regression model.

PD-N vs PDD

The logistic regression showed that the combination of the salience NW, the limbic NW, the frontostriatal NW and posterior DMN together in this order was successful in discriminating the PD-N from PDD ($\chi^2 = 26.69$, df=4, $p < 0.001$) with an overall accuracy of 85.3% (83.3-87.5%) with the final model ($R^2 = 0.726$). The mean expression of these networks is displayed in Figure 3-2. While, the expression scores of the limbic NW and frontostriatal NW were lower in PDD compared to PD-N, the expression scores of the DMN and salience NW were higher for the PDD group. The mean and range of the effect size (odds ratio) of the corresponding networks are: salience NW: 18.666 (1.436-242.564, $p = 0.025$), limbic NW: 0.007 (0.0-0.754, $p = 0.038$), frontostriatal NW: 0.004 (0.0-0.486, $p = 0.025$), posterior DMN: 5.737 (0.946-34.782, $p = 0.057$) (Figure 3-2).

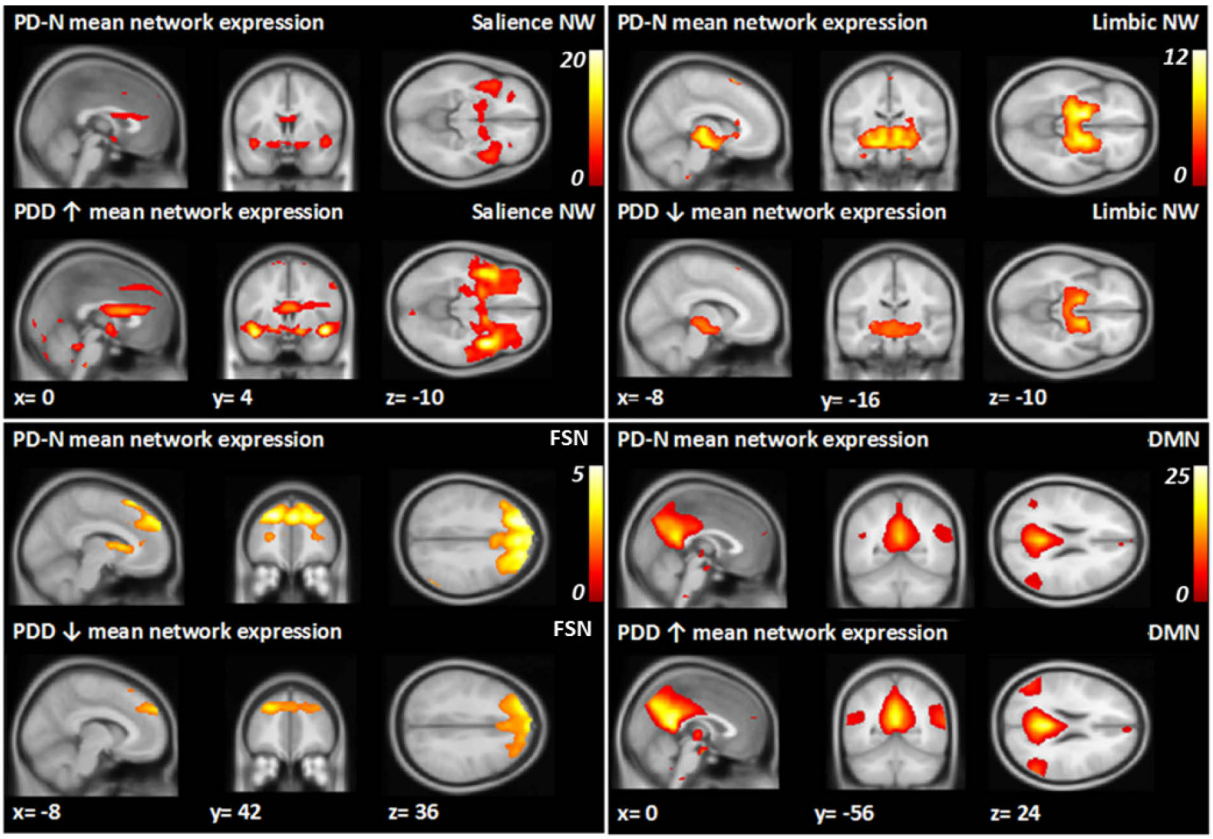

Figure 3-2: The group means of the salience NW, the limbic NW, the frontostriatal NW and the DMN in the PD-N and PDD are displayed on the MNI-152 T1 weighted standard template and the respective MNI coordinates are shown below each picture. The color coding represents % signal change.

PD-MCI vs PDD

When comparing the PD-MCI and PDD, the logistic regression showed, that the limbic NW, the DMN and posterior temporal NW together where most successful in discriminating these groups (χ^2 = 21.009, df=3, p < 0.001) with an overall correct prediction of 83.3% (83.3% and 83.3%) for the final model (R^2 = 0.589). The mean expression of these networks is displayed in Figure 3-3. Compared to PD-MCI, the PDD group expressed a stronger DMN but weaker limbic NW and posterior temporal NW connectivity. The effect size (odds ratio) of the corresponding networks are: DMN: 7.473 (1.371-40.721, p = 0.02), the limbic NW: 0.01 (0.0-0.269, p = 0.006) and the posterior temporal NW: 0.117 (0.01-1.133, p = 0.064) (Figure 3-3).

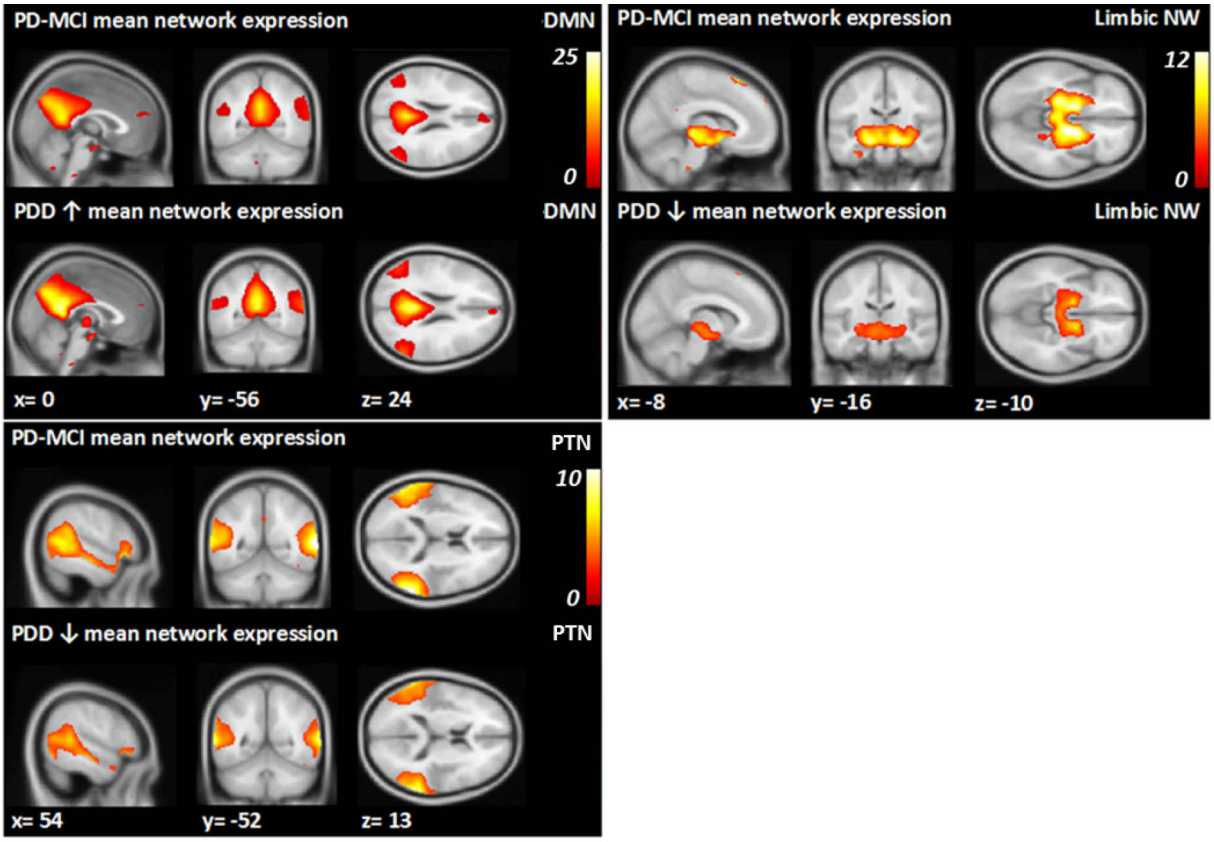

Figure 3-3: The means of the DMN, the limbic NW and the posterior temporal NW in the PD-MCI and PDD groups are displayed superimposed on the MNI-152 T1 weighted template and the respective MNI coordinates are shown below each picture. The color coding represents % signal change.

PD-non-demented vs PDD

When the PD-N and PD-MCI together were tested against the PDD, the logistic regression showed an overall correct prediction of 84.6% (77.8-88.2%) (R^2= 0.593) in the final model that included the limbic NW, DMN, frontostriatal NW and salience NW (χ^2 = 29.208, df=4, $p < 0.001$). The mean expression of these networks is displayed in Figure 3-4. The limbic and frontostriatal NW showed lower expression scores for the PDD, while the expression scores for the posterior DMN and salience NW were increased in PDD. The effect sizes (odds ratio) of the corresponding networks are: limbic NW: 0.024 (0.001-0.373, p = 0.008), frontostriatal NW: 0.028 (0.001-0.515, p = 0.016), DMN: 3.377 (0.933-12.219, p = 0.064), salience NW: 4.130 (0.983-17.357, p = 0.053) (Figure 3-4).

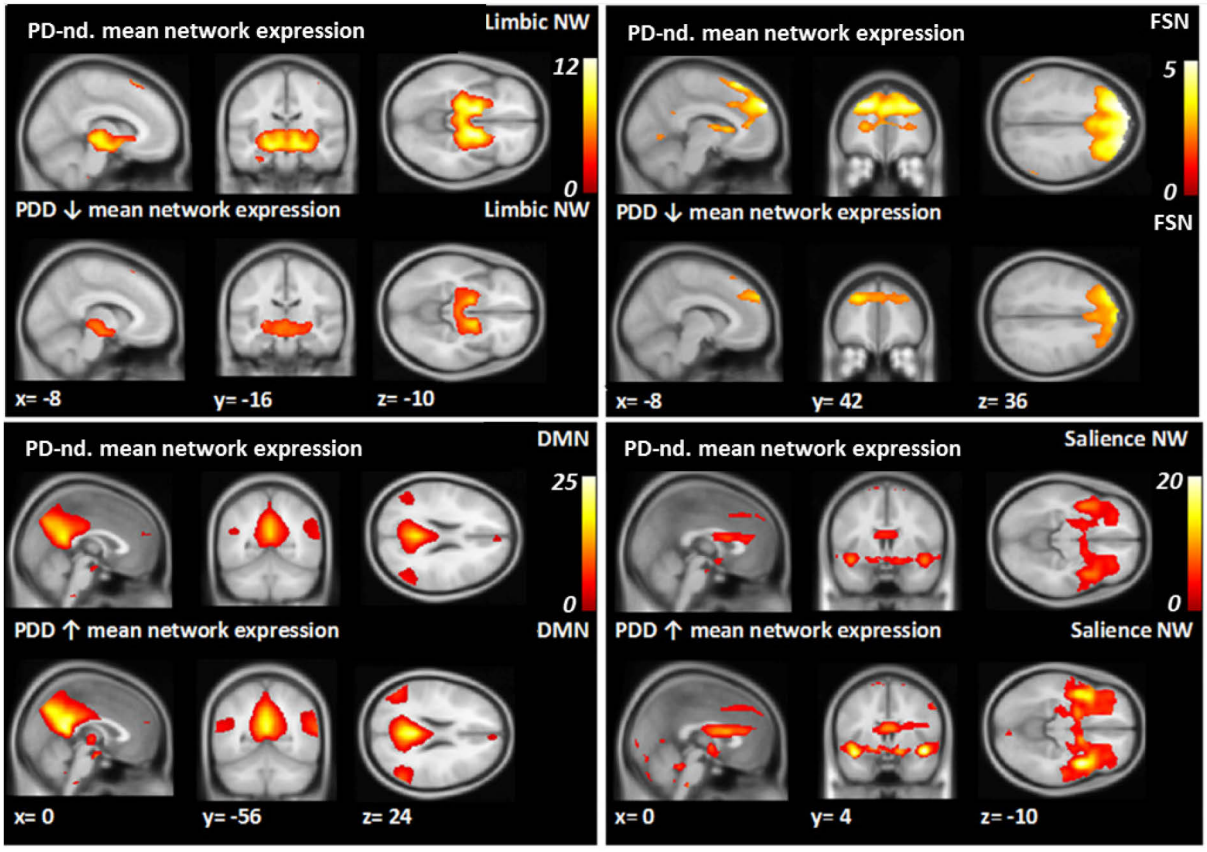

Figure 3-4: The group means of the limbic NW, DMN, frontostriatal NW and salience NW in the PD-non-demented (PD-nd.) and PDD groups are displayed superimposed on the MNI-152 T1 weighted standard template, and the respective MNI coordinates are shown below each picture. The color coding represents % signal change.

PD-N vs PD-MCI

The logistic regression analysis did not reveal any significant difference in network expression levels between the PD-N and PD-MCI. However, the two important RSNs, DMN and SN, that showed significant effect in the regression model between the PDD and PD-non-demented groups actually showed a progressive increase in intrinsic functional connectivity from PD-N through PD-MCI and PDD, that is along the progression of the cognitive decline (Figure 3-5).

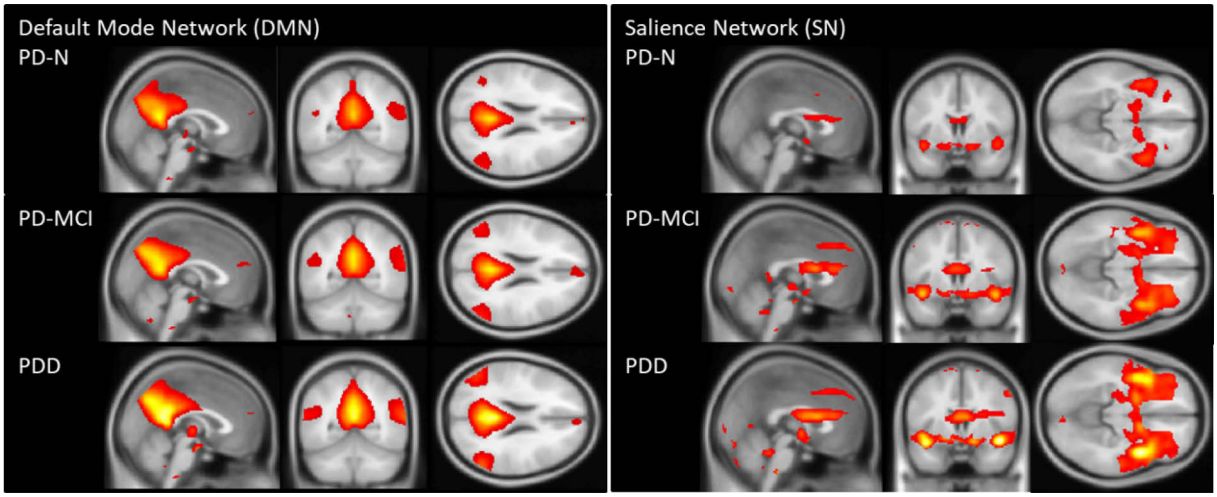

Figure 3-5: The group means of the default mode network (DMN) and salience network (SN) in the three PD groups are displayed superimposed on the MNI-152 T1 weighted standard template. The color coding represents % signal change.

3.6.1.2 VOXEL-BASED COMPARISON for FUNCTIONAL CONNECTIVITY

While we used the logistic regression analysis on the expression scores of the networks for the evaluation of the discriminative power of the overall network pattern between the patient groups, in a second step we also applied voxel-based two sample t-test comparisons as implemented in the second-level analysis module of the SPM8 software in order to determine the specific regions of each network that show the strongest intrinsic connectivity difference between different patient groups. We tested the following contrasts: PD-N vs PDD, PD-MCI vs PDD, PD-non-demented vs PDD and PD-N vs PD-MCI.

In order to run the comparisons within the specific spatial extent of each network, explicit mask of each network was created based on a one-sample t-test carried out on the reconstructed network maps of all subjects. Only voxels with a t value above 3 were included in the explicit mask. By this way, a common solution space was created for each network

before the group comparisons are carried out by two sample t-tests with family-wise error (FWE) correction. The clusters obtained with an uncorrected height-threshold of $p < 0.001$ were compared between pairs of patient groups and clusters with cluster-level FWE-corrected $p < 0.05$ are reported.

The PD-N vs PDD

Complementary to the results of the binary logistic regression analysis, we found locally significant differences in the functional connectivity of the limbic NW and salience NW between PD-N and PDD.

Limbic Network

Compared to PD-N, PDD showed significantly reduced functional connectivity ($p = 0.027$) in a cluster of 206 voxels in the limbic NW with peak coordinates in the right thalamus (12 -14 4). The cluster also included the lentiform nucleus and putamen (Figure 3-6).

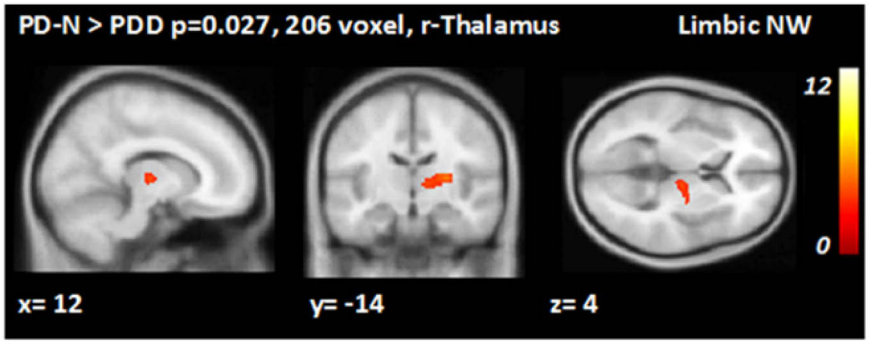

Figure 3-6: Significant cluster of decreased functional connectivity in the right thalamus of the limbic NW in PDD compared to PD-N.

Salience Network - SN

Other than in the limbic NW, we found increased functional connectivity in two clusters of the salience NW in the PDD group compared to PD-N (Figure 3-7). One significant cluster ($p = 0.046$) composed of 147 voxels covers mainly extra nuclear space and cingulum in addition to a small portion of the caudate body. The other cluster with a FWE-corrected p value close to significance ($p = 0.056$) of 137 voxels was in the right insula (peak) and included also parts of the superior temporal gyrus.

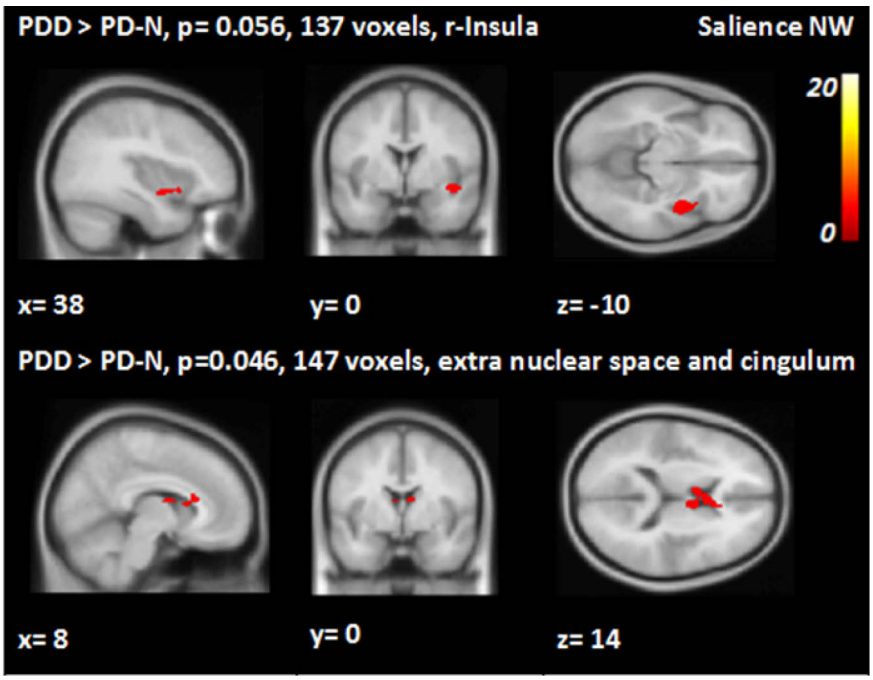

Figure 3-7: Two significant clusters of increased functional connectivity in the right insula and extra- nuclear space within the salience NW of PDD compared to PD-N patients.

PD-MCI vs PDD

As in the binary logistic regression analysis, we found significant differences in the functional connectivity within the limbic network between PDD and PD-MCI using the voxel-wise comparison method.

Limbic Network

Compared to PD-MCI, PDD showed significantly reduced functional connectivity in two different clusters: one significant cluster (p = 0.004) of 312 voxels with its peak in the left hippocampus and another significant cluster (p = 0.014) of 233 voxels with its peak in the right hippocampus (Figure 3-8). In the same network, we also found the opposite contrast for PDD, namely increased functional connectivity in a significant cluster (p < 0.001) of 693 voxels mainly located on extra-nuclear space and white matter (corpus callosum).

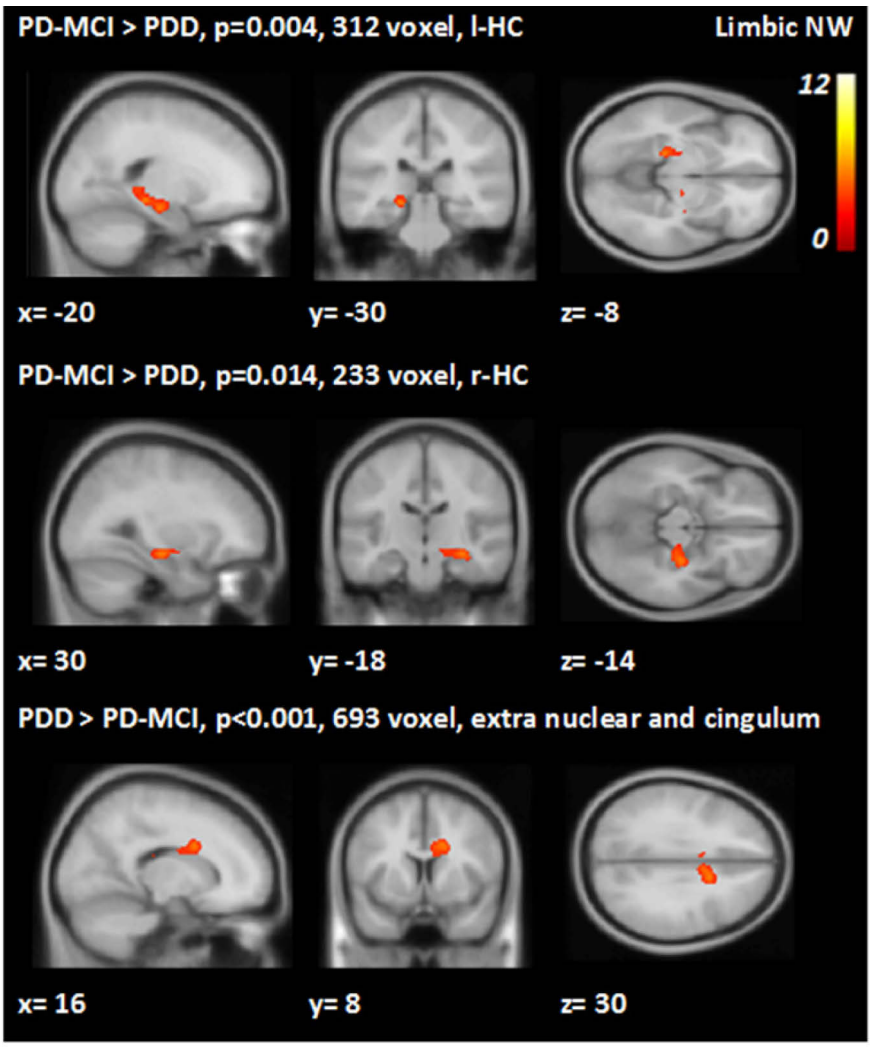

Figure 3-8: Three significant cluster within the limbic NW when comparing PD-MCI and PDD. Significant decreased functional connectivity in the left and right hippocampus in the PDD and significantly increased functional connectivity mainly located on extra-nuclear space and white matter (corpus callosum).

PD-non-demented vs PDD

When the data of the PD-N and PD-MCI were brought together and tested against the PDD group, significant differences in functional connectivity were found in the limbic NW and the frontostriatal NW.

Limbic NW

As in the PD-N vs PDD and PD-MCI vs PDD comparison, we could identify three significant clusters in the limbic NW for PDD vs PD-non-demented (Figure 3-9). The PDD group showed significantly decreased functional connectivity in one cluster (282 voxels) in the left hippocampus (p = 0.008) and in another cluster (326 voxels) located on the right thalamus

(p = 0.004). The cluster with its peak in the right thalamus covers mostly the thalamus (the ventral lateral and the medial dorsal nuclei) and parts of the basal ganglia (lentiform nucleus, putamen, lateral globus pallidus). In the third cluster (850 voxels), the PDD group showed significantly increased functional connectivity (p < 0.001) compared to PD-non-demented, but an important part of this cluster resides in white matter and extra-nuclear space.

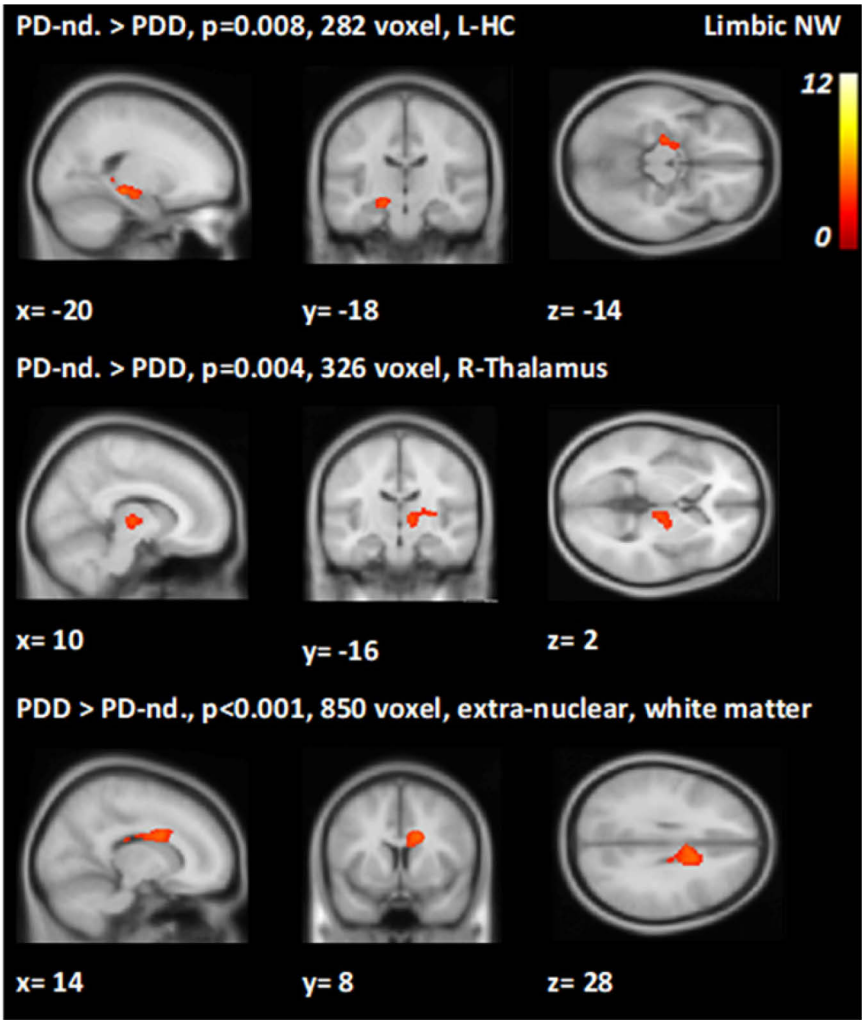

Figure 3-9: Three significant clusters within the limbic NW in the comparison PDD vs PD-non-demented (PD-nd.). Significantly decreased functional connectivity is obtained in the left hippocampus and right thalamus in the PDD and significantly increased functional connectivity in a cluster that mainly resides in white matter and extra-nuclear space.

Frontostriatal NW - FSN

For the frontostriatal NW, we could find significantly decreased functional connectivity in a cluster of 641 voxels (p = 0.032) for the PDD when using a height-threshold of $p < 0.005$ but not with a height threshold of $p < 0.001$ as applied in all other comparisons (Figure 3-10). However, this result is still worth of reporting, because the same network did significantly contribute to the binary logistic regression model that discriminated the PDD form PD-non-demented patients. The cluster covers mostly the left caudate head and body, parts of the putamen, the lentiform nucleus and to a lesser part the right caudate.

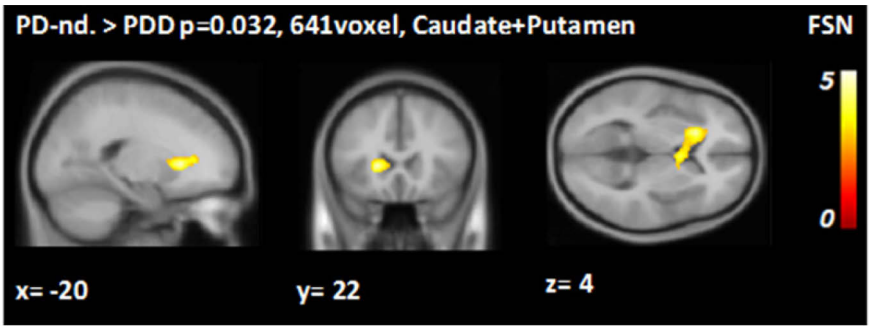

Figure 3-10: Significant cluster at height-threshold $p < 0.005$ showing decreased functional connectivity in the caudate, putamen and lentiform nucleus within the frontostriatal NW in PDD when compared to PD-non-demented (PD-nd.).

PD-N vs PD-MCI

No significant differences in functional connectivity were found between the PD-N and PD-MCI groups.

3.6.1.3 SUMMARY OF THE RS-FMRI DATA

Both the logistic regression and voxel-based analyses delivered complementary results. Based on the resting state data we can summarize, that the PDD patients show significantly lower expression of the limbic network, posterior temporal network and frontostriatal network compared to non-demented PD patients, which are supported by decreased functional connectivity in the thalamus, hippocampus and the caudate/putamen in voxel-based comparisons. Opposite to that, the overall expression of the DMN and salience network are stronger in PDD patients, where the stronger expression of the salience network is supported by increased functional connectivity in the right insula in voxel-based comparison of PD-N vs PDD groups (Table 3-9).

Table 3-9: Summary for the binary logistic regression results of the expression scores and the voxel- based comparisons for functional connectivity of the rs-fMRI data

Comparison	*RSNs*	*Logistic regression – NW expression*	*Voxel-based – Functional connectivity*
PD-N vs PDD	**Limbic NW**	**↓**	**R - Thalamus↓**
	FSN	↓	-
	DMN	↑	-
	Salience NW	**↑**	Caudate ↑ **& R - Insula ↑**
PD-MCI vs PDD	**Limbic NW**	**↓**	**L- HC ↓, R - HC ↓,** Caudate ↑
	PTN	↓	-
	DMN	↑	-
PD-nd. vs PDD	**Limbic NW**	**↓**	**L-HC↓, R-Thalamus↓,** Caudate↑
	FSN	**↓**	**Caudate, Putamen ↓**
	DMN	↑	-
	Salience NW	↑	-

3.6.1.4 Correlations of the RSNs with Clinical and Neuropsychological Variables

In order to associate the cognitive dysfunctions and motor symptoms of the PD patients with the functional connectivities, one-tailed non-parametric (Spearman's) bivariate correlation analyses were carried out for the significant findings obtained with the expression of the RSNs and the clinical and neuropsychological data collected from the 52 PD patients.

For Bonferroni correction, the clinical/neuropsychological variables were grouped into categories and based on the numbers of parameter in each category the alpha was adjusted: clinical data ($p < 0.05/5 = 0.01$; UPDRS-total, UPDRS-III, UPDRS-cognitive score, Hoehn &Yahr, GDS), global neuropsychological tests ($p < 0.05/7 = 0.0071$; ACE-R, Semantic fluency, phonemic fluency, pentagon copying, cube copying, clock drawing, MOCA) and specific neuropsychological tests ($p < 0.05/7 = 0.0071$; Stroop-mistakes and Stroop-effect, SDMT-total and SDMT-correct, WCST-category and WCST-error, JOLO).

The analyses showed that the expression of the limbic NW was negatively correlated with disease duration, the UPDRS - total and the UPDRS - cognitive score ($p < 0.01$), while the expression of the DMN was positively correlated with education and the Hoehn & Yahr score ($p < 0.01$). Beyond these, the expression of the FSN was positively correlated with better clock drawing performance ($p < 0.0071$), which is in line with stronger FSN expression and better performance in the clock drawing test in PD-N and PD compared to PDD. Finally, the salience network showed negative correlation with semantic fluency ($p < 0.0071$), which is reasonable as the PDD group showed bad performance in semantic fluency compared to PD-N and

PD-MCI and at the same time displayed stronger SN expression. The correlation analyses results for the RSNs are displayed in (Table 3-10).

Table 3-10: Correlation of RSN expression and the clinical and neuropsychological parameters

Expression scores of the RSNs						
Clinical / neuropsychological variables		PTN	DMN	Limbic NW	FSN	SN
Education [a)]	Corr.Coef. p (1-tailed)	0.247 0.039	0.334 0.008	0.071 NS	0.023 NS	0.026 NS
Disease Duration [a)]	Corr.Coef. p (1-tailed)	0.037 NS	0.145 NS	-0.344 0.006	0.049 NS	0.164 NS
UPDRS – total [b)]	Corr.Coef. p (1-tailed)	-0.230 NS	0.194 NS	-0.328 0.009	-0.126 NS	0.242 NS
UPDRS - Cognitive [b)]	Corr.Coef. p (1-tailed)	-0.124 NS	0.138 NS	-0.386 0.002	-0.242 NS	0.159 NS
Hoehn & Yahr [b)]	Corr.Coef. p (1-tailed)	-0.187 NS	0.344 0.006	-0.260 NS	-0.036 NS	0.296 NS
Semantic Fluency [c)]	Corr.Coef. p (1-tailed)	0.135 NS	-0.314 NS	0.244 NS	0.119 NS	-0.366 0.004
Clock Drawing [c)]	Corr.Coef. p (1-tailed)	0.036 NS	-0.202 NS	0.246 NS	0.336 0.007	-0.316 NS

Remarks: a) $p < 0.05$, b) $p < 0.01$, c) $p < 0.0071$.

3.6.2 DTI-Results

DTI data from all the PD patients were collected in order to gain information about the underlying structural white matter changes associated with cognitive decline in PD.

We used a ROI-based approach for white-matter analysis using 20 white-matter-tracts from the Johns Hopkins University–ICBM atlas (JHU-ICBM-tracts-maxprob-thr0-1mm) (Figure 3-12) and compared the mean FA, MD, RD and AD values of the voxels within these ROIs among the three groups by one-way ANOVA. After correcting the ANOVA results for the multiple comparisons in 20 ROIs, post-hoc two-sample t-tests were carried out between the following pairs of groups: PD-N vs PDD, PD-MCI vs PDD and PD-N vs PD-MCI (see methods).

For this purpose, the FA maps of all patients were first averaged and voxels of the obtained mean image with FA < 0.2 were excluded in order to exclude GM and CSF and obtain a study-specific white-matter mask corresponding to the investigated subjects (Figure 3-11). The JHU-ICBM atlas was multiplied with the study-specific white matter mask in order to obtain the study-specific ROIs (Figure 3-12, Table 3-11). In an automatized process using the

FSlstats command in FSL, each subject's mean FA, MD, RD and AD values for each of the study-specific ROIs have been calculated.

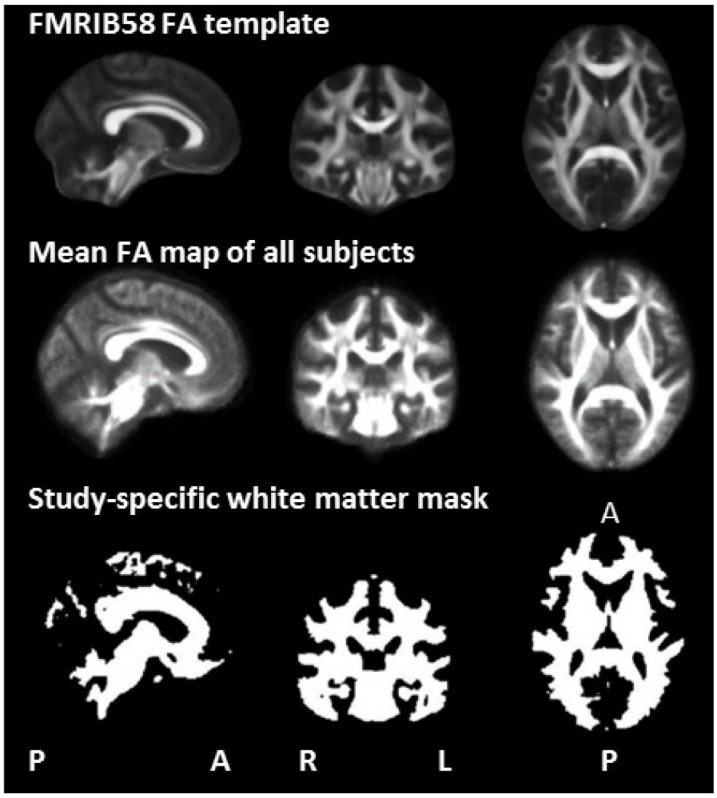

Figure 3-11: Computation of the study-specific white matter mask. In the first row the FMRIB58 FA template is displayed. The second row shows the mean FA map of all subjects in our study and in the third row the thresholded (> 0.2) white-matter mask is displayed.

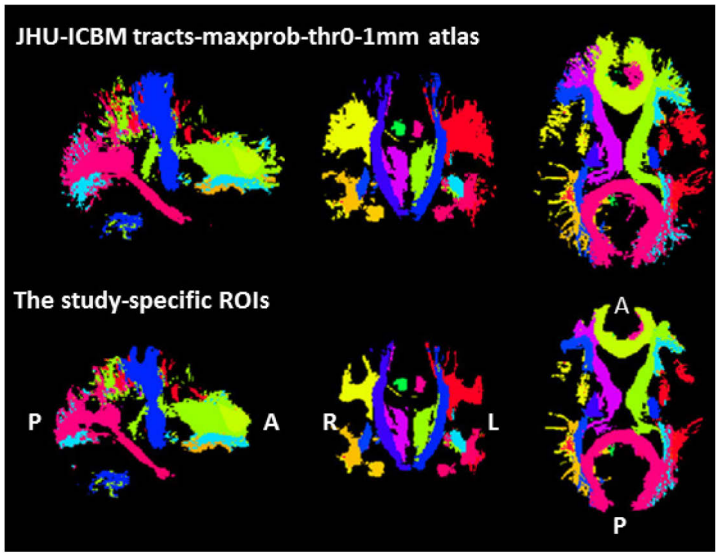

Figure 3-12: Computation of the study-specific ROIs. The original ROIs of the JHU-ICBM tracts-maxprob-thr0-1mm atlas are shown in the first and the study-specific ROIs obtained by voxel-wise multiplication of this atlas with the study-specific white matter mask (Fig. 3-11) in the second row. The study-specific ROIs in the second row consist of a sub-set of voxels of the same ROIs in the original atlas.

Table 3-11: ROI-size in total voxel number used in DTI ROI-based analyses

	Study-specific ROI-size		Original ROI-size	
ROI	**Left**	**Right**	**Left**	**Right**
ATR	37105	33182	54291	49337
CST	26706	28528	36577	37946
Cingulum-Cingulate	17670	13672	26228	18969
Cingulum-HC	6157	6881	9858	10118
IFOF	25111	33720	41508	51961
ILF	25900	25380	46905	42441
SLF	51617	49266	103293	94044
Uncinate	7103	5973	12074	10524
SLF-temp	808	3562	1390	4635
Forceps major	31617	-	49803	-
Forceps Minor	28730	-	56701	-

Remark: ROI-size displayed in number of voxels

3.6.2.1 ANOVA analyses among the 3 patient groups

For comparisons of the PD-N, PD-MCI and PDD groups one-way ANOVAs were first performed for FA values of each of the 20 ROIs with Bonferroni adjusted alpha ($p < 0.0025$). The results showed that anterior thalamic radiation (ATR) R, corticospinal tract (CST) L and R, cingulum cingulate gyrus L and R, inferior fronto-occipital fasciculus (IFOF) L and R, inferior longitudinal fasciculus (ILF) L and R, superior longitudinal fasciculus (SLF) L and R, superior longitudinal fasciculus – temporal region (SLF-temp.) L show significant differences among the 3 patient groups (Table 3-12).

For those ROIs showing significant FA difference after Bonferroni correction, mean MD, RD and AD values were further tested with one-way ANOVAs among the groups with the same adjusted alpha ($p < 0.0025$). The results showed that the mean MD values differed significantly among the 3 groups in cingulum cingulate gyrus L and R, IFOF L, ILF L and R, SLF L and SLF temp. L (Table 3-13), while RD values significantly differed in cingulum cingulate gyrus L, IFOF L, ILF L and R, SLF L and SLF-temp. L (Table 3-14) and mean AD values significantly differed between the 3 groups in cingulum cingulate gyrus L, IFOF, ILF L and R and SLF L (Table 3-15).

Overall, the FA values resulted in significant differences in 12 of the investigated 20 WM tracts (Figure 3-13).

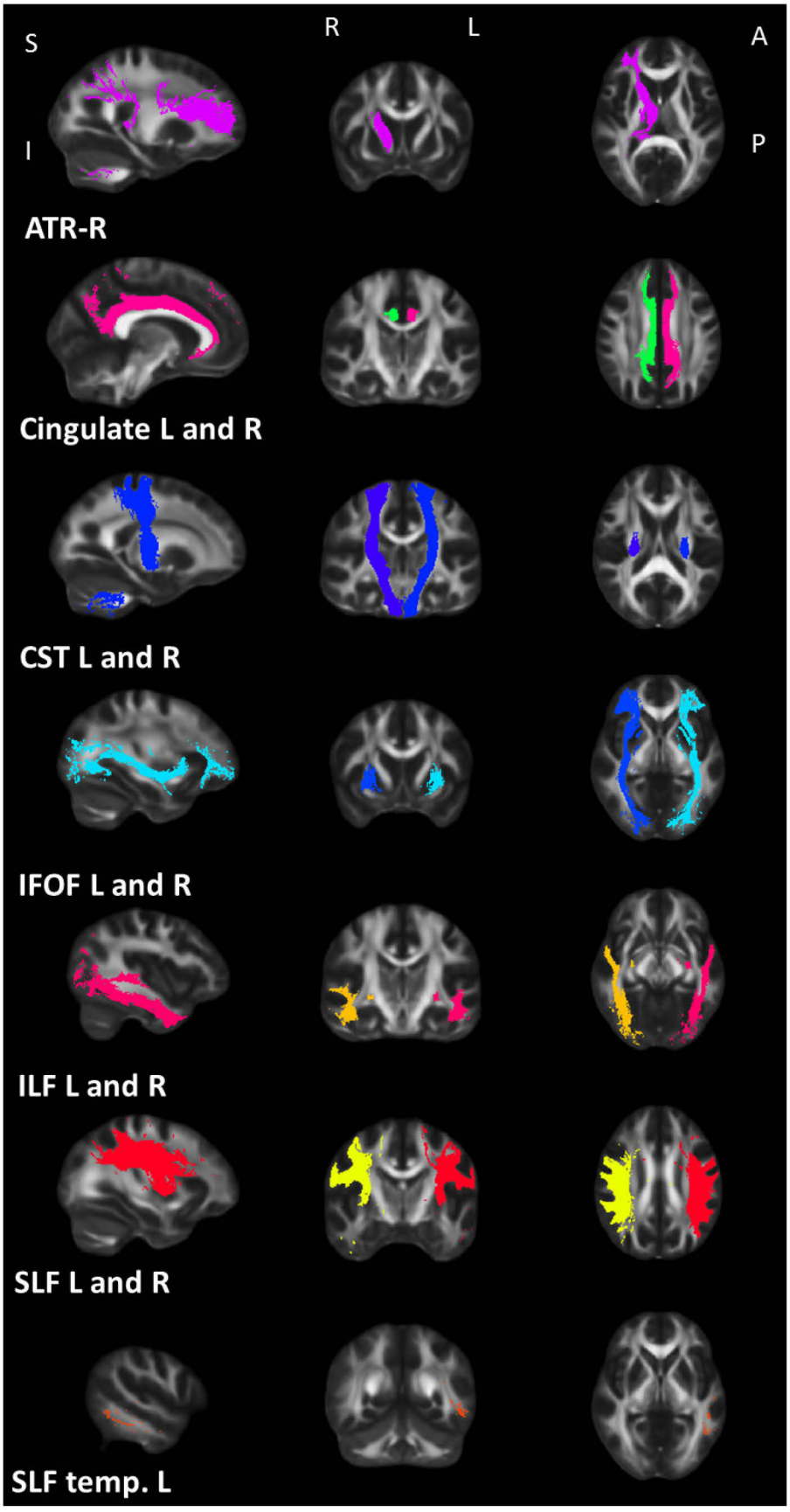

Figure 3-13: ROIs with significant FA differences among the 3 patient groups displayed on FMRIB58 FA template.

Table 3-12: Mean FA values of the PD-N, PD-MCI and PDD patients and one-way ANOVA results for 20 ROIs

	PD-N n=16		PD-MCI n=18		PDD n=18		ANOVA	
ROIs	***M***	***sd***	***M***	***sd***	***M***	***sd***	***F* (2,49)**	***p***
ATR-L	0.390	0.027	0.379	0.031	0.355	0.033	6.001	NS
ATR-R	0.397	0.023	0.390	0.022	0.367	0.027	7.558	0.001
CST-L	0.468	0.016	0.468	0.023	0.444	0.022	8.360	0.001
CST-R	0.468	0.015	0.462	0.024	0.439	0.022	9.082	0.000
Cing. Cingulate. Gyr-L	0.390	0.018	0.384	0.020	0.361	0.024	9.220	0.000
Cing. Cingulate. Gyr-R	0.367	0.018	0.364	0.021	0.342	0.025	7.088	0.002
Cing.- HC.-L	0.305	0.017	0.299	0.014	0.288	0.018	4.622	NS
Cing.- HC.-R	0.318	0.014	0.317	0.015	0.301	0.021	5.527	NS
Forc.-Major	0.418	0.025	0.408	0.038	0.383	0.038	4.873	NS
Forc.-Minor	0.423	0.027	0.412	0.033	0.385	0.040	5.744	NS
IFOF-L	0.369	0.018	0.364	0.020	0.341	0.021	9.709	0.000
IFOF-R	0.382	0.021	0.375	0.025	0.351	0.027	7.401	0.002
ILF-L	0.355	0.014	0.344	0.024	0.326	0.021	8.843	0.001
ILF-R	0.345	0.018	0.337	0.024	0.319	0.020	6.975	0.002
SLF-L	0.360	0.017	0.352	0.024	0.330	0.022	9.569	0.000
SLF-R	0.357	0.017	0.347	0.025	0.328	0.021	8.415	0.001
Uncinate-Fasc.-L	0.357	0.024	0.352	0.016	0.339	0.026	2.997	NS
Uncinate-Fasc.-R	0.347	0.035	0.346	0.028	0.340	0.030	0.276	NS
SLF-temp-L	0.379	0.024	0.371	0.024	0.344	0.022	10.807	0.000
SLF-temp-R	0.414	0.018	0.404	0.032	0.381	0.033	6.124	NS

Remark: Bonferroni adjusted alpha = p < 0.0025.

Table 3-13: Mean MD values of the PD-N, PD-MCI and PDD patients and one-way ANOVA results for 12 ROIs

	PD-N n=16		PD-MCI n=18		PDD n=18		ANOVA	
ROIs	***M***	***sd***	***M***	***sd***	***M***	***sd***	***F*** (2,49)	***P***
ATR-R	98.156 E-5	12.48 E-5	102.54 E-5	11.77 E-5	112.35 E-5	12.407 E-5	6.108	NS
CST-L	88.313 E-5	6.849 E-5	91.711 E-5	9.171 E-5	98.456 E-5	11.940 E-5	4.931	NS
CST-R	87.450 E-5	7.076 E-5	91.122 E-5	8.413 E-5	97.944 E-5	11.320 E-5	5.778	NS
Cing.gyr.-L	83.806 E-5	4.145 E-5	86.333 E-5	4.998 E-5	91.594 E-5	7.787 E-5	7.776	0.001
Cing.gyr.-R	83.544 E-5	4.041 E-5	85.622 E-5	5.489 E-5	91.000 E-5	7.659 E-5	7.151	0.002
IFOF-L	90.188 E-5	5.468 E-5	92.672 E-5	5.085 E-5	98.639 E-5	6.981 E-5	9.299	0.000
IFOF-R	89.988 E-5	7.379 E-5	93.117 E-5	6.686 E-5	98.367 E-5	7.844 E-5	5.743	NS
ILF-L	87.138 E-5	3.285 E-5	90.017 E-5	5.160 E-5	95.900 E-5	5.684 E-5	14.46	0.000
ILF-R	85.475 E-5	4.157 E-5	89.156 E-5	5.596 E-5	94.861 E-5	6.538 E-5	12.35	0.000
SLF-L	84.675 E-5	4.602 E-5	88.239 E-5	7.237 E-5	94.083 E-5	8.731 E-5	7.567	0.001
SLF-R	85.263 E-5	5.289 E-5	87.889 E-5	7.218 E-5	93.617 E-5	8.141 E-5	6.338	NS
SFL temp.-L	82.975 E-5	4.632 E-5	85.028 E-5	5.112 E-5	90.406 E-5	6.177 E-5	8.821	0.001

Remark: Bonferroni adjusted alpha = p < 0.0025.

Table 3-14: Mean RD values of the PD-N, PD-MCI and PDD patients and one-way ANOVA results for 12 ROIs

	PD-N n=16		PD-MCI n=18		PDD n=18		ANOVA	
ROIs	***M***	***sd***	***M***	***sd***	***M***	***sd***	***F* (2,49)**	***p***
ATR-R	78.882 E-5	12.53 E-5	83.128 E-5	12.28 E-5	93.256 E-5	12.765 E-5	6.002	NS
CST-L	65.956 E-5	6.773 E-5	68.928 E-5	9.381 E-5	76.333 E-5	11.985 E-5	5.227	NS
CST-R	65.294 E-5	6.882 E-5	68.772 E-5	8.810 E-5	76.1 E-5	11.232 E-5	6.153	NS
Cing.Gyr-L	65.456 E-5	4.559 E-5	68.067 E-5	5.814 E-5	74.167 E-5	8.635 E-5	7.845	0.001
Cing.Gyr-R	66.825 E-5	4.689 E-5	68.906 E-5	6.610 E-5	75.122 E-5	8.659 E-5	6.743	NS
IFOF-L	72.45 E-5	5.927 E-5	75.0 E-5	5.778 E-5	81.417 E-5	7.162 E-5	9.193	0.000
IFOF-R	71.775 E-5	7.949 E-5	74.867 E-5	7.597 E-5	80.778 E-5	8.431 E-5	5.619	NS
ILF-L	70.669 E-5	4.051 E-5	74.022 E-5	6..292 E-5	80.261 E-5	6.525 E-5	12.145	0.000
ILF-R	69.925 E-5	4.755 E-5	73.772 E-5	6.565 E-5	79.828 E-5	6.811 E-5	11.241	0.000
SLF-L	68.9 E-5	5.243 E-5	72.533 E-5	8.177 E-5	79.128 E-5	9.409 E-5	7.409	0.002
SLF-R	69.838 E-5	5.949 E-5	72.589 E-5	8.247 E-5	78.939 E-5	8.653 E-5	6.224	NS
SFL temp.-L	65.775 E-5	5.571 E-5	68.089 E-5	6.429 E-5	74.617 E-5	7.184 E-5	8.721	0.001

Remark: Bonferroni adjusted alpha = $p < 0.0025$.

Table 3-15: Mean AD values of the PD-N, PD-MCI and PDD patients and one-way ANOVA results for 12 ROIs

	PD-N n=16		PD-MCI n=18		PDD n=18		ANOVA	
ROIs	***M***	***sd***	***M***	***sd***	***M***	***sd***	***F* (2,49)**	***p***
ATR-R	136.706 E-5	12.61 E-5	141.378 E-5	10.997 E-5	150.539 E-5	12.018 E-5	6.051	NS
CST-L	133.025 E-5	7.134 E-5	137.278 E-5	8.898 E-5	142.700 E-5	11.930 E-5	4.338	NS
CST-R	131.763 E-5	7.647 E-5	135.822 E-5	7.710 E-5	141.633 E-5	11.574 E-5	4.949	NS
Cing.Gyr-L	120.507 E-5	3.925 E-5	122.867 E-5	3.734 E-5	126.450 E-5	6.393 E-5	6.458	NS
Cing.Gyr-R	116.981 E-5	3.357 E-5	119.056 E-5	3.628 E-5	122.756 E-5	6.016 E-5	7.141	0.002
IFOF-L	125.663 E-5	4.755 E-5	128.017 E-5	3.999 E-5	133.083 E-5	6.840 E-5	8.635	0.001
IFOF-R	126.413 E-5	6.560 E-5	129.617 E-5	5.088 E-5	133.544 E-5	6.850 E-5	5.655	NS
ILF-L	120.075 E-5	2.436 E-5	122.006 E-5	3.745 E-5	127.178 E-5	4.615 E-5	16.586	0.000
ILF-R	116.575 E-5	3.416 E-5	119.922 E-5	3.955 E-5	124.928 E-5	6.221 E-5	13.481	0.000
SLF-L	116.225 E-5	3.651 E-5	119.650 E-5	5.586 E-5	123.994 E-5	7.540 E-5	7.463	0.001
SLF-R	116.113 E-5	4.250 E-5	118.489 E-5	5.382 E-5	122.972 E-5	7.355 E-5	6.073	NS
SFL Temp.-L	117.375 E-5	3.927 E-5	118.906 E-5	3.954 E-5	121.983 E-5	5.259 E-5	4.803	NS

Remark: Bonferroni adjusted alpha = $p < 0.0025$.

3.6.2.2 Post-hoc multiple comparisons of FA, MD, RD, and AD values between pairs of patient groups

According to the 12 significant overall ANOVA results on FA values, the post-hoc two-sample t-tests between pairs of patient groups have been corrected with a Bonferroni adjusted alpha ($p < 0.0042$). The PDD patients showed significantly reduced mean FA values compared to the PD-N in all of the 12 ROIs, while only CST-L, IFOF-L and SLF-temp.-L displayed significant FA decrease in PDD compared with the PD-MCI group (Table 3-16). On the other hand, PD-MCI

group showed no significant difference in any of the investigated ROIs in comparison to the PD-N group.

Significantly increased MD values were obtained in the cingulum cingulate gyrus L and R, IFOF-L, ILF-L, SLF-L and SLF temp.-L of the PDD patients compared with the PD-N group. A similar pattern of increased RD was obtained in the PDD group with the exception of no significant difference in cingulum cingulate gyrus R compared with the PD-N group. Interestingly, the AD values also increased in PDD patients, but only in cingulum cingulate gyrus R, IFOF L, ILF L and R and SLF-L. On the other hand, none of the investigated WM structures showed a significant MD, RD and AD difference between the PDD and PD-MCI groups except for the increased MD and AD values in ILF-L.

Table 3-16: Bonferroni corrected (group) multiple comparisons results for FA, RD, MD and AD

	FA		**MD**		**RD**		**AD**	
	PD-N > PDD	**PD-MCI > PDD**	**PD-N < PDD**	**PD-MCI < PDD**	**PD-N < PDD**	**PD-MCI < PDD**	**PD-N < PDD**	**PD-MCI < PDD**
ROIs	***p***	***p***	***p***	***p***	***p***	***p***	***p***	***p***
ATR-R	0.002	NS	-	-	-	-	-	-
CST-L	0.003	0.003	-	-	-	-	-	-
CST-R	0.001	NS	-	-	-	-	-	-
Cing. Gyr-L	0.001	NS	0.001	NS	0.001	NS	-	-
Cing. Gyr-R	0.004	NS	0.002	NS	-	-	0.002	NS
IFOF-L	0.000	0.004	0.000	NS	0.000	NS	0.001	NS
IFOF-R	0.002	NS	-	-	-	-		
ILF-L	0.000	NS	0.000	.002	0.000	NS	0.000	0.000
ILF-R	0.002	NS	0.000	NS	0.000	NS	0.000	NS
SLF-L	0.000	NS	0.001	NS	0.001	NS	0.001	NS
SLF-R	0.001	NS	-	-	-		-	-
SFL Temp.-L	0.000	0.004	0.001	NS	0.001	NS	-	-

Remark: Bonferroni adjusted alpha p < 0.00042.

3.6.2.3 Correlations of the White Matter Changes with Clinical and Neuropsychological Variables

To associate the cognitive dysfunctions and motor symptoms of the PD patients with the structural changes, one-tailed non-parametric (Spearman's) bivariate correlation analyses were carried out for the FA, MD, RD and AD values of the tracts that significantly differed among the patient groups in ANOVA tests and the clinical and neuropsychological data collected from all 52 PD patients.

For Bonferroni correction, the parameters were grouped into categories and based on the numbers of parameter in the groups the alpha was adjusted: clinical data ($p < 0.01$), global neuropsychological tests ($p < 0.0071$) and specific neuropsychological tests ($p < 0.0071$).

3.6.2.3.1 DTI - FA

The neuropsychological test and clinical parameters displayed significant correlations with the DTI-derived FA values (Table 3-17). The increasing age lead to decreased FA in all ROIs ($p < 0.05$) except for SLF-L. The increases of disease duration and UPDRS – total and UPDRS – cognitive scores, that correspond to worse disease symptoms, similarly resulted in lower FA of the CST-R, the cingulum-L, the IFOF-L, the ILF-L, the SLF-L and R, and the SLF-temp.-L, while the increasing UPDRS- cognitive scores were further associated with decreased FA in the ATR-R, right cingulum, right IFOF and right ILF ($p < 0.01$). The Hoehn & Yahr score representing the severity of the motor symptoms correlated negatively with the FA values of the ILF-L, SLF-L and SLF-temp.-L ($p < 0.01$), while the ACE-R as a measure for cognitive functions was positively correlated with the FA of CST-R, ILF-L and SLF-temp.-L ($p < 0.0071$). The pentagon copying performance was positively correlated with FA values of all ROIs, while phonemic fluency displayed positive correlation with ILF-L and SLF-L, and clock drawing performance was positively correlated with CST-R and SLF-temp.-L ($p < 0.0071$). The MOCA test as a global cognitive screening instrument showed a broad positive correlation with the FA of most ROIs ($p < 0.0071$) except for the ATR-R, Cingulum-L and SLF-L, while WCST-category was positively correlated with ATR-R, cingulum-L, IFOF-R, ILF-L and R, SLF-L and R and the SLF-temp.-L ($p < 0.0071$).

Interestingly, the FA values of ILF-L, SLF-temp.-L showed mostly a non-specific pattern of correlation with all parameters except the clock drawing and phonemic fluency.

Table 3-17: Correlation of DTI-derived FA findings and the clinical and neuropsychological parameters

Fractional Anisotropy - FA													
Clinical / neuropsychological variables		ATR - R	CST - L	CST - R	Cing. cingulate gyr.-L	Cing. cingulate gyr.-R	IFOF - L	IFOF - R	ILF - L	ILF - R	SLF - L	SLF - R	SLF-temp.-L
Age [a]	Corr.Coef.	-0.414	-0.291	-0.383	-0.433	-0.423	-0.410	-0.465	-0.394	-0.430	-0.306	-0.410	-0.442
	p (1-tailed)	0.001	0.018	0.003	0.001	0.001	0.001	0.000	0.002	0.001	NS	0.001	0.001
Disease Duration [a]	Corr.Coef.	-0.142	-0.166	-0.233	-0.252	-0.181	-0.274	-0.177	-0.306	-0.218	-0.261	-0.272	-0.311
	p (1-tailed)	NS	NS	0.049	0.036	NS	0.025	NS	0.014	NS	0.031	0.025	0.012
UPDRS - total [b]	Corr.Coef.	-0.312	-0.317	-0.395	-0.368	-0.301	-0.367	-0.308	-0.438	-0.397	-0.373	-0.398	-0.443
	p (1-tailed)	NS	NS	0.002	0.004	NS	0.004	NS	0.001	0.002	0.003	0.002	0.001
UPDRS – Cognitive [b]	Corr.Coef.	-0.427	-0.300	-0.410	-0.476	-0.374	-0.458	-0.440	-0.407	-0.426	-0.360	-0.414	-0.499
	p (1-tailed)	0.001	NS	0.001	0.000	0.003	0.000	0.001	0.001	0.001	0.004	0.001	0.000
Hoehn & Yahr [b]	Corr.Coef.	-0.231	-0.221	-0.296	-0.281	-0.194	-0.285	-0.228	-0.330	-0.290	-0.284	-0.327	-0.381
	p (1-tailed)	NS	NS	NS	NS	NS	NS	NS	0.008	NS	NS	0.009	0.003
ACE-R [c]	Corr.Coef.	0.267	0.245	0.342	0.313	0.220	0.310	0.245	0.342	0.305	0.322	0.327	0.379
	p (1-tailed)	NS	NS	0.006	NS	NS	NS	NS	0.007	NS	NS	NS	0.003
Phonemic Fluency [c]	Corr.Coef.	0.232	0.280	0.327	0.302	0.252	0.272	0.270	0.345	0.298	0.363	0.293	0.318
	p (1-tailed)	NS	NS	NS	NS	NS	NS	NS	0.006	NS	0.004	NS	NS
Pentagon Copy [c]	Corr.Coef.	0.337	0.437	0.453	0.408	0.369	0.448	0.369	0.453	0.363	0.411	0.424	0.387
	p (1-tailed)	0.007	0.001	0.000	0.001	0.004	0.000	0.004	0.000	0.004	0.001	0.001	0.002
Clock Drawing [c]	Corr.Coef.	0.209	0.303	0.352	0.263	0.126	0.290	0.248	0.311	0.294	0.266	0.304	0.383
	p (1-tailed)	NS	NS	0.005	NS	NS	NS	NS	NS	NS	NS	NS	0.003
MOCA [c]	Corr.Coef.	0.361	0.406	0.488	0.404	0.330	0.397	0.398	0.393	0.381	0.359	0.428	0.421
	p (1-tailed)	NS	0.004	0.001	0.004	NS	0.005	0.005	0.006	0.007	NS	0.003	0.003
WCST – Categories c]	Corr.Coef.	0.395	0.330	0.366	0.423	0.318	0.361	0.430	0.457	0.443	0.424	0.400	0.486
	p (1-tailed)	0.006	NS	NS	0.003	NS	NS	0.003	0.002	0.002	0.003	0.005	0.001

Remarks: a) $p < 0.05$, b) $p < 0.01$, c) $p < 0.0071$. L: left, R: right, ATR: anterior thalamic radiation, CST: cortico spinal tract, Cingulum cingulate gyrus, IFOF: inferior fronto occipital fasciculus, ILF: inferior longitudinal fasciculus, SLF: superior longitudinal fasciculus, SLF-temp.: superior longitudinal fasciculus temporal.

3.6.2.3.2 DTI - MD

Generally, the DTI-derived MD values of the evaluated ROIs were positively correlated with the clinical and demographic parameters but negatively correlated with the NPT scores (Table 3-18).

All tracts that showed a significant MD difference among the groups in previous ANOVA tests, that are the Cingulum cingulate gyr.-L and R, IFOF-L, ILF-L and R, SLF-L and SLF temp.-L, significantly increased with increasing age and UPDRS scores. Disease duration was also positively correlated with MD values of the investigated ROIs except the IFOF-L and SLF temp.-L, and Hoehn & Yahr score was positively correlated with the MD values of cingulum cingulate gyr.-L, ILF-L and R and SLF temp.-L.

On the other hand, decreased ACE-R and MOCA scores representing worsening of the global cognitive performance of the subjects and decreasing Pentagon Copy test scores were correlated with increased MD values of all investigated tracts. Decrease of the WCST-Categories score was associated in a similar non-specific manner with increased MD values in all of these tracts except cingulum cingulate gyr.-R. Beyond these global patterns, worse scores in phonemic fluency test were specifically associated with increased MD in Cingulum cingulate gyr.-L and ILF-L, while worsening semantic fluency performance was associated with increased MD in ILF-L and R and SLF temp.-L. Lower scores in clock drawing test were also correlated with increased MD in ILF-L and R and SLF temp.-L. Finally, increased number of errors in the WCST test were associated with increased MD values in ILF-R and SLF temp.-L.

Table 3-18: Correlation of DTI-derived MD findings and the clinical and neuropsychological parameters

Mean Diffusivity (MD)								
Clinical / neuropsychological variables		Cing. cingulate gyr.-L	Cing. cingulate gyr.-R	IFOF-L	ILF-L	ILF-R	SLF-L	SLF temp.-L
Age [a)]	Corr.Coef.	0.549	0.527	0.634	0.597	0.556	0.496	0.451
	p (1-tailed)	0.000	0.000	0.000	0.000	0.000	0.000	0.000
Disease Duration [a)]	Corr.Coef.	0.301	0.256	0.165	0.318	0.322	0.273	0.214
	p (1-tailed)	0.015	0.034	NS	0.011	0.010	0.025	NS
UPDRS – total [b)]	Corr.Coef.	0.445	0.384	0.408	0.548	0.572	0.441	0.517
	p (1-tailed)	0.000	0.002	0.001	0.000	0.000	0.001	0.000
UPDRS - III [b)]	Corr.Coef.	0.383	0.347	0.364	0.478	0.525	0.383	0.445
	p (1-tailed)	0.003	0.006	0.004	0.000	0.000	0.003	0.000
UPDRS - Cognitive [b)]	Corr.Coef.	0.435	0.414	0.506	0.558	0.517	0.380	0.474
	p (1-tailed)	0.001	0.001	0.000	0.000	0.000	0.003	0.000
Hoehn & Yahr [b)]	Corr.Coef.	0.341	0.307	0.318	0.449	0.450	0.318	0.382
	p (1-tailed)	0.007	NS	NS	0.000	0.000	NS	0.003
ACE-R [c)]	Corr.Coef.	-0.387	-0.336	-0.360	-0.483	-0.495	-0.353	-0.426
	p (1-tailed)	0.002	0.007	0.004	0.000	0.000	0.005	0.001
Phonemic Fluency [c)]	Corr.Coef.	-0.337	-0.293	-0.233	-0.338	-0.331	-0.311	-0.328
	p (1-tailed)	0.007	NS	NS	0.007	NS	NS	NS
Semantic Fluency [c)]	Corr.Coef.	-0.296	-0.280	-0.309	-0.416	-0.445	-0.316	-0.373
	p (1-tailed)	NS	NS	NS	0.001	0.000	NS	0.003
Pentagon Copy [c)]	Corr.Coef.	-0.403	-0.416	-0.349	-0.547	-0.470	-0.412	-0.427
	p (1-tailed)	0.002	0.001	0.006	0.000	0.000	0.001	0.001
Clock Drawing [c)]	Corr.Coef.	-0.227	-0.209	-0.270	-0.367	-0.382	-0.246	-0.342
	p (1-tailed)	NS	NS	NS	0.004	0.003	NS	0.006
MOCA [c)]	Corr.Coef.	-0.414	-0.384	-0.475	-0.509	-0.507	-0.427	-0.418
	p (1-tailed)	0.004	0.007	0.001	0.000	0.000	0.003	0.003
WCST - Categories [c)]	Corr.Coef.	-0.408	-0.353	-0.498	-0.521	-0.584	-0.453	-0.495
	p (1-tailed)	0.005	NS	0.001	0.000	0.000	0.002	0.001
WCST - Error [c)]	Corr.Coef.	0.235	0.169	0.358	0.322	0.401	0.302	0.428
	p (1-tailed)	NS	NS	NS	NS	0.005	NS	0.003

Remarks: a) $p < 0.05$, b) $p < 0.01$, c) $p < 0.0071$.

3.6.2.3.3 DTI – RD

The RD values of the investigated tracts display the same pattern of positive correlations with the demographic and clinical parameters and negative correlation with the NPTs similar to the correlation pattern of the MD values (Table 3-18, Table 3-19). The RD generally seems to be less specific, as the RD of almost all tracts show correlations with all parameters but phonemic fluency.

While increasing age, UPDRS-total, UPDRS-III and UPDRS cognitive scores were associated with increase in RD of all investigated tracts, increasing ACE-R, pentagon copying, MOCA and

WCST- category scores were associated with decreased RD of all ROIs. The disease duration was positively correlated with the RD of all ROIs except the left IFOF and the Hoehn & Yahr score was positively correlated with the RD in all ROIs but not the left SLF. The semantic fluency was negatively correlated with the RD in the left and right ILF and the left temporal SLF, while the worse clock drawing performance and number of error in the WCST were correlated with higher RD values of the same ROIs, namely the right ILF and the left temporal SLF.

Table 3-19: Correlation of DTI-derived RD findings and the clinical and neuropsychological parameters

Radial Diffusivity (RD)							
Clinical / neuropsychological variables		Cing. cingulate gyr.-L	IFOF-L	ILF-L	ILF-R	SLF-L	SLF temp.-L
Age [a)]	Corr.Coef.	0.563	0.619	0.592	0.550	0.490	0.491
	p (1-tailed)	0.000	0.000	0.000	0.000	0.000	0.000
Disease Duration [a)]	Corr.Coef.	0.297	0.203	0.292	0.288	0.263	0.245
	p (1-tailed)	0.016	NS	0.018	0.019	0.030	0.040
UPDRS - total [b)]	Corr.Coef.	0.433	0.417	0.526	0.554	0.427	0.526
	p (1-tailed)	0.001	0.001	0.000	0.000	0.001	0.000
UPDRS - III [b)]	Corr.Coef.	0.370	0.361	0.465	0.499	0.367	0.444
	p (1-tailed)	0.003	0.004	0.000	0.000	0.004	0.000
UPDRS - Cognitive [b)]	Corr.Coef.	0.432	0.511	0.514	0.502	0.376	0.498
	p (1-tailed)	0.001	0.000	0.000	0.000	0.003	0.000
Hoehn & Yahr [b)]	Corr.Coef.	0.341	0.326	0.401	0.408	0.305	0.390
	p (1-tailed)	0.007	0.009	0.002	0.001	NS	0.002
ACE-R [c)]	Corr.Coef.	-0.360	-0.360	-0.439	-0.466	-0.343	-0.428
	p (1-tailed)	0.004	0.004	0.001	0.000	0.006	0.001
Phonemic Fluency [c)]	Corr.Coef.	-0.301	-0.238	-0.324	-0.328	-0.306	-0.335
	p (1-tailed)	NS	NS	NS	NS	NS	NS
Semantic Fluency [c)]	Corr.Coef.	-0.292	-0.318	-0.380	-0.407	-0.325	-0.389
	p (1-tailed)	NS	NS	0.003	0.001	NS	0.002
Pentagon Copy [c)]	Corr.Coef.	-0.385	-0.375	-0.498	-0.443	-0.386	-0.403
	p (1-tailed)	0.002	0.003	0.000	0.001	0.002	0.002
Clock Drawing [c)]	Corr.Coef.	-0.239	-0.286	-0.326	-0.365	-0.259	-0.369
	p (1-tailed)	NS	NS	NS	0.004	NS	0.004
MOCA [c)]	Corr.Coef.	-0.409	-0.469	-0.483	-0.499	-0.419	-0.442
	p (1-tailed)	0.004	0.001	0.001	0.000	0.003	0.002
WCST - Categories [c)]	Corr.Coef.	-0.404	-0.487	-0.550	-0.568	-0.440	-0.526
	p (1-tailed)	0.005	0.001	0.000	0.000	0.002	0.000
WCST - Error [c)]	Corr.Coef.	.228	0.339	0.338	0.387	0.281	0.427
	p (1-tailed)	NS	NS	NS	0.007	NS	0.003

Remarks: a) $p < 0.05$, b) $p < 0.01$, c) $p < 0.0071$.

3.6.2.3.4 DTI - AD

The correlation pattern for the AD with the other parameters was similar to the RD correlations (Table 3-20). Age, UPDRS-total, UPDRS-III, UPDRS-cognitive scores were positively and the ACE-R and pentagon copying were negatively correlated with the AD in all ROIs. Whereas the disease duration was positively correlated with the AD in all ROIs but not the IFOF-L, the Hoehn & Yahr scale was positively correlated with AD in all ROIs but the SLF-L. The phonemic and semantic fluency were both negatively correlated with the AD of left and right ILF. The clock drawing abilities were negatively correlated with the AD of left and right ILF and the left SLF, while the MOCA and WCST-categories were negatively correlated with the AD in all ROIs but the right cingulum cingulate gyrus. Finally, the WCST-error was positively correlated with the AD of the left IFOF and the right ILF.

Table 3-20: Correlation of DTI-derived AD findings and the clinical and neuropsychological parameters

Axial Diffusivity (AD)						
Clinical / neuropsychological variables		Cing.cingulate gyr.-R	IFOF-L	ILF-L	ILF-R	SLF-L
Age [a)]	Corr.Coef.	0.423	0.644	0.535	0.491	0.489
	p (1-tailed)	0.001	0.000	0.000	0.000	0.000
Disease Duration [a)]	Corr.Coef.	0.271	0.135	0.298	0.346	0.231
	p (1-tailed)	0.026	NS	0.016	0.006	0.050
UPDRS - total [b)]	Corr.Coef.	0.370	0.401	0.507	0.605	0.451
	p (1-tailed)	0.003	0.002	0.000	0.000	0.000
UPDRS - III [b)]	Corr.Coef.	0.335	0.373	0.442	0.566	0.396
	p (1-tailed)	0.008	0.003	0.001	0.000	0.002
UPDRS - Cognitive [b)]	Corr.Coef.	0.382	0.472	0.570	0.494	0.358
	p (1-tailed)	0.003	0.000	0.000	0.000	0.005
Hoehn &- Yahr [b)]	Corr.Coef.	0.356	0.344	0.478	0.493	0.313
	p (1-tailed)	0.005	0.006	0.000	0.000	NS
ACE-R [c)]	Corr.Coef.	-0.364	-0.355	-0.515	-0.566	-0.357
	p (1-tailed)	0.004	0.005	0.000	0.000	0.005
Phonemic Fluency [c)]	Corr.Coef.	-0.295	-0.196	-0.339	-0.348	-0.281
	p (1-tailed)	NS	NS	0.007	0.006	NS
Semantic Fluency [c)]	Corr.Coef.	-0.282	-0.320	-0.448	-0.514	-0.276
	p (1-tailed)	NS	NS	0.000	0.000	NS
Pentagon Copy [c)]	Corr.Coef.	-0.474	-0.332	-0.598	-0.532	-0.402
	p (1-tailed)	0.000	0.008	0.000	0.000	0.002
Clock Drawing [c)]	Corr.Coef.	-0.240	-0.232	-0.391	-0.416	-0.198
	p (1-tailed)	NS	NS	0.002	0.001	NS
MOCA [c)]	Corr.Coef.	-0.349	-0.463	-0.520	-0.537	-0.428
	p (1-tailed)	NS	0.001	0.000	0.000	0.003
WCST - Categories [c)]	Corr.Coef.	-0.314	-0.508	-0.498	-0.596	-0.456
	p (1-tailed)	NS	0.000	0.001	0.000	0.002
WCST - Error [c)]	Corr.Coef.	0.155	0.390	0.369	0.447	0.356
	p (1-tailed)	NS	0.006	NS	0.002	NS

Remarks: a) $p < 0.05$, b) $p < 0.01$, c) $p < 0.0071$.

3.6.3 ASL Results

The ASL based cerebral blood flow (CBF) maps for all 52 subjects were calculated and registered to the 152-MNI standard space (Figure 3-14). As the ASL data were collected from a restricted field of view (FOV) during the scanning sessions and differed slightly regarding their position, due to anatomical differences of the patients, we chose a ROI-based approach for the calculation of differences in CBF. Seventy pre-defined ROIs were extracted from the lateralized Harvard Cortical Structural Atlas and the mean CBF from voxels within the ROIs were calculated and statistically compared between the patient groups (Table 3-21).

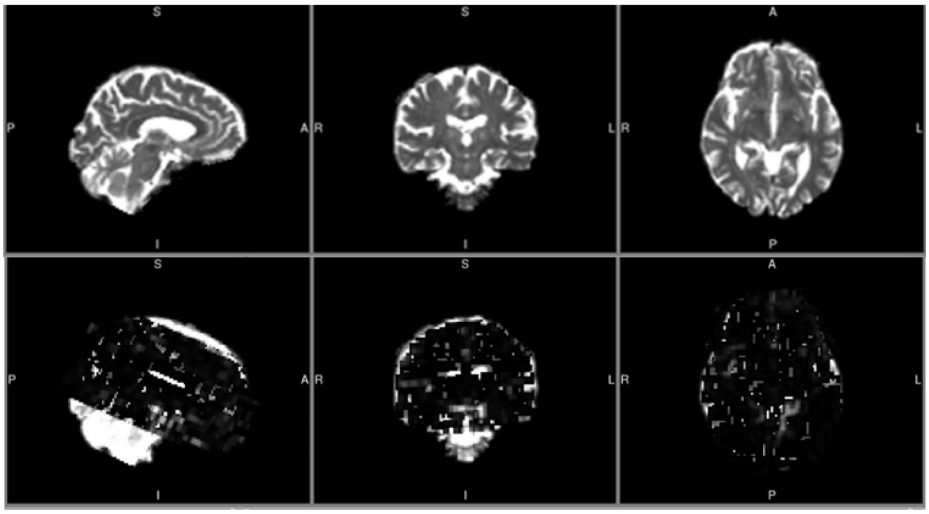

Figure 3-14: Example of a PDD patients registered T2-weighted image to 152-MNI standard space in the first row and the co-registered CBF maps in the lower row.

3.6.3.1 ANOVA analyses among the 3 patient groups

For comparisons of the PD-N, PD-MCI and PDD groups one-way ANOVAs were performed for the 70 ROIs with Bonferroni adjusted alpha ($p < 0.0007$). While an overall progressive decrease of the CBF was observed from PD-N through PD-MCI to PDD groups, the differences among the 3 groups were significant only in 9 ROIs: the right inferior temporal gyrus posterior (Inf. Temp. G.-P), the right inferior temporal gyrus temporo-occipital region (Inf. Temp. gyr.–TO), right middle frontal gyrus (Mid. Front. gyr.), left middle temporal gyrus anterior portion (Mid. Temp. G.-A), left and right superior frontal gyrus (Sup. Front. gyr.), left superior temporal gyrus anterior portion (Sup. Temp. gyr.-A), right temporal fusiform cortex posterior portion (Temp. Fus. C.-P) and right temporal occipital fusiform cortex (Temp. Occ. Fus. C.) (Table 3-21).

Table 3-21: The mean CBF values of 70 lateralized ROIs in PD-N, PD-MCI and PDD patient groups and ANOVA results.

		Left			Right			One-Way NAOVA	
		N	***M***	***sd***	***N***	***M***	***sd***	***F***	***p***
Inf. Temp. gyr. post.	PD-N	15	43.91	25.45	16	49.80	17.46	L F (2,47) = 3,146	0.052
	PD-MCI	18	36.94	17.29	18	45.75	10.49	**R F (2,48)=13,234**	**0.000**
	PDD	17	28.20	6.61	17	29.36	6.55		
Inf. Temp. gyr. temp.-occ.	PD-N	15	36.13	26.18	16	46.25	20.85	L F (2,44) = 1,907	0.161
	PD-MCI	15	32.77	16.19	18	38.25	8.39	**R F(2,48) =14,910**	**0.000**
	PDD	17	24.30	6.13	17	21.97	5.52		
Middle Frontal gyr	PD-N	14	54.36	24.91	16	50.98	22.62	L F (2,45) = 7,056	0.002
	PD-MCI	16	51.88	21.06	18	50.89	17.47	**R F(2,49) =10,273**	**0.000**
	PDD	18	32.02	8.64	18	28.70	7.71		
Middle Temp. gyr. ant.	PD-N	12	53.45	27.10	16	49.43	25.37	**L F (2,37)=11,768**	**0.000**
	PD-MCI	11	60.08	14.43	18	47.74	18.59	R F (2,48) = 5,573	0.007
	PDD	17	30.50	6.74	17	30.36	6.54		
Superior Frontal gyr	PD-N	16	61.10	17.28	16	57.98	20.86	**L F (2,49)=16,815**	**0.000**
	PD-MCI	18	57.83	13.50	18	57.85	16.22	**R F (2,49) = 9,764**	**0.000**
	PDD	18	37.83	5.50	18	38.27	4.79		
Superior Temp. gyr ant.	PD-N	13	57.41	28.67	16	52.29	32.82	**L F (2,37)=12,013**	**0.000**
	PD-MCI	10	69.03	14.41	18	49.78	26.92	R F (2,48) = 1,889	0.162
	PDD	17	35.48	5.03	17	36.95	5.37		
Temporal Fusiform Cortex post	PD-N	16	44.57	26.48	16	52.31	16.16	L F (2,48) = 1,733	0.188
	PD-MCI	18	36.81	17.24	18	51.00	10.41	**R F (2,48) = 9,417**	**0.000**
	PDD	17	32.95	4.76	17	37.07	4.96		
Temporal Occipital Fusiform	PD-N	16	39.65	26.10	16	50.78	19.22	L F (2,48) = 1,002	0.375
	PD-MCI	18	35.04	21.64	18	48.07	13.69	**R F (2,48) = 9,664**	**0.000**
	PDD	17	29.99	4.03	17	31.63	4.03		

Remark: Bonferroni adjusted alpha p < 0.0007.

3.6.3.2 Post-hoc multiple comparisons of BF values between pairs of patient groups

The post-hoc two-sample t-tests for these 9 ROIs (Figure 3-15) between pairs of patient groups, each of which are initially Bonferroni corrected for 3 between-group comparisons, have been further corrected with the Bonferroni adjusted alpha ($p < 0.0055$) against the 9 repeated comparisons (Table 3-22). The CBF significantly decreased in all of the 9 ROIs in the PDD group compared to PD-MCI and PD-N, but the significance level did not survive for the left superior temporal gyrus between PDD and PD-N after Bonferroni correction ($p = 0.007$). The PD-N and PD-MCI groups did not show any significant CBF difference in the investigated ROIs.

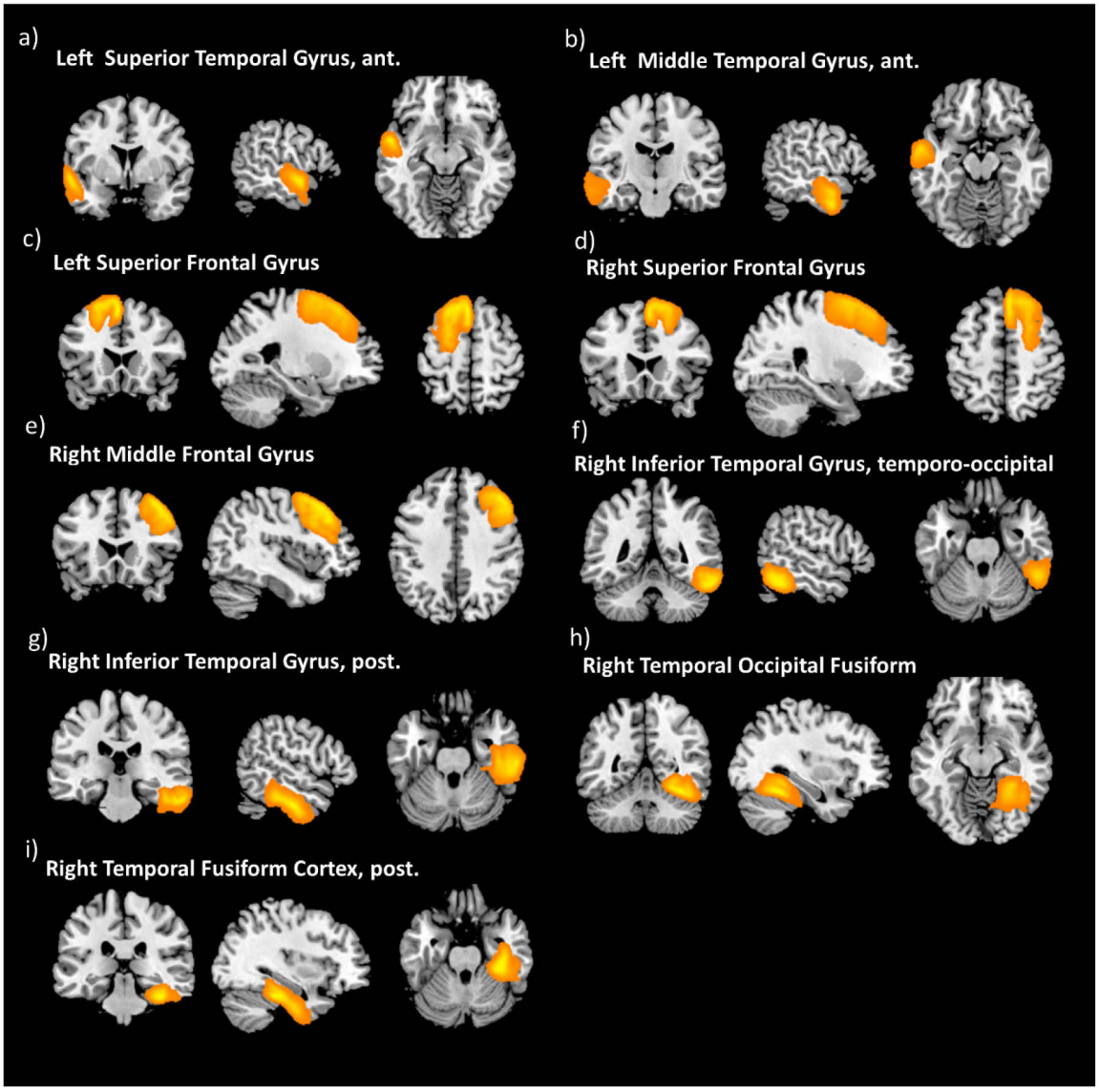

Figure 3-15: ROIs for which significant decreased CBF in PDD patients were found. The ROIs are displayed on the 152-MNI standard template.

Table 3-22: Bonferroni corrected post-hoc multiple comparison results for CBF ROI analysis

	PD-N > PDD		***PD-MCI > PDD***	
	Left	**Right**	**Left**	**Right**
ROIs	***p***	***p***	***p***	***p***
Inf. Tmp. gyr. - post.	-	0.000	-	0.001
Inf. Tmp. gyr. - TO.	-	0.000	-	0.002
Mid. Frt. gyr.	-	0.001	-	0.001
Mid. Tmp. gyr. - ant.	0.003	-	0.000	-
Sup. Frt. gyr.	0.000	0.001	0.000	0.001
Sup. Temp. gyr.	NS	-	0.000	-
Tmp. Fus. C. - post.	-	0.001	-	0.002
Tmp. Occ. Fus	-	0.001	-	0.003

Remark: Bonferroni adjusted alpha for 9 ROIs ($p<0.0055$).

3.6.3.3 Correlations of the CBF values with Clinical and Neuropsychological Variables

In order to further investigate the dependency of the clinical and neuropsychological status of the PD patients on cerebral blood flow changes in various parts of the brain, one-tailed non-parametric (Spearman's) bivariate correlation analyses were carried out for the significant findings obtained in ASL analyses and the clinical and neuropsychological data collected from the 52 PD patients.

For Bonferroni correction, the parameters were grouped in categories and based on the numbers of parameter in the groups the alpha was adjusted: clinical data ($p < 0.01$), global neuropsychological tests ($p < 0.0071$) and specific neuropsychological tests ($p < 0.0071$).

The correlation analysis of the CBF in the investigated ROIs of the ASL analyses and the clinical and neuropsychological variables delivered a rich set of multiple correlations (Table 3-23). The CBF in all investigated ROIs were positively correlated with disease duration and negatively correlated with clock drawing. The SDMT and cube copying showed positive correlations only with the temporo-occipital region of the right inferior temporal gyrus. The semantic fluency and pentagon copying were similarly correlated with the CBF of all ROIs except with the anterior part of the superior temporal gyrus. The phonemic fluency positively correlated with the posterior and temporo-occipital regions of the right inferior temporal gyrus. The UPDRS – total, UPDRS - cognitive score, Hoehn & Yahr scale, and ACE-R showed similar negative correlations with the CBF values of most of the ROIs, while the UPDRS-III was negatively correlated only with the left superior frontal gyrus and the temporo-occipital region of the right inferior temporal gyrus.

The MOCA showed positive correlations with the CBF of the left superior frontal gyrus, the right middle frontal gyrus and posterior and the temporo-occipital parts of the right inferior temporal gyrus. The number of the mistakes during the Stroop test was negatively correlated with the CBF of the right inferior temporal gyrus and the right temporal fusiform cortex. Finally, the number of the categories of the WCST was positively and the number of WCST errors was negatively correlated with the CBF of the left superior frontal gyrus, right middle frontal gyrus, the posterior and temporo-occipital parts of the right inferior temporal gyrus, the posterior part of the temporal fusiform cortex and the right temporal occipital fusiform cortex.

Table 3-23: Correlation of ASL findings and the clinical and neuropsychological parameters

Arterial Spin Labeling - ROIs										
Clinical / neuropsychological variables		MTG-ant.-L	STG-ant.-L	SFG-L	ITG-post.-R	ITG-TO-R	MFG-R	SFG-R	*TFC-post*.-R	*TOFC*.-R
Disease Duration [a)]	Corr.Coef.	-0.466	-0.373	-0.324	-0.304	-0.450	-0.321	-0.234	-0.284	-0.308
	p (1-tailed)	0.001	0.009	0.009	0.015	0.000	0.010	0.047	0.022	0.014
UPDRS – Total [b)]	Corr.Coef.	-0.375	-0.302	-0.410	-0.392	-0.425	-0.334	-0.330	-0.325	-0.220
	p (1-tailed)	0.009	NS	0.001	0.002	0.001	0.008	0.009	0.010	NS
UPDRS – III [b)]	Corr.Coef.	-0.279	-0.237	-0.362	-0.312	-0.367	-0.282	-0.302	-0.260	-0.215
	p (1-tailed)	NS	NS	0.004	NS	0.004	NS	NS	NS	NS
UPDRS – Cognitive [b)]	Corr.Coef.	-0.495	-0.351	-0.408	-0.472	-0.507	-0.380	-0.258	-0.439	-0.414
	p (1-tailed)	0.001	NS	0.001	0.000	0.000	0.003	NS	0.001	0.001
Hoehn & Yahr [b)]	Corr.Coef.	-0.373	-0.388	-0.475	-0.344	-0.373	-0.418	-0.411	-0.326	-0.269
	p (1-tailed)	0.009	0.007	0.000	0.007	0.003	0.001	0.001	0.010	NS
ACE-R [c)]	Corr.Coef.	0.445	0.299	0.484	0.502	0.598	0.425	0.319	0.445	0.437
	p (1-tailed)	0.002	NS	0.000	0.000	0.000	0.001	NS	0.001	0.001
Phonemic Fluency [c)]	Corr.Coef.	0.314	0.298	0.331	0.371	0.406	0.273	0.261	0.326	0.305
	p (1-tailed)	NS	NS	NS	0.004	0.002	NS	NS	NS	NS
Semantic Fluency [c)]	Corr.Coef.	0.499	0.324	0.469	0.434	0.502	0.416	0.411	0.421	0.398
	p (1-tailed)	0.001	NS	0.000	0.001	0.000	0.001	0.001	0.001	0.002
Pentagon Copy [c)]	Corr.Coef.	0.462	0.366	0.477	0.444	0.540	0.514	0.479	0.383	0.377
	p (1-tailed)	0.001	NS	0.000	0.001	0.000	0.000	0.000	0.003	0.003
Cube Copy [c)]	Corr.Coef.	0.254	0.128	0.221	0.316	0.421	0.250	0.156	0.282	0.310
	p (1-tailed)	NS	NS	NS	NS	0.001	NS	NS	NS	NS
Clock Drawing [c)]	Corr.Coef.	0.440	0.294	0.424	0.452	0.548	0.451	0.344	0.401	0.459
	p (1-tailed)	0.002	NS	0.001	0.000	0.000	0.000	0.006	0.002	0.000
MOCA [c)]	Corr.Coef.	0.301	0.118	0.391	0.393	0.532	0.409	0.228	0.349	0.370
	p (1-tailed)	NS	NS	0.006	0.006	0.000	0.004	NS	NS	NS
Stroop - Mistakes [c)]	Corr.Coef.	-0.244	-0.261	-0.357	-0.447	-0.296	-0.220	-0.284	-0.425	-0.237
	p (1-tailed)	NS	NS	NS	0.001	NS	NS	NS	0.002	NS
SDTM - Total [c)]	Corr.Coef.	0.056	0.034	0.343	0.330	0.424	0.302	0.234	0.272	0.271
	p (1-tailed)	NS	NS	NS	NS	0.003	NS	NS	NS	NS
SDTM - Correct [c)]	Corr.Coef.	0.084	0.033	0.337	0.340	0.400	0.292	0.227	0.283	0.276
	p (1-tailed)	NS	NS	NS	NS	0.005	NS	NS	NS	NS
WCST - Categories [c)]	Corr.Coef.	0.242	0.343	0.452	0.455	0.456	0.389	0.384	0.481	0.427
	p (1-tailed)	NS	NS	0.002	0.002	0.002	0.007	0.007	0.001	0.003
WCST - Error [c)]	Corr.Coef.	-0.205	-0.285	-0.357	-0.507	-0.430	-0.414	-0.343	-0.492	-0.350
	p (1-tailed)	NS	NS	NS	0.000	0.003	0.004	NS	0.001	NS

Remarks: a) $p < 0.05$, b) $p < 0.01$, c) $p < 0.0071$. R: right, L: left, MTG-ant.: medial temporal gyrus, STG-ant.: superior temporal gyrus anterior, SFG: superior frontal gyrus, ITG-post.: inferior temporal gyrus posterior, ITG-TO: inferior temporal gyrus temporooccipital, MFG: middle frontal gyrus, TFC-post.: temporal fusiform cortex posterior, TOFC: temporal occipital fusiform cortex.

3.6.4 MR Spectroscopic Imaging (MRSI)

In order to investigate the metabolical changes related to cognitive decline in PD, we measured the resonances of NAA+NAAG, creatine (Cr), choline (Cho), glutamine/glutamate complex (Glx) and myo-Inosytol (mI) from two separate FOVs (Figure 3-16) obtained in two separate proton MR spectroscopic imaging (1H-MRSI) scans on two FOVs and evaluated the metabolite ratios with respect to creatin: NAA+NAAG/Cr, Cho/Cr, Glx/Cr, and mI/Cr. Because of the high temporal requirements of the MRSI measurements, whole brain coverage is not feasible, hence the two FOVs have been placed in such a way that mainly areas possibly related with cognitive dysfunctions in PDD were covered.

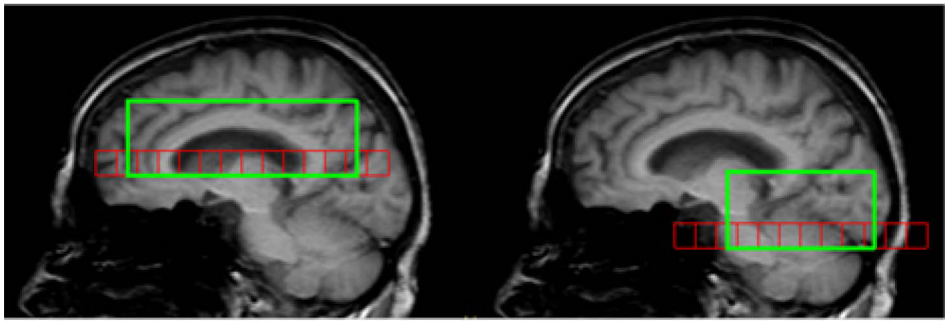

Figure 3-16: Example of the two FOV positions displayed on an original PDD patient's brain

The MRSI data of all patients were obtained but due to a failure in the data set of two PD-N patients, the analyzed data set was composed of 50 patients.

Using the LCModel and the recently developed software by Cengiz and Öztürk-Isık (2016a and b), the metabolite concentrations were estimated and evaluated using the ROI-based approach. In total, 54 ROIs were extracted from the Harvard-Oxford Cortical Structural Atlas, the MNI Structural Atlas and the Harvard-Oxford Subcortical Structural Atlas.

Because of the relatively higher variability of the MRSI variables among the investigated population, we limit the between-group comparisons for MRSI data to focus on the differences between the PDD patients and the rest of the PD-non-demented group (PD-N and PD-MCI together).

3.6.4.1 Independent samples T-test

The mean metabolite ratios of voxels within the ROIs were compared for PDD vs PD-non-demented by using t-tests. The adjustment of alpha for multiple comparisons ($p < 0.05/54 = 0.00093$) was very conservative for MRSI results, thus no significant differences survived the

comparisons. Therefore, we report the results for uncorrected data with $p < 0.05$, which, however, will only be discussed in terms of their conjunction with significant results in other MRI modalities.

The PDD group showed significantly reduced NAA+NAAG/Cr ratios in the posterior portion of the left middle temporal gyrus (L-mid. temp. gyr.-P), the left and right precuneus (L and R-precuneus), the right angular gyrus (R-angular gyr.), the right central opercular cortex (R-central opercular C.), the right superior frontal gyrus (R-sup. front. gyr.) and caudate nucleus compared to the non-demented PD group ($p < 0.05$) (Table 3-24).

The PDD patients further displayed significantly increased Cho/Cr in the temporo-occipital portion of both the right inferior temporal gyrus (R-inf. temp. gyr.-TO.) and the right middle temporal gyrus (R-mid. temp. gyr.-TO.) compared to PD-non-demented ($p < 0.05$) (Table 3-25).

Beyond that, the PDD group displayed significantly higher Glx/Cr in the left and right superior frontal gyrus (L- and R-sup. front. gyr.), the temporo-occipital region of the right middle temporal gyrus (R-mid. temp. gyr.-TO.) and the juxtapositional lobule cortex when compared to PD-non-demented ($p < 0.05$) (Table 3-26).

Finally, the PDD group displayed significantly increased mI/Cr ratios in the left superior frontal gyrus (L-sup. front. gyr.) compared to PD-non-demented ($p < 0.05$) (Table 3-27).

Table 3-24: NAA+NAAG/Cr comparison between PDD and PD-non-demented

NAA+NAAG/Cr					**Independent t-test**	
ROI	**Group**	***n***	***M***	***sd***	***t***	***p***
L-mid. temp. gyr.-P	PD-nd.	27	4.33	2.16	2.057	0.046
	PDD	18	3.21	1.48		
L-precuneus	PD-nd.	32	1.49	0.08	2.458	0.021
	PDD	18	1.41	0.12		
R-precuneus	PD-nd.	32	1.62	0.39	2.112	0.041
	PDD	18	1.46	0.13		
R-angular g.	PD-nd.	32	1.97	0.89	2.058	0.046
	PDD	18	1.62	0.32		
R-central opercular C.	PD-nd.	32	1.64	1.04	2.178	0.035
	PDD	17	1.19	0.41		
R-sup. front. gyr.	PD-nd.	31	1.80	0.86	2.125	0.040
	PDD	17	1.45	0.24		
Caudate	PD-nd.	32	1.29	0.17	2.811	0.009
	PDD	18	1.11	0.22		

Remarks: p < 0.05

Table 3-25: Cho/Cr comparison between PDD and PD-non-demented

Cho/Cr					**Independent t - test**	
ROI	**Group**	***N***	***M***	***sd***	***t***	***p***
R-inf. temp.gyr.-TO.	PD-nd.	31	0.27	0.05	-3.362	0.002
	PDD	18	0.33	0.06		
R-mid. temp. gyr.-TO.	PD-nd.	32	0.28	0.06	-3.209	0.003
	PDD	18	0.34	0.06		

Remarks: $p < 0.05$

Table 3-26: Glx/Cr comparison between PDD and PD-non-demented

Glx/Cr					**Independent t - test**	
ROI	**Group**	***N***	***M***	***sd***	***t***	***p***
L-sup. front. gyr.	PD-nd.	31	2.60	1.11	-2.139	0.044
	PDD	17	3.70	1.96		
R-sup. front. gyr.	PD-nd.	31	2.27	0.92	-3.631	0.002
	PDD	16	4.19	2.00		
R-angular gyr.	PD-nd.	30	3.63	2.22	-2.106	0.041
	PDD	18	5.12	2.60		
R-mid. temp. gyr.-TO.	PD-nd.	30	2.77	1.56	-2.403	0.025
	PDD	17	4.42	2.57		
Juxtapositional Lobule C.	PD-nd.	31	1.87	0.84	-2.173	0.043
	PDD	17	3.00	2.04		

Remarks: $p < 0.05$.

Table 3-27: mI/Cr comparison between PDD and PD-non-demented

mI/Cr					**Independent t - test**	
ROI	**Group**	***N***	***M***	***sd***	***t***	***p***
L-sup. front. gyr.	PD-nd.	31	1.32	0.23	-2.094	0.042
	PDD	17	1.50	0.39		

Remarks: $p < 0.05$.

3.6.5 Discriminant analyses for the combination of significant multimodal MRI findings for the diagnosis of PDD

In a final step, we tried to create a multimodal model based on the variables of various neuroimaging methods that when tested in a single modality resulted in significant differences between the patient groups. This is carried out by testing the performance of a discriminant function by stepwise entering the variables from rs-fMRI, DTI and ASL modalities for the correct classification of the PDD cases with leave-one-out cross-validation technique. For this purpose, we entered in three main steps the expression scores of the RSNs that best discriminated the three groups from each other, mean values of the FA, MD, RD and AD values in the DTI ROIs and mean CBF values obtained from the ROIs of the ASL measurements that resulted in significant group differences in variance analyses among the three groups in a stepwise discriminant analysis and evaluated the performance of the resulting discriminant functions in discriminating the PDD patients from PD-N or PD-MCI groups. The results of the discriminant analyses are shown in Table 3-28 and Table 3-29.

Table 3-28: Discriminant analyses using the RSNs

PDD vs PD-N (RSN)				**PDD vs PD-MCI (RSN)**			
Limbic NW		**PD-N**	**PDD**			**PD-MCI**	**PDD**
	PD-N	11	5	**DMN**	PD-MCI	13	5
FSN	PDD	3	15		PDD	4	14
	%	68.8	31.3	**Limbic NW**	%	72.2	27.8
SN		16.7	83.3			22.2	77.8

Table 3-29: Discriminant analyses using the combined RSNs and DTI-derived FA, MD, RD and AD values

PDD vs PD-N (RSN + DTI)				**PDD vs PD-MCI (RSN + DTI)**			
FA-SLF temp.-L		**PD-N**	**PDD**			**PD-MCI**	**PDD**
MD-Cingulum cingulat gyr.-L	PD-N	15	1		PD-MCI	15	3
	PDD	0	18	**AD ILF-L**	PDD	3	15
AD-ILF-L		93.8	6.3			83.3	16.7
FSN	%			**Limbic NW**	%		
		0.0	100.0			16.7	83.3
SN							

The rs-fMRI variables resulted in a cross-validated accuracy of 76.5% with 83.3% sensitivity and 68.8% specificity for the discrimination of the PDD patients from the PD-N patients, while the cross-validated classification accuracy for the PDD vs PD-MCI discrimination was 75.0% with 77.8% sensitivity and 72.2% specificity. With the inclusion of the DTI variables in the discriminant model, the performance for the PDD vs PD-N discrimination increased to 97.1% overall accuracy with 100.0% sensitivity and 93.8% specificity, while for the PDD vs PD-MCI classification the performance increased to 83.3% overall accuracy with 83.3% sensitivity and specificity. Further inclusion of the ASL variables into the stepwise discriminant analysis did not further increase, but even slightly decrease the accuracy for the PDD vs PD-N classification to 88.2% with 100.0% sensitivity but 75.0% specificity. A similar effect was also observed with the inclusion of the ASL values for the discrimination of PDD cases from PD-MCI cases, yielding 80.0% overall accuracy with 100.0% sensitivity but only 61.1% specificity. In short, the discriminant analyses performed best when rs-fMRI and DTI parameters were used in a multimodal manner for the discrimination of PDD group from both PD-N and PD-MCI groups.

4 DISCUSSION

Cognitive decline is common in Parkinson's disease, that is primarily considered as a movement disorder, and the presence of mild cognitive impairment in PD may represent a prodromal state for the specific type of dementia observed in PD patients. Still, it is not well understood, whether PD-MCI and PDD display different severity stages of the disease progression or whether they may indeed represent different pathological patterns. Therefore, it is important to identify the clinical and neuropathological characteristics of different stages of cognitive decline in PD and to identify the predictors for the development of PDD. Although clinical diagnostic criteria for cognitive decline have been developed in recent years (Litvan et al., 2012; Emre et al., 2007), the diagnosis of PD-MCI and PDD is still only based on the judgment of a clinician and arbitrarily set cut-off values of neuropsychological test scores. So far, there are no reliable biomarkers available that directly represent the underlying pathophysiological processes in PD-MCI and PDD or that can be used for the identification of PD patients with high dementia risk.

Being able to follow the neuropathological changes along the progression of cognitive deficits with methods that have anatomical localization capability and sensitivity to pathological changes in the brain tissue will help to define a discriminative biomarker for cognitive decline in PD, and help to identify PD patients with increased risk of developing dementia.

In this study, we investigated the progressive neuropathological changes occurring at different stages of cognitive decline in Parkinson's disease using multimodal MRI techniques, with the aim to derive a discriminative biomarker for dementia in PD.

Therefore, we analyzed the combined clinical, neuropsychological and multimodal MRI data from 52 age-matched PD-N, PD-MCI and PDD patients.

4.1 Demographic and Clinical Observations

The PDD showed significantly longer disease duration and severe motor deficits than PD-N and PD-MCI as indicated by their scores for the UPDRS and Hoehn & Yahr scale. Disease duration and symmetry of motor symptoms have already been reported to be risk factors for PDD (Emre et al., 2007). As PD-N and PD-MCI did not differ significantly from each other in any of the demographic or clinical parameters, our findings for the non-demented patients and PDD exactly support the described findings in the literature. The cognitive score obtained from

the UPDRS revealed to be quite accurate, as the PDD group scored significantly worse than the PD-N and PD-MCI, while the PD-N and PD-MCI did not differ significantly from each other. As high age is known to be one major risk factor for PDD (Hanagasi et al., 2017), we matched the mean age of the groups and thereby tried to investigate the cognitive decline in PD independent form age but related to the neuropathological changes. Still, the PD-N showed significantly higher education level than PDD, which is also in line with findings about lower education being a risk factor for the development of cognitive decline.

4.2 Differences in Neuropsychological Test Performance

The Addenbrooke's Cognitive Examination Revised proofed to be a handy global test for quick administration and examination of most of the cognitive domains. Still, during examination it became clear, that the ACE-R was more sensitive for higher educated patients than patients with lower education. However, supported by other test performances, the chosen cut-off of ≤ 83 for PD-MCI diagnosis seems to be appropriate.

The ACE-R and MOCA test results differed significantly between the PD-N, PD-MCI and PDD groups, while the MMSE scores did not differ between the PD-N and the PD-MCI groups.

None of the groups showed significant difference regarding the Navon, number of spontaneous corrections in the Stroop and the % of perseverative errors in the Wisconsin Card Sorting Test.

PD-MCI and PDD did neither differ regarding their performance in the JOLO, the phonemic fluency test, the Stroop effect, the WCST nor the SDMT. In contrast, significantly worse performance in the semantic fluency, pentagon copying, cube copying and clock drawing as well as the number of mistakes in the Stroop test seems to be specific for PDD, as we did observe significant differences between PDD vs PD-MCI groups and between PDD vs PD-N groups, but not in PD-N vs PD-MCI comparison.

The findings may proof that the cognitive decline in PD starts with executive dysfunction (Emre et al, 2007) and that the additional dysfunction of more temporally located abilities (semantic fluency), visuo-spatial and visuo-construction abilities as well as planning skills may be an indicator or risk factor for dementia in PDD (Williams-Gray et al., 2007 and 2009).

Although, the PDD and PD-MCI did not differ significantly for the JOLO test, the amount of PDD patients not being able to complete the JOLO test might be an indicator for an even more

affected visuospatial function in PDD. Most of the PDD patients, who could not complete the JOLO test, understood the task, but, due to unsuccessful performance in the training part, their tests could not be scored.

In summary, the clinical and neuropsychological observations confirmed the correct assignment of the PD patients to the related study groups, namely the PD-N, PD-MCI and PDD, which was necessary for the reliable analysis of the related MRI data.

4.3 Dementia related resting-state fMRI differences in PD

After the resting-state networks (RSN) in the rs-fMRI data were obtained using the GIFT toolbox based on the independent component analysis (ICA), we used two different methods for the analysis of the RSN differences among the patient groups, namely the binary logistic regression based on the expression level of each RSN in each single subject and voxel-based comparison of the RSNs between pairs of patient groups.

The expression score of each RSN in each subject is a scalar value that represents the level of the similarity of the subject's RSN topography with that of the aggregate RSN representing the whole group of patients. As a result, these scalar expression scores create a comprehensive but significantly reduced set of variables that represent efficiently the whole spectrum of large-scale neural networks existing in the resting-state data. The mathematical constraint of the spatial ICA algorithm for the estimation of the RSNs to be spatially maximally independent from each other, allows for optimal application of multivariate regression analyses on these expression scores, as already applied for various brain disorders in previous studies (Gruner et al., 2014). Therefore, the discriminative power of the RSN expression scores among the patient groups was tested by means of binary logistic regression analyses.

Based on the logistic regression analyses we identified the combination of the RSNs that best discriminated PDD from the non-demented PD patients. Those networks discriminating PDD from PD-N or PDD from the combined group of PD-N and PD-MCI (PD-non-demented) were the limbic network, frontostriatal network (FSN), default mode network (DMN) and salience network (SN) with lower expression of the first two networks and stronger expression of the latter two networks in PDD. Furthermore, the lower expression of the posterior-temporal network (PTN) in combination with the lower expression of the limbic network and higher expression of the DMN was successful in discriminating PDD from PD-MCI.

While the decreasing expression of the PTN representing generally the ventral visual stream, the limbic network and the frontostriatal network in PDD are more or less in accordance with the general pattern of the cognitive impairments in visuo-spatial, memory and executive domains, the increased intrinsic connectivities of both DMN and SN builds a contra-intuitive pattern, because in many disorders the DMN hypo-connectivity is the main correlate of the cognitive decline as it is a characteristic feature in Alzheimer pathology (Seeley et al., 2009. Additionally, DMN hypo-connectivity was also previously reported in several studies on cognitively unimpaired PD patients vs healthy controls (Tessitore et al., 2012; Amboni et al., 2015, Goettlich et al., 2013).

On the other hand, several studies (Eimeren et al., 2009; Ibarretxe-Bilbao et al., 2011) pronounced the reduced level of deactivation of the posterior DMN nodes in PD patients during an executive task independent from the age of the patients, while Baggio and colleagues (2015) reported even increased connectivity between the DMN and occipito-parietal regions that were associated with visuospatial dysfunction in PD-MCI. As the progressive increase of the DMN connectivity in our results is observed in PD patients with increasing cognitive symptoms, it is possible that, when compared to age-matched healthy controls, our data would also yield an overall reduced DMN connectivity in-line with the results of first group of studies. On the other hand, as the identified DMN in our study displays a more posteriorly weighted spatial pattern, with almost no fronto-medial involvement, our finding of a progressively increasing DMN connectivity from PD-N to PDD groups is generally in accordance with the reports on the posterior DMN reactivity in the task-based fMRI studies by Eimeren et al (2009) and Baggio et al. (2015).

One might speculate that the anti-dementia drugs (acetylcholinesterase inhibitors) and anti-psychotics (quetiapine, lithium, clozapine) used only in the PDD group might have an effect on the higher DMN expression, but although the expression of the DMN was statistically significant in the PDD group, the PD-MCI group also exhibited a stronger DMN compared to the PD-N suggesting that the DMN hyperactivity stems not from this type of drug treatment.

Finally, there are studies suggesting a modulatory effect of L-Dopa, in terms of restoring the reduced DMN deactivation during task based fMRI (Deleveau et al., 2010,). As, however, similar number of patients in our 3 patient groups received L-Dopa treatment, the progressive increase of the DMN connectivity along the PD-N to PDD axis cannot be explained by the effect of L-Dopa administration.

In summary, the DMN related findings in PD and PDD dementia in recent literature are controversial but mostly related to reduced deactivation pattern in task-fMRI studies, where our finding of the increased posterior DMN connectivity in PDD in resting-state shows that such dysfunctional property of the DMN can also be obtained in resting-state recordings without the need of applying a complex cognitive task.

Similar to the DMN pattern we also observed a progressive increase of the SN connectivity from PD-N through PD-MCI to PDD, while the difference reached significance only between the PDD vs PD-N or PD-non-demented patients. This pattern of the increasing DMN and SN connectivities with increasing cognitive decline is in contrast to the decreased DMN vs increased SN connectivity pattern in Alzheimer's dementia (AD) and increased DMN vs decreased SN connectivity pattern in behavioral variant of the fronto-temporal dementia (bvFTD) (Zhou et al., 2010). According to the model proposed by Bressler and Menon (2010), under physiological conditions SN acts as a dynamic switch that in the presence of salient events gets activated and suppresses the DMN and mobilizes the cognitive resources in favor of the central-executive network, while in the absence of salient events the decreased activation of SN results in increased DMN activity. This model explains the anticorrelated activation of SN vs DMN, which seems to be disrupted in PDD.

Christopher et al (2013 and 2014) by using PET found combined striatal dopamine denervation and D2 receptor loss in the bilateral insula to be related with cognitive decline in PD-MCI that seems especially associated with the executive dysfunction. This reduction of the inhibitory input to insula might lead to aberrant connectivity within the SN, which than cannot efficiently modulate the DMN and executive networks. In fact, alpha-synuclein deposition in the insula in the later stage of the disease (stage 5 of 6) has been described by Braak et al. (2003), and the deposition might be responsible for various alterations regarding neural activity, synaptic function and receptor modulation leading to altered within-network connectivities (Christopher et al., 2013 and 2014).

Studies on the functional connectivity of the insula in healthy subjects (Cauda et al., 2011) suggest the involvement of the insula in two major networks. The connections of the anterior insula with the middle temporal, inferior temporal and anterior cingulate cortex, corresponding by large to the SN, associates the insula with the limbic network, while the posterior insula connects by large with the middle posterior cingulate cortex, the premotor, sensorimotor and supplementary motor areas related with sensorimotor integration. The

reduced functional connectivity in parts of the limbic network in the PDD group in our data might therefore be an indirect result of abnormal insula functional connectivity pattern.

While the two important modulatory RSNs, DMN and SN, increase their intrinsic connectivity with increasing cognitive decline, other RSNs related with executive, memory and visuo-spatial functions, namely FSN, limbic network and PTN showed significant reductions of their intrinsic connectivity, which will be discussed in detail below in connection with correlated findings in other MRI modalities.

The findings of the functional connectivity analysis using whole-brain voxel-based comparisons by large supported the findings from the logistic regression analysis (Table 3-9), but could further shed light on the spatial details of the dysfunctions in the RSNs. We found decreased functional connectivity in the thalamus as part of the limbic network and increased functional connectivity in the right insula of the salience network in PDD compared to PD-N. When PD-MCI and PDD were compared, decreased functional connectivity was found in PDD in the left and right hippocampi as part of the limbic network. Furthermore, the PDD group showed decreased functional connectivity in the left hippocampus and right thalamus within the limbic network when compared to PD-non-demented group in addition to decreased functional connectivity of the caudate and putamen in the frontostriatal network. Our findings about the decreased functional connectivity in limbic network are in accordance with previous reports on atrophies in various limbic structures in PDD (Goldman, 2012). Additionally, decrease of the functional connectivity in the FSN of PDD patients, specifically in the caudate, has been previously reported by Seibert and colleagues using a seed-based approach in native-space analyses of rs-fMRI data (Seibert et al., 2012), which is also in-line with our FSN findings.

In short, in terms of large-scale functional network characteristics the FSN, limbic NW and PTN related with executive functions, memory and visuo-spatial functions show significant decreases in intrinsic connectivities specifically in PDD patients, while the two modulatory neuro-cognitive networks, DMN and SN, show a progressive increase in network connectivity. These findings, in general, point to that in fMRI signals the degeneration in neuro-cognitive networks directly related with the functional loss in PDD are manifested in relatively late stages of the process, while the dysfunctional signals in the neuro-modulatory networks appear in earlier stages of the cognitive decline. In the present study, the increases in DMN and SN connectivities that reached significance in the PDD group were still observable in

PD-MCI group, although at a non-significant level. This might depend on the fact that around 50% of the PD-MCI cases that will convert to PDD in long term (Hanagasi et al., 2017; Pigott et al., 2015) show this pattern, while the non-converters dilute the finding to a non-significant level. On the other hand, when tested on a larger group of PD-MCI cases with sub-grouping according to longitudinal evaluation of conversion to PDD, the DMN and SN features might be predictive markers for dementia development.

4.4 Dementia related structural changes in PD revealed by DTI data

Additional to the functional data, we collected DTI data to gain information about structural changes related to cognitive decline in PD. A ROI-based approach was used in order to investigate white matter changes for the study groups. We evaluated the fractional anisotropy (FA) values among the groups and identified 12 regions of interest (ROIs) with significantly differing FA values, stemming from decreased FA values in PDD patients compared to PD-N in the right anterior thalamic radiation (ATR-R), left and right cortico spinal tract (CST-L and R), the left and right cingulum cingulate gyrus (Cing. Cingulate gyr-L and R), left and right inferior fronto-occipital fasciculus (IFOF-L and R), the inferior fronto longitudinal fasciculus (ILF-L and R), the left and right superior longitudinal fasciculus (SLF-L and R) and the left temporal superior longitudinal fasciculus (SFL Temp.-L) as well as decreased FA values of the PDD group in the CST-L, IFOF-L and SFL Temp.-L compared to PD-MCI, while PD-MCI did not show any significant FA difference compared with PD-N.

We further investigated the corresponding mean diffusivity (MD), radial diffusivity (RD) and axial diffusivity (AD) values in the same RIOs and found in general increased MD, RD and AD values in PDD. While increased MD and RD values support the white matter degeneration in ROIs with low FA, the increase of AD seems to be inconsistent with decreased FA values. However, it has been reported before, that simultaneous increase of AD in parallel with stronger increase in RD is consistent with decreased FA values in degenerating WM fibers (Mascalchi et al., 2015).

Notably, although the ROI based approach had the trade-off of rather large-sized ROIs, which were limited in localization sensitivity within the tracts, the obtained measurements were strong enough to reveal significant differences in DTI measurements among the patient groups which points to a global white matter disruption in PDD compared to the non-demented patients.

Our findings further suggest a mainly bilateral pattern of white matter changes in various white matter tracts in the PDD patients compared to PD-N but a left lateralization pattern when compared to PD-MCI. Hence, the degeneration in the left CST, left IFOF and the left temporal SLF as indicated by reduced FA values may be crucial for the discrimination between MCI and dementia in PD, and as the MD and AD of the left ILF were further significantly increased in PDD compared to PD-MCI, we will discuss these tracts in more detail in the following.

The SLF consists of three sub-parts (I, II, III), with the SLF II representing its main component. While the dorsally located SLF I is mostly known to be involved in the regulation of motor aspects and the initiation of motor activity by connecting the supplementary and premotor areas with the superior parietal and medial parietal cortex (Schmahmann et al., 2008), the SLF II is located more lateral and links the caudal inferior parietal cortex and parietooccipital areas with the dorsolateral prefrontal cortex. Based on the anatomical connection of the SLF II it is suggested that it contributes largely to the dorsal visual stream (Ffytche et al., 2010) and thereby is important for visual awareness and spatial attention (Schmahmann et al., 2008). Finally, the ventrally in the operculum located SLF III is thought to play a major role in the transfer of somatosensory information between the operculum, the premotor areas and parietal lobe (supramarginal gyrus) and therefore is thought to be important for articulatory and phonemic language aspects (Schmahmann et al., 2008).

The IFOF on the other hand is especially known for its involvement in the ventral visual stream by linking the occipital lobe with parts of the parietal lobe, temporal lobe and the frontal lobe. The IFOF therefore is important for the integration of peripheral vision and the processing of visual spatial information (Ffytche et al., 2010; Migliaccio et al., 2012). The ILF is like the IFOF considered to be part of the ventral visual stream as it connects the occipital and temporal cortices and is thought to be involved in the symptoms of visual agnosia after damage of this tract (Migliaccio et al., 2012).

To summarize, the SLF, ILF and IFOF contribute in large parts to both the ventral and dorsal visual streams and therefore play a major role for the visuo-spatial and visuo-perceptive function. The structural changes in these tracts correlated with the pentagon copying and clock drawing performance among the whole study-group but also with test scores for the executive functions. This finding may be especially important in terms of the proposed

concept of stronger exhibited visuo-spatial dysfunction as a risk factor and marker for PDD (Williams-Gray et al., 2007 and 2009).

The corticospinal tract on the other hand plays a major role in the control of movement, as it contains descending fibers, mainly originating from the motor cortex including the premotor area, supplementary motor area towards the cingulum, brainstem and spinal cord. As the CST also connects parts of the prefrontal, parietal and ventral temporal cortex, including the parahippocampal gyrus and entorhinal cortex the CST is thought to be further involved in somatic sensation, attention and motivation (Schmahmann et al., 2008). As such, these WM changes are related with increasing motor symptoms in PDD.

The anterior thalamic radiation on the other hand is a portion of the anterior limb of the internal capsule (ALIC) and relates the prefrontal cortex and the thalamus (Mamah et al., 2010). The changes in this tract might be associated with the functional connectivity decrease observed in the FSN.

Our findings are in line with widespread cerebral white matter deterioration in PDD patients previously shown by Hattori et al. (2012) and Kamagata (2013). Neural degeneration and white matter lesions together with Lewy body deposition may characterize the white matter changes, which in turn lead to the motor and cognitive symptoms in PD and are displayed in the significant decrease of FA and increase of MA, RD and AD values in the PDD compared to the PD-N and PD-MCI patients. Agosta and co-workers (2013) showed that the dysfunction of global cognitive abilities correlates with the degree of structural changes in the white matter and that the involvement of structural changes exceeding the nigrostriatal system correlates with increasing clinical stage.

4.5 Dementia related perfusion changes in PD revealed by ASL data

The ASL method was used to track changes in cerebral blood flow related with cognitive decline in PD. Various lateralized ROIs were used to compare the CBF among the patient groups, and the PDD groups showed significant hypoperfusion in regions including the posterior part of the right inferior temporal gyrus, the right temporo-occipital part of the inferior temporal gyrus, the right middle frontal gyrus, the anterior portion of the left middle temporal gyrus, bilateral superior frontal gyrus, left superior temporal gyrus and the posterior portion of the right temporal fusiform cortex together with the right temporal occipital

fusiform cortex compared to PD-N and PD-MCI, while there were no significant differences in CBF between PD-N and PD-MCI.

The identified extensive cortical hypo-perfusion in PDD patients support the recent literature findings of decreased CBF in PDD and PD compared to healthy controls (Kamagata et al., 2011, Lin et al., 2016). However, as we found the CBF decrease specifically in the PDD compared to PD-N and PD-MCI groups, this may point to a PDD specific decrease of CBF.

On the other hand, Lin and colleagues (2016) demonstrated an inverse effect of dopaminergic therapy on cortical perfusion in PD patients, showing a higher perfusion decrease under L-Dopa therapy, though the modulation effect becomes less in PDD patients as the perfusion was significantly decreased during both on and off L-Dopa states in their study. On the contrary, Le Heron et al. (2014) reported comparable pattern of hypoperfusion for PDD and AD patients, pointing to shared mechanisms of neurodegeneration leading to dementia. In our study, where similar number of patients in each of the PD-N, PD-MCI and PDD groups receive L-Dopa treatment, the hypoperfusion in PDD patients has to depend on biological changes rather than the L-Dopa treatment.

The performed correlation analyses for the investigation of the dependency of the clinical and neuropsychological status of the PD patients on cerebral blood flow changes revealed a rather broad pattern of CBF correlations of the significant ROIs and the demographical, clinical and NPT scores, indicating a non-specific global decrease of CBF in PDD.

4.6 Dementia related metabolite changes in PD revealed by MRSI data

MRSI data were evaluated for PDD vs PD patients, in order to compare differences in prominent metabolite ratios within various ROIs. The investigated ROIs were chosen according to the rs-fMRI, DTI and ALS findings and the FOV size of the MRSI measurements. While many studies investigated a limited amount of voxel, our FOV size allowed the investigation of a larger area at the same time.

We did not obtain significant differences for the corrected statistics between the two groups, thus the uncorrected statistical results for the NAA+NAAG/Cr, Glx/Cr, Cho/Cr and mI/Cr ratios will only be discussed in the framework of their conjunction with results in other modalities.

4.7 Integrative Evaluation of the Multimodal Neuroimaging Findings

The findings from the different MRI modalities complement each other in in the following ways.

Divisions of the higher expressed DMN in PDD patients overlapped with white matter tracts in which structural changes were found for the PDD group. The increased connectivity within the DMN network is focused to the posterior part of the network with a rather missing connectivity to the medial prefrontal region, which is in-line with the decreased fractional anisotropy of the left and right cingulum in PDD patients, that connects the anterior and posterior parts of the DMN (Greicius et al., 2009). Additionally, MRSI data showed reduced NAA+NAAG/Cr in the left and right precuneus of PDD patients indicating a loss of neuronal integrity within that region (Figure 4-1). While the increased DMN in PDD patients may represent a compensatory mechanism for neuronal loss, it might also be related to the altered insula activation pattern we observed in PDD patients in the salience network, which has regulatory influence on the DMN activity under normal physiological conditions.

The increased functional connectivity of the insula within the salience network of the PDD patients compared to PD-N patients seems to depend mainly on the reduced inhibitory input to the insula due to combined striatal dopamine denervation and D2 receptor loss as shown in a previous study on PD-MCI (Christopher et al., 2013). Additionally, Braak et al. (2003) described alpha-synuclein deposition in the insula in the later stage of the disease, which might also count for alteration of the network connectivity (Christopher et al., 2014). On the other hand, the aberrant connectivity within the SN of the PDD patients is accompanied by WM degeneration in the left and right inferior fronto-occipital fasciculus (IFOF) and partly inferior longitudinal fasciculus (ILF), which might play a role in the connections of the insular region with the temporo-occipital regions (Figure 4-1).

The reduced NAA+NAAG/Cr in the right central operculum of PDD patients might complement these findings on the MRSI basis, as the opercular cortex borders and slightly overlaps with the insular cortex and partly connects with the ILF, although the operculum is mainly related with the SLF-III. The SLF-III on the other hand is considered to play a crucial role not only in articulatory but also in phonemic language aspects which was also displayed by correlation of the FA values of the SLF with phonemic fluency. The expression of the salience network as

well as the MD, RD and AD values of the bilateral ILF were negatively correlated with semantic fluency performance (Figure 4-1).

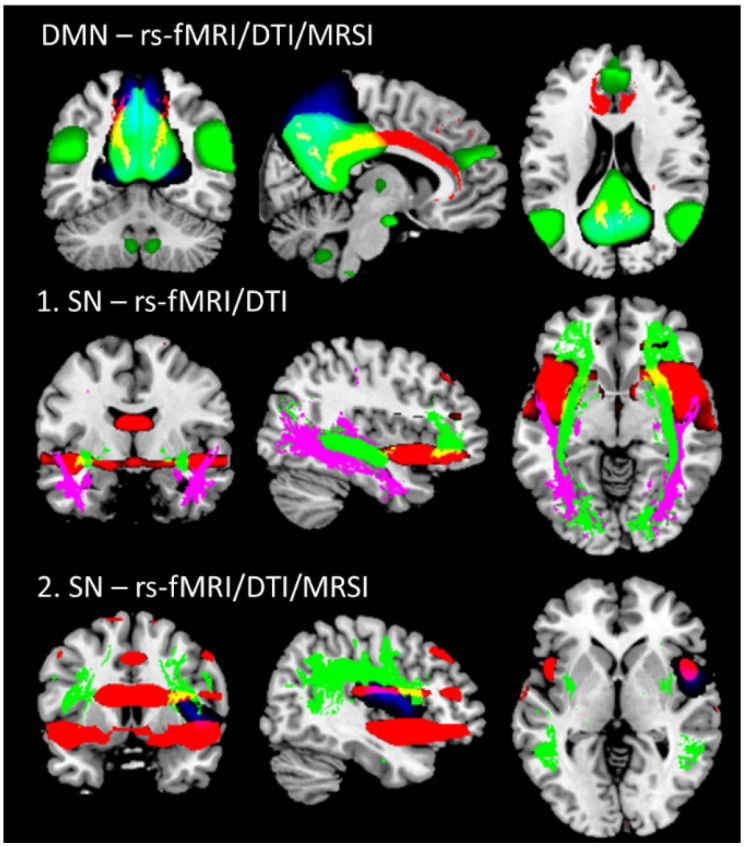

Figure 4-1: Complementary multimodal MRI findings for the default mode network (DMN) and the salience network (SN). DMN: The stronger expressed DMN in PDD is green, the right and left cingulum with decreased FA in PDD are in red and the precuneus with reduced NAA+NAAG/Cr in PDD is in blue. The additive overlap is indicated in yellow and turquoise. 1.SN: The stronger expressed SN is red, the IFOF with decreased FA is green and the ILF is violet. IFOF and SN overlaps are yellow. 2.SN: The SN is red, the SLF is green and the central opercular cortex blue. Overlaps are pink and yellow.

The lower expression of the limbic network together with the reduced functional connectivity of the right thalamus derived from the functional data in PDD patients compared to PD-N, might be partly complemented with the structural changes of the right anterior thalamic radiation obtained with DTI measurements in the PDD group (Figure 4-2). The right anterior thalamic radiation spatially also overlaps with clusters of the lower expressed frontostriatal network, in which we obtained reduced functional connectivity mainly in parts of the caudate and putamen in PDD patients compared to non-demented PD patients, and these findings might be supported by the metabolic changes displayed by the reduced NAA+NAAG/Cr in the

caudate of PDD patients revealed by MRSI data. Furthermore, the hypo-perfusion and metabolic changes in the middle and superior frontal gyrus revealed by ASL measurements also correspond to structures of the FSN, which may lead to an overall lower expression of the FSN in PDD (Figure 4-3).

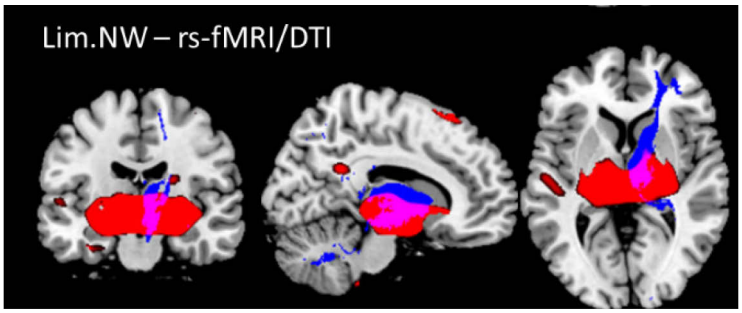

Figure 4-2: Complementary multimodal MRI findings for the limbic network (Lim.NW).
The decreased limbic network in PDD is in red and the right anterior thalamic radiation with decreased FA is in blue. The overlap is in pink.

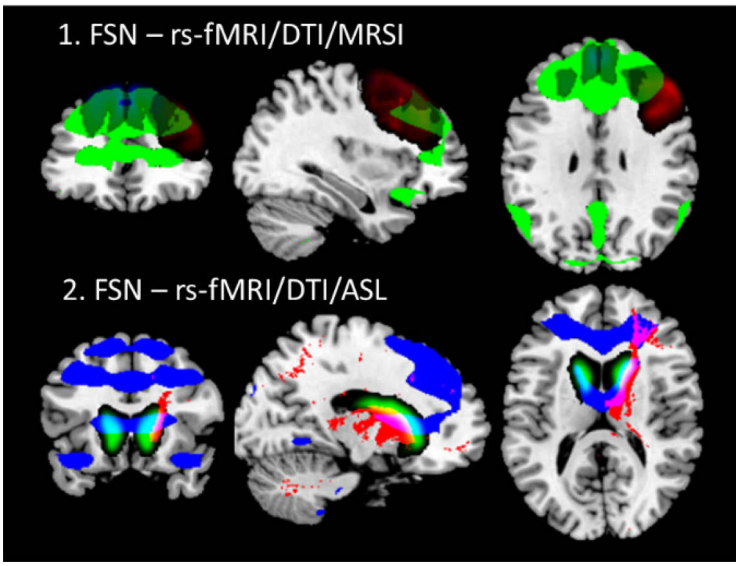

Figure 4-3: Complementary multimodal MRI findings for the frontostriatal network (FSN).
1.FSN: The decreased FSN in PDD is in green and the right left and right superior frontal gyri in blue and the right middle frontal gyrus in red displaying hypoperfusion in PDD. The overlap is dark green. 2.FSN: The decreased FSN in PDD is in blue, the right anterior thalamic radiation with decreased FA is in red and the caudate with decreased NAA+NAAG/Cr is green. The overlap is in pink, turquoise and yellow.

The posterior- temporal network (PTN), that was previously also introduced as ventral stream network in other literature (Veer et al., 2010), highly corresponds to the ventral visual stream and the reduced expression of this network in PDD patients therefore might correspond to

the structural changes of the ILF, SLF and SLF-temp in the PDD groups, as these tracts are known to be parts of the ventral stream. The changes within the PTN are also represented by decreased perfusion in the parts of the left superior and middle temporal gyri and the changes of NAA+NAAG/Cr, Cho/Cr and Glx/Cr within this region in PDD patients. While the expression level of the PTN simultaneously decreased with the years of education, the FA, MD, RD and AD values of the ILF, SLF and SLF-temp showed various correlations with the pentagon and cube copying test and the clock drawing performance over the whole group, which could represent the biological counterpart of disturbed visuo-spatial dysfunction in PDD together with the hypoperfusion in the occipital region in PDD (Figure 4-4).

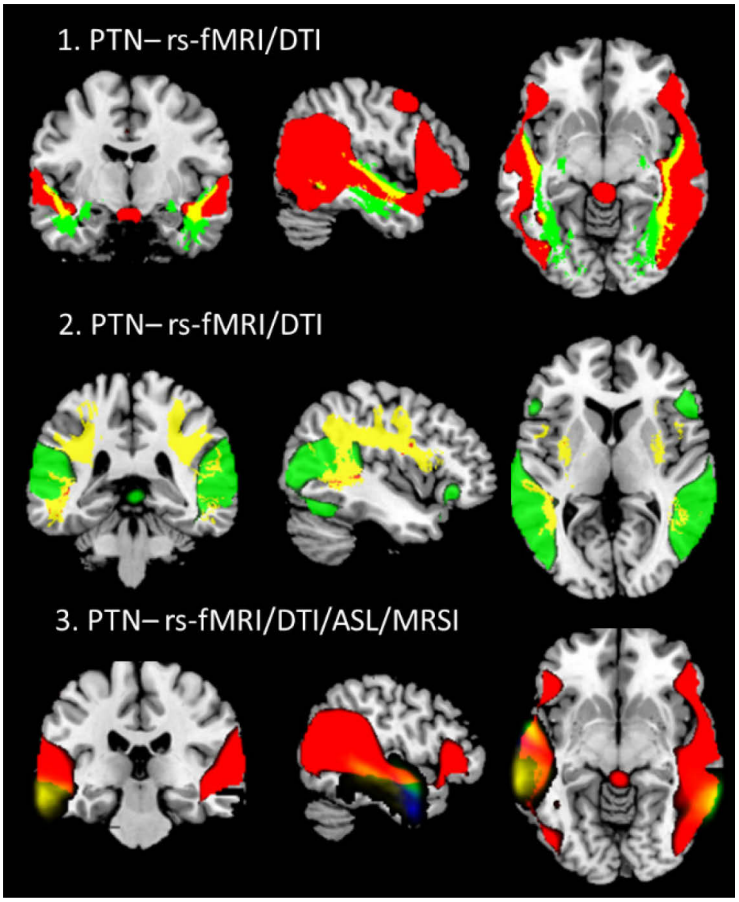

Figure 4-4: Complementary multimodal MRI findings for the posterior-temporal network (PTN). 1.PTN: The decreased PTN in PDD is in red and the right left and right ILF with decreased FA in PDD are green. The overlap is yellow. 2.PTN: The decreased PTN in PDD is in green and the right left and right SLF with decreased FA in PDD are yellow and the left SLF-temporal is orange but only very few voxels can be seen. 3.PTN: The PTN is red, the left anterior middle temporal gyrus is blue, the left posterior middle temporal gyrus is yellow and the left anterior superior temporal gyrus is green. The right temporo-occipital middle temporal gyrus is also green. Overlaps are yellow.

Finally, the severity of motor-dysfunction may be related to the degenerations in the SLF and CST of PDD patients and the metabolic changes in the supplementary motor cortex, as the mean FA of the SLF and CST were correlated with the UPDRS and Hoehn & Yahr scores (Figure 4-5).

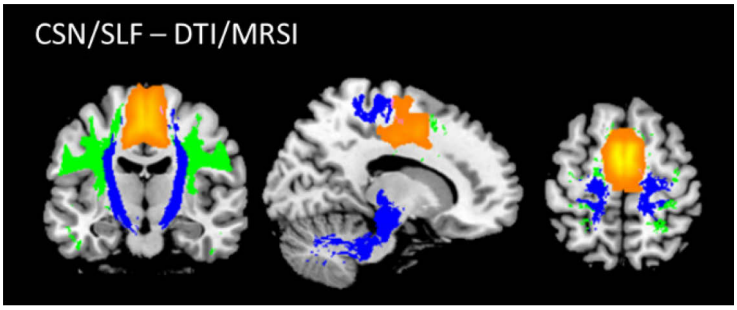

Figure 4-5: Complementary multimodal MRI findings for the corticospinal tract (CST), superior longitudinal fasciculus (SLF) and the supplementary motor area. The CST is blue and the SLF is green both showing decreased FA in PDD and the supplementary motor area with increased Glx/Cr in PDD is orange.

4.8 Discriminant analyses on multimodal MRI data

The above presented framework of multimodal MRI findings may provide insights about the evolution of neuropathological changes in PD that lead to cognitive decline and dementia. On the other hand, our results also provide a pragmatic approach for the classification of PD cases in demented and non-demented subgroups by means of a logistic regression model created on the basis of multiple RSNs obtained from fMRI data. In a last step, we will discuss the possibility to enhance the sensitivity and specificity of such regression model in discriminating the demented patients by adding significant variables of other MRI modalities into the model.

As the MRSI differences among the patient groups did not survive the statistical correction procedures, variables obtained with the rs-fMRI, DTI and ASL neuroimaging methods were fed stepwise into a discriminant analysis in order to build a multimodal regression model for the correct identification of PDD patients. For this purpose, we limited the variables to those that when tested in a single modality resulted in significant differences between the patient groups.

Indeed, the addition of the DTI variables into the model with leave-one-out cross-validation resulted in significant increases for both sensitivity and specificity, which reached 100% and 93.8% for the discrimination of PDD from PD-N and to 83.3% and 83.3% for the discrimination of the PDD from PD-MCI cases, respectively.

The variables displayed by the model for PDD vs PD-N patient discrimination were the FA values of the SLF temp.-L, MD values of cing.-cingulate gyr.-L, AD values of ILF-L and the intrinsic connectivities of frontostriatal and salience networks, while the AD value of the ILF-L and the intrinsic connectivity of the limbic network efficiently discriminated PDD and PD-MCI cases.

Both results are very strong in terms of classification power, and if validated with data of larger patient groups, can reliably be used as biomarkers for PDD. The further addition of ASL data did not further increase but rather decreased the sensitivity and specificity of the model, hence the two easier applicable modalities of rs-fMRI and DTI are sufficient for a classifier design for determination of dementia in PD.

4.9 Limitations for this study

In future work, it would be of big advantage being able to refine the normalization process of the data in a way that the subject's brains would be registered to an age matched and/or disease-related standard template or even to work directly in the subject space, instead of registering the patient's brains to a standard template obtained from the average of 152 healthy subjects of different ages. Although the usage of the MNI-152 template is the common way in reference literature, we believe the usage of a specific template and atlas-tools would improve the data analyses and this, in addition to the need of a gray matter mask, might also be the reason why some of the identified clusters around the ventricle obtained with rs-fMRI data analysis in this study partly resided in white-matter.

But indeed, there is fMRI literature directly addressing the investigation of WM activity, and as the BOLD signal depends on the blood in the tissue, it isn't too surprising also detecting activity in the WM, but less strong than in the gray matter (Gawryluk 2014).

As we collected the data from a patient group, we cannot fully exclude the impact of any medication treatment on the functional MRI data and neuropsychological assessment, but it would be ethically unacceptable to pause the patients drug intake and cause a worsening of the patient's symptoms. On the other hand, we would also risk motion artifacts due to severe motor-symptoms during the MRI scans when the Parkinson-related drugs would be stopped for that period, hence all recordings were performed during on-stage of the patients. But, as the type of Parkinson-related medication was balanced within the three patient groups and

we did not compare our data to a healthy control group, we believe that our results are not biased by the medication of the patients.

5 CONCLUSION

To conclude, in this study we were able to provide novel information about the mechanisms underlying the pathogenesis and progression of the cognitive decline from PD-N to PDD using multimodal MRI techniques.

By this, we first obtained the RSNs that yield discriminative power among the three patient groups, which were the DMN, SN, FSN, PTN and the limbic network. Contra intuitively, the expression of the DMN and SN, which are functionally related in a way that the SN regulates the activation and deactivation of the DMN and the CEN in the presence/absence of salient stimuli, were simultaneously increased in the PDD group, pointing to an altered switching mechanism in PDD patients that is different from altered activation pattern that have been described for AD and bvFTD cases. Although the DMN and SN increase became statistically significant only in the PDD group, the intrinsic functional connectivity of the DMN and SN increased from PD-N trough PD-MCI to PDD. As not all PD-MCI patient will evolve into PDD, the non-converters might have diluted this effect and it would be interesting to follow the long-term progression of those patients within the PD-MCI group with and without increased DMN and SN functional connectivity in terms of prognostic features of alterations of these networks.

The FSN, PTN and limbic network on the other hand showed decreased intrinsic functional connectivity in the PDD group and relate to the executive, visuo-spatial and memory dysfunction in PDD patients.

We were further able to show complementary DTI derived differences in various white matter tracts that not only indicate global neurodegenerative processes in PDD but were also linked the structural changes of specific tracts with the RSN alterations observed in PDD. Additionally, the ASL and MRSI techniques provided sensitive information about various pattern of hypoperfusion and altered metabolite ratios in the PDD group that were supportive for the RSN and white matter findings.

Furthermore, the biological results obtained with the different MRI techniques significantly correlated with motor-symptom severity and the cognitive decline among the groups. As for example the FSN was related with clock drawing performance, the SN with semantic fluency

and the limbic network showed several correlations with the UPDRS-cognitive score, UPDRS-total score and disease duration, it seems that semantic fluency and clock drawing performance are indeed valuable tests for fast clinical evaluation of the cognitive state of the PD patients and poor performance in these tests point to dementia risk.

In a second step, we were able to create a multimodal neuroimaging-based biomarker for the discrimination of PDD cases from PD-N and PD-MCI based on the significant parameters of the rs-fMRI analysis together with the significant changes within DTI derived parameters, and obtained a discrimination model with 100.0% sensitivity for the discrimination of PDD from PD-N and 83.3% sensitivity between PDD and PD-MCI cases. The obtained discriminative function of the combined modalities was even more successful than the logistic regression model using the expression of the RSNs alone.

As the rs-fMRI and DTI data can be easily recorded during the MRI and yielded reliable discriminative power in this study, the application of these measurements in clinical diagnosis and follow-up of the PD patients cognitive status would provide the clinicians an eminent tool for the reliable diagnosis and the generation of appropriate treatment strategies for the individual patient. The establishment of a reference value of RSN expression for PD-MCI and PDD would allow the fast diagnosis of newly diseased patients by comparing the individual scores with the reference value and the early intervention for an optimal treatment would be of great interest for the slowing of the patient's symptoms.

On the other hand, our results exposed neuro-pathological changes in the brains of PD patients at different stages of cognitive decline that can predict PDD and represent important inside in the PDD specific disease pattern in contrast to other forms of dementia. This identified regions could represent promising targets for innovative therapies that yet have to be developed.

6 LITERATURE

1. Aarsland, D., Andersen, K., Larsen, J. P., & Lolk, A. (2003). Prevalence and characteristics of dementia in Parkinson disease: an 8-year prospective study. *Archives of neurology*, *60*(3), 387-392.
2. Aarsland, D., Zaccai, J., & Brayne, C. (2005). A systematic review of prevalence studies of dementia in Parkinson's disease. *Movement disorders*, *20*(10), 1255-1263.
3. Agosta, F., Canu, E., Stefanova, E., Sarro, L., Tomić, A., Špica, V., ... & Filippi, M. (2014). Mild cognitive impairment in Parkinson's disease is associated with a distributed pattern of brain white matter damage. *Human brain mapping*, *35*(5), 1921-1929.
4. Agosta, F., Canu, E., Stojković, T., Pievani, M., Tomić, A., Sarro, L., ... & Filippi, M. (2013). The topography of brain damage at different stages of Parkinson's disease. *Human brain mapping*, *34*(11), 2798-2807.
5. Al-Bachari, S., Parkes, L. M., Vidyasagar, R., Hanby, M. F., Tharaken, V., Leroi, I., & Emsley, H. C. (2014). Arterial spin labelling reveals prolonged arterial arrival time in idiopathic Parkinson's disease. *NeuroImage: Clinical*, *6*, 1-8.
6. Albert, M. S., DeKosky, S. T., Dickson, D., Dubois, B., Feldman, H. H., Fox, N. C., ... & Snyder, P. J. (2011). The diagnosis of mild cognitive impairment due to Alzheimer's disease: Recommendations from the National Institute on Aging-Alzheimer's Association workgroups on diagnostic guidelines for Alzheimer's disease. *Alzheimer's & dementia*, *7*(3), 270-279.
7. Alexander, GE., Crutcher, MD, DeLong, MR. (1990). Basal ganglia-thalamocortical circuits: Parallel substrates for motor, occulomotor,'prefrontal' and 'limbic' functions. Prog BrainRes 85:119-146.
8. Amboni, M., Tessitore, A., Esposito, F., Santangelo, G., Picillo, M., Vitale, C., ... & Tedeschi, G. (2015). Resting-state functional connectivity associated with mild cognitive impairment in Parkinson's disease. *Journal of neurology*, *262*(2), 425-434.
9. Andersson, J. L., & Sotiropoulos, S. N. (2016). An integrated approach to correction for off-resonance effects and subject movement in diffusion MR imaging. *Neuroimage*, *125*, 1063-1078.
10. Andersson, J. L., Jenkinson, M., & Smith, S. (2007). Non-linear registration, aka Spatial normalisation FMRIB technical report TR07JA2. *FMRIB Analysis Group of the University of Oxford*, *2*.

11. Andersson, J. L., Skare, S., & Ashburner, J. (2003). How to correct susceptibility distortions in spin-echo echo-planar images: application to diffusion tensor imaging. *Neuroimage*, *20*(2), 870-888.
12. Arslan, D. B. & Öztürk-Işık, E. (2016a). Masterthesis: Measurement of cerebral perfusion in Parkinson's disease with mild cognitive impairment using arterial spin labeling. The Institute of Biomedical Engineering, Boğaziçi University, 2016.
13. Arslan, D. B., Kicik, A., Cengiz, S., Erdogdu, E., Buker, S., ... & Öztürk-Işık, E. (2016b). Cerebral Perfusion Correlates of MAPT and COMT Genotypes for Mild Cognitive Impairment in Parkinson's Disease at 3T, In Proceedings of the 33rd Annual Meeting of European society for magnetic resonance in medicine and biology (ESMRMB) Abstract 2016: Vienna, Austria.
14. Baggio, H. C., Sala-Llonch, R., Segura, B., Marti, M. J., Valldeoriola, F., Compta, Y., ... & Junqué, C. (2014). Functional brain networks and cognitive deficits in Parkinson's disease. *Human brain mapping*, *35*(9), 4620-4634.
15. Baggio, H. C., Segura, B., Sala-Llonch, R., Marti, M. J., Valldeoriola, F., Compta, Y., ... & Junqué, C. (2015). Cognitive impairment and resting-state network connectivity in Parkinson's disease. *Human brain mapping*, *36*(1), 199-212.
16. Baldo, J. V., Schwartz, S., Wilkins, D., & Dronkers, N. F. (2006). Role of frontal versus temporal cortex in verbal fluency as revealed by voxel-based lesion symptom mapping. *Journal of the International Neuropsychological Society*, *12*(06), 896-900.
17. Beck, A. T., Epstein, N., Brown, G., & Steer, R. A. (1988). An inventory for measuring clinical anxiety: psychometric properties. *Journal of consulting and clinical psychology*, *56*(6), 893.
18. Behrens, T. E., Woolrich, M. W., Jenkinson, M., Johansen-Berg, H., Nunes, R. G., Clare, S., ... & Smith, S. M. (2003). Characterization and propagation of uncertainty in diffusion-weighted MR imaging. *Magnetic resonance in medicine*, *50*(5), 1077-1088.
19. Benton, A. L., Varney, N. R., & deS Hamsher, K. (1978). Visuospatial judgment: A clinical test. *Archives of Neurology*, *35*(6), 364-367.
20. Berg, E. A. (1948). A simple objective technique for measuring flexibility in thinking. *The Journal of general psychology*, *39*(1), 15-22.
21. Biswal, B., Zerrin Yetkin, F., Haughton, V. M., & Hyde, J. S. (1995). Functional connectivity in the motor cortex of resting human brain using echo-planar mri. *Magnetic resonance in*

medicine, *34*(4), 537-541.

22. Bohnen, N. I., Kaufer, D. I., Hendrickson, R., Ivanco, L. S., Lopresti, B. J., Constantine, G. M., ... & DeKosky, S. T. (2006). Cognitive correlates of cortical cholinergic denervation in Parkinson's disease and parkinsonian dementia. *Journal of neurology*, *253*(2), 242-247.
23. Bohnen, N. I., Koeppe, R. A., Minoshima, S., Giordani, B., Albin, R. L., Frey, K. A., & Kuhl, D. E. (2011). Cerebral glucose metabolic features of Parkinson disease and incident dementia: longitudinal study. *Journal of Nuclear Medicine*, *52*(6), 848-855.
24. Braak, H., Del Tredici, K., Bratzke, H., Hamm-Clement, J., Sandmann-Keil, D., & Rüb, U. (2002). Staging of the intracerebral inclusion body pathology associated with idiopathic Parkinson's disease (preclinical and clinical stages). *Journal of neurology*, *249*, III-1.
25. Braak, H., Del Tredici, K., Rüb, U., de Vos, R. A., Steur, E. N. J., & Braak, E. (2003). Staging of brain pathology related to sporadic Parkinson's disease. *Neurobiology of aging*, *24*(2), 197-211.
26. Bressler, S. L., & Menon, V. (2010). Large-scale brain networks in cognition: emerging methods and principles. *Trends in cognitive sciences*, *14*(6), 277-290.
27. Buxton, R. B., Frank, L. R., Wong, E. C., Siewert, B., Warach, S., & Edelman, R. R. (1998). A general kinetic model for quantitative perfusion imaging with arterial spin labeling. *Magnetic resonance in medicine*, *40*(3), 383-396.
28. Calhoun, V. D., Adali, T., Pearlson, G. D., & Pekar, J. J. (2001). A method for making group inferences from functional MRI data using independent component analysis. *Human brain mapping*, *14*(3), 140-151.
29. Calhoun, V. D., Liu, J., & Adalı, T. (2009). A review of group ICA for fMRI data and ICA for joint inference of imaging, genetic, and ERP data. *Neuroimage*, *45*(1), S163-S172.
30. Camicioli, R. M., Korzan, J. R., Foster, S. L., Fisher, N. J., Emery, D. J., Bastos, A. C., & Hanstock, C. C. (2004). Posterior cingulate metabolic changes occur in Parkinson's disease patients without dementia. *Neuroscience letters*, *354*(3), 177-180.
31. Castillo, M., Kwock, L., & Mukherji, S. K. (1996). Clinical applications of proton MR spectroscopy. *American journal of neuroradiology*, *17*, 1-16.
32. Cauda, F., D'agata, F., Sacco, K., Duca, S., Geminiani, G., & Vercelli, A. (2011). Functional connectivity of the insula in the resting brain. *Neuroimage*, *55*(1), 8-23.
33. Cengiz, S., Kicik, A., Erdogdu, E., Arslan, D.B., Buker, S., ...& Öztürk-Işık, E. (2016a) Proton MR spectroscopic imaging of Parkinson's disease with mild cognitive impairment or

normal cognition registered to MNI-152 brain atlas, in In Proceedings of the 33rd Annual Meeting of European society for magnetic resonance in medicine and biology (ESMRMB) Abstract: Vienna, Austria.

34. Cengiz, S. & Öztürk-Işık, E. (2016b) Masterthesis: Determination of biomarkers for mild cognitive impairment in parkinson's disease using magnetic resonance spectroscopic imaging (Manyetik rezonans spektroskopik görüntüleme kullanarak hafif kognitif bozukluğu olan parkinson hastalarında biyoişaretleciyilerin belirlenmesi), The Institute of Biomedical Engineering, Boğaziçi University, 2016 67p.
35. Chen, B., Fan, G. G., Liu, H., & Wang, S. (2015). Changes in anatomical and functional connectivity of Parkinson's disease patients according to cognitive status. *European journal of radiology*, *84*(7), 1318-1324.
36. Christopher, L., Koshimori, Y., Lang, A. E., Criaud, M., & Strafella, A. P. (2014). Uncovering the role of the insula in non-motor symptoms of Parkinson's disease. *Brain*, *137*(8), 2143-2154.
37. Christopher, L., Marras, C., Duff-Canning, S., Koshimori, Y., Chen, R., Boileau, I., ... & Houle, S. (2013). Combined insular and striatal dopamine dysfunction are associated with executive deficits in Parkinson's disease with mild cognitive impairment. *Brain*, awt337.
38. Chung, K. K., Zhang, Y. I., Lim, K. L., Tanaka, Y., Huang, H., Gao, J., ... & Dawson, T. M. (2001). Parkin ubiquitinates the α-synuclein–interacting protein, synphilin-1: implications for Lewy-body formation in Parkinson disease. *Nature medicine*, *7*(10), 1144-1150.
39. Compta, Y., Pereira, J. B., Ríos, J., Ibarretxe-Bilbao, N., Junqué, C., Bargalló, N., ... & Martí, M. J. (2013). Combined dementia-risk biomarkers in Parkinson's disease: a prospective longitudinal study. *Parkinsonism & related disorders*, *19*(8), 717-724.
40. de Frias, C. M., Dixon, R. A., Fisher, N., & Camicioli, R. (2007). Intraindividual variability in neurocognitive speed: a comparison of Parkinson's disease and normal older adults. *Neuropsychologia*, *45*(11), 2499-2507.
41. De Lau, L. M., & Breteler, M. M. (2006). Epidemiology of Parkinson's disease. The Lancet Neurology, 5(6), 525-535
42. Delaveau, P., Salgado-Pineda, P., Fossati, P., Witjas, T., Azulay, J. P., & Blin, O. (2010). Dopaminergic modulation of the default mode network in Parkinson's disease. *European Neuropsychopharmacology*, *20*(11), 784-792.
43. Deng, B., Zhang, Y., Wang, L., Peng, K., Han, L., Nie, K., ... & Wang, J. (2013). Diffusion

tensor imaging reveals white matter changes associated with cognitive status in patients with Parkinson's disease. *American Journal of Alzheimer's Disease & Other Dementias®*, *28*(2), 154-164.

44. Derejko, M., Slawek, J., Lass, P., & Nyka, W. M. (2001). Cerebral blood flow changes in Parkinson's disease associated with dementia. *Nucl Med Rev Cent East Eur*, *4*(2), 123-127.
45. Detre, J. A., Zhang, W., Roberts, D. A., Silva, A. C., Williams, D. S., Grandis, D. J., ... & Leigh, J. S. (1994). Tissue specific perfusion imaging using arterial spin labeling. *NMR in Biomedicine*, *7*(1-2), 75-82.
46. Dickson, D. W. (2012). Parkinson's disease and parkinsonism: neuropathology. *Cold Spring Harbor perspectives in medicine*, *2*(8), a009258.
47. Dubois, B., & Pillon, B. (1996). Cognitive deficits in Parkinson's disease. *Journal of neurology*, *244*(1), 2-8.
48. Dubois, B., Burn, D., Goetz, C., Aarsland, D., Brown, R. G., Broe, G. A., ... & Korczyn, A. (2007). Diagnostic procedures for Parkinson's disease dementia: recommendations from the movement disorder society task force. *Movement Disorders*, *22*(16), 2314-2324.
49. Duncan, G. W., Firbank, M. J., O'Brien, J. T., & Burn, D. J. (2013). Magnetic resonance imaging: a biomarker for cognitive impairment in Parkinson's disease?. *Movement Disorders*, *28*(4), 425-438.
50. Eling, P., Derckx, K., & Maes, R. (2008). On the historical and conceptual background of the Wisconsin Card Sorting Test. *Brain and cognition*, *67*(3), 247-253.
51. Emre, M., Aarsland, D., Brown, R., Burn, D. J., Duyckaerts, C., Mizuno, Y., ... & Goldman, J. (2007). Clinical diagnostic criteria for dementia associated with Parkinson's disease. *Movement disorders*, *22*(12), 1689-1707.
52. Fama, R., Sullivan, E. V., Shear, P. K., Stein, M., Yesavage, J. A., Tinklenberg, J. R., & Pfefferbaum, A. (2000). Extent, pattern, and correlates of remote memory impairment in Alzheimer's disease and Parkinson's disease. *Neuropsychology*, *14*(2), 265.
53. Feldman, H. M., Yeatman, J. D., Lee, E. S., Barde, L. H., & Gaman-Bean, S. (2010). Diffusion tensor imaging: a review for pediatric researchers and clinicians. *Journal of developmental and behavioral pediatrics: JDBP*, *31*(4), 346.
54. Fernández-Seara, M. A., Mengual, E., Vidorreta, M., Castellanos, G., Irigoyen, J., Erro, E., & Pastor, M. A. (2015). Resting state functional connectivity of the subthalamic nucleus in Parkinson's disease assessed using arterial spin-labeled perfusion fMRI. *Human brain*

mapping, *36*(5), 1937-1950.

55. ffytche DH, Blom JD, Catani M. (2010), Disorders of visual perception, *Journal of Neurology, Neurosurgery & Psychiatry,* 81:1280-1287.
56. Folstein, M. F., Folstein, S. E., & McHugh, P. R. (1975). "Mini-mental state": a practical method for grading the cognitive state of patients for the clinician. *Journal of psychiatric research*, *12*(3), 189-198.
57. Forno, L. S. (1996). Neuropathology of Parkinson's disease. *Journal of Neuropathology & Experimental Neurology*, *55*(3), 259-272.
58. Fox, M. D., & Raichle, M. E. (2007). Spontaneous fluctuations in brain activity observed with functional magnetic resonance imaging. *Nature Reviews Neuroscience*, *8*(9), 700-711.
59. Galtier, I., Nieto, A., Lorenzo, J. N., & Barroso, J. (2016). Mild cognitive impairment in Parkinson's disease: Diagnosis and progression to dementia. *Journal of clinical and experimental neuropsychology*, *38*(1), 40-50.
60. Ganguli, M., Blacker, D., Blazer, D. G., Grant, I., Jeste, D. V., Paulsen, J. S., ... & Sachdev, P. S. (2011). Classification of neurocognitive disorders in DSM-5: a work in progress.
61. Garraux, G., Phillips, C., Schrouff, J., Kreisler, A., Lemaire, C., Degueldre, C., ... & Salmon, E. (2013). Multiclass classification of FDG PET scans for the distinction between Parkinson's disease and atypical parkinsonian syndromes. *NeuroImage: Clinical*, *2*, 883-893.
62. Gawryluk, J. R., Mazerolle, E. L., & D'Arcy, R. C. (2014). Does functional MRI detect activation in white matter? A review of emerging evidence, issues, and future directions. *Frontiers in neuroscience*, *8*, 239.
63. Gibb, W. R., & Lees, A. J. (1988). The relevance of the Lewy body to the pathogenesis of idiopathic Parkinson's disease. *Journal of Neurology, Neurosurgery & Psychiatry*, *51*(6), 745-752.
64. Goldman, J. G., Holden, S., Bernard, B., Ouyang, B., Goetz, C. G., & Stebbins, G. T. (2013). Defining optimal cutoff scores for cognitive impairment using Movement Disorder Society Task Force criteria for mild cognitive impairment in Parkinson's disease. *Movement Disorders*, *28*(14), 1972-1979.
65. Goldman, J. G., Stebbins, G. T., Bernard, B., Stoub, T. R., Goetz, C. G., & deToledo-Morrell, L. (2012). Entorhinal cortex atrophy differentiates Parkinson's disease patients with and

without dementia. *Movement Disorders, 27*(6), 727-734.

66. Goldman, J. G., Litvan, L. (2011). Mild Cognitive Impairment in Parkinson's Disease*, Minerva Med.102*(6):441-459*.*
67. Goldman, W. P., Baty, J. D., Buckles, V. D., Sahrmann, S., & Morris, J. C. (1998). Cognitive and motor functioning in Parkinson disease: subjects with and without questionable dementia. *Archives of Neurology*, *55*(5), 674-680.
68. González-Redondo, R., García-García, D., Clavero, P., Gasca-Salas, C., García-Eulate, R., Zubieta, J. L., ... & Rodríguez-Oroz, M. C. (2014). Grey matter hypometabolism and atrophy in Parkinson's disease with cognitive impairment: a two-step process. *Brain*, *137*(8), 2356-2367.
69. Goodman, W. K., Price, L. H., Rasmussen, S. A., Mazure, C., Fleischmann, R. L., Hill, C. L., ... & Charney, D. S. (1989). The Yale-Brown obsessive compulsive scale: I. Development, use, and reliability. *Archives of general psychiatry*, *46*(11), 1006-1011.
70. Goris, A., Williams-Gray, C. H., Clark, G. R., Foltynie, T., Lewis, S. J., Brown, J., ... & Chinnery, P. F. (2007). Tau and α-synuclein in susceptibility to, and dementia in, Parkinson's disease. *Annals of neurology*, *62*(2), 145-153.
71. Göttlich, M., Münte, T. F., Heldmann, M., Kasten, M., Hagenah, J., & Krämer, U. M. (2013). Altered resting state brain networks in Parkinson's disease. *PloS one*, *8*(10), e77336.
72. Grace, J., Amick, M. M., D'abreu, A., Festa, E. K., Heindel, W. C., & Ott, B. R. (2005). Neuropsychological deficits associated with driving performance in Parkinson's and Alzheimer's disease. *Journal of the International Neuropsychological Society*, *11*(06), 766-775.
73. Greicius, M. D., Supekar, K., Menon, V., & Dougherty, R. F. (2009). Resting-state functional connectivity reflects structural connectivity in the default mode network. *Cerebral cortex*, *19*(1), 72-78.
74. Griffith, H. R., den Hollander, J. A., Okonkwo, O. C., O'Brien, T., Watts, R. L., & Marson, D. C. (2008). Brain metabolism differs in Alzheimer's disease and Parkinson's disease dementia. *Alzheimer's & Dementia*, *4*(6), 421-427.
75. Gruner, P., Vo, A., Argyelan, M., Ikuta, T., Degnan, A. J., John, M., ... & Szeszko, P. R. (2014). Independent component analysis of resting state activity in pediatric obsessive-compulsive disorder. *Human brain mapping*, *35*(10), 5306-5315.
76. Gullett, J. M., Price, C. C., Nguyen, P., Okun, M. S., Bauer, R. M., & Bowers, D. (2013).

Reliability of three Benton Judgment of Line Orientation short forms in idiopathic Parkinson's disease. *The Clinical Neuropsychologist*, *27*(7), 1167-1178.

77. Hanagasi, H. A., Tufekcioglu, Z., & Emre, M. (2017). Dementia in Parkinson's disease. *Journal of the Neurological Sciences*.
78. Hattori, T., Orimo, S., Aoki, S., Ito, K., Abe, O., Amano, A., ... & Mizusawa, H. (2012). Cognitive status correlates with white matter alteration in Parkinson's disease. *Human brain mapping*, *33*(3), 727-739.
79. Hely MA, Reid WGJ, Adena MA, Halliday GM, Morris JGL. The Sydney Multicenter Study of Parkinson's disease: The inevitability of dementia at 20 years. Mov Disord. 2008;23(6):837-844. doi:10.1002/mds.21956.
80. Hilker, R., Thomas, A. V., Klein, J. C., Weisenbach, S., Kalbe, E., Burghaus, L., ... & Heiss, W. D. (2005). Dementia in Parkinson disease functional imaging of cholinergic and dopaminergic pathways. *Neurology*, *65*(11), 1716-1722.
81. Hoehn M, Yahr M (1967). "Parkinsonism: onset, progression and mortality.". Neurology. 17 (5): 427–42. doi:10.1212/wnl.17.5.427. PMID 6067254.
82. Hoehn, M. M., & Yahr, M. D. (1967). Parkinsonism onset, progression, and mortality. *Neurology*, *17*(5), 427-427.
83. Huang, C., Mattis, P., Perrine, K., Brown, N., Dhawan, V., & Eidelberg, D. (2008). Metabolic abnormalities associated with mild cognitive impairment in Parkinson disease. *Neurology*, *70*(16 Part 2), 1470-1477.
84. Hughes, A. J., Daniel, S. E., Kilford, L., & Lees, A. J. (1992). Accuracy of clinical diagnosis of idiopathic Parkinson's disease: a clinico-pathological study of 100 cases. *Journal of Neurology, Neurosurgery & Psychiatry*, *55*(3), 181-184.
85. Hyvärinen, A., & Oja, E. (2000). Independent component analysis: algorithms and applications. *Neural networks*, *13*(4), 411-430.
86. Ibarretxe-Bilbao, N., Zarei, M., Junque, C., Marti, M. J., Segura, B., Vendrell, P., ... & Tolosa, E. (2011). Dysfunctions of cerebral networks precede recognition memory deficits in early Parkinson's disease. *Neuroimage*, *57*(2), 589-597.
87. Janvin, C. C., Larsen, J. P., Aarsland, D., & Hugdahl, K. (2006). Subtypes of mild cognitive impairment in Parkinson's disease: progression to dementia. *Movement Disorders*, *21*(9), 1343-1349.
88. Jellinger, K. A. (2013). Mild cognitive impairment in Parkinson disease: heterogenous

mechanisms. *Journal of Neural Transmission*, *120*(1), 157-167.

89. Jenkinson, M., & Smith, S. (2001). A global optimization method for robust affine registration of brain images. *Medical image analysis*, *5*(2), 143-156.
90. Jenkinson, M., Bannister, P., Brady, M., & Smith, S. (2002). Improved optimization for the robust and accurate linear registration and motion correction of brain images. *Neuroimage*, *17*(2), 825-841.
91. Jenkinson, M., Pechaud, M., & Smith, S. (2005, June). BET2: MR-based estimation of brain, skull and scalp surfaces. In *Eleventh annual meeting of the organization for human brain mapping* (Vol. 17, p. 167).
92. Jeste, D., Blacker, D., Blazer, D., Ganguli, M., Grant, I., Paulsen, J., & Sachdev, S. (2010). Neurocognitive disorders: a proposal from the DSM-5 Neurocognitive Disorders Work Group. *Neurocognitive Criteria Draft, American Psychiatric Association*.
93. Kamagata, K., Motoi, Y., Hori, M., Suzuki, M., Nakanishi, A., Shimoji, K., ... & Mizuno, Y. (2011). Posterior hypoperfusion in Parkinson's disease with and without dementia measured with arterial spin labeling MRI. *Journal of Magnetic Resonance Imaging*, *33*(4), 803-807.
94. Kamagata, K., Motoi, Y., Tomiyama, H., Abe, O., Ito, K., Shimoji, K., ... & Kuwatsuru, R. (2013). Relationship between cognitive impairment and white-matter alteration in Parkinson's disease with dementia: tract-based spatial statistics and tract-specific analysis. *European radiology*, *23*(7), 1946-1955.
95. Kandel, ER., Schwartz, JH., Jessell, TM. (2000). Principles of Neural Science, 4/e, The McGraw-Hill Companies , New York, USA.
96. Kandiah, N., Zainal, N. H., Narasimhalu, K., Chander, R. J., Ng, A., Mak, E., ... & Tan, L. C. (2014). Hippocampal volume and white matter disease in the prediction of dementia in Parkinson's disease. *Parkinsonism & related disorders*, *20*(11), 1203-1208.
97. Lawrence, B. J., Gasson, N., & Loftus, A. M. (2016). Prevalence and Subtypes of Mild Cognitive Impairment in Parkinson's Disease. *Scientific Reports*, *6*.
98. Le Heron, C. J., Wright, S. L., Melzer, T. R., Myall, D. J., MacAskill, M. R., Livingston, L., ... & Anderson, T. J. (2014). Comparing cerebral perfusion in Alzheimer's disease and Parkinson's disease dementia: an ASL-MRI study. *Journal of Cerebral Blood Flow & Metabolism*, *34*(6), 964-970.
99. Lebedev, A. V., Westman, E., Simmons, A., Lebedeva, A., Siepel, F. J., Pereira, J. B., &

Aarsland, D. (2014). Large-scale resting state network correlates of cognitive impairment in Parkinson's disease and related dopaminergic deficits. *Frontiers in systems neuroscience*, *8*, 45.

100. Lee, J. E., Cho, K. H., Song, S. K., Kim, H. J., Lee, H. S., Sohn, Y. H., & Lee, P. H. (2013). Exploratory analysis of neuropsychological and neuroanatomical correlates of progressive mild cognitive impairment in Parkinson's disease. *Journal of Neurology, Neurosurgery & Psychiatry*, jnnp-2013.

101. Lee, J. E., Park, H. J., Park, B., Song, S. K., Sohn, Y. H., Lee, J. D., & Lee, P. H. (2010). A comparative analysis of cognitive profiles and white-matter alterations using voxel-based diffusion tensor imaging between patients with Parkinson's disease dementia and dementia with Lewy bodies. *Journal of Neurology, Neurosurgery & Psychiatry*, *81*(3), 320-326.

102. Lima, C. F., Meireles, L. P., Fonseca, R., Castro, S. L., & Garrett, C. (2008). The Frontal Assessment Battery (FAB) in Parkinson's disease and correlations with formal measures of executive functioning. *Journal of neurology*, *255*(11), 1756-1761.

103. Lin, C. H., & Wu, R. M. (2015). Biomarkers of cognitive decline in Parkinson's disease. *Parkinsonism & related disorders*, *21*(5), 431-443.

104. Lin, W. C., Chen, P. C., Huang, Y. C., Tsai, N. W., Chen, H. L., Wang, H. C., ... & Lu, C. H. (2016). Dopaminergic Therapy Modulates Cortical Perfusion in Parkinson Disease With and Without Dementia According to Arterial Spin Labeled Perfusion Magnetic Resonance Imaging. *Medicine*, *95*(5).

105. Litvan, I., Aarsland, D., Adler, C. H., Goldman, J. G., Kulisevsky, J., Mollenhauer, B., ... & Weintraub, D. (2011). MDS task force on mild cognitive impairment in Parkinson's disease: Critical review of PD-MCI. *Movement disorders*, *26*(10), 1814-1824.

106. Litvan, I., Goldman, J. G., Tröster, A. I., Schmand, B. A., Weintraub, D., Petersen, R. C., ... & Aarsland, D. (2012). Diagnostic criteria for mild cognitive impairment in Parkinson's disease: Movement Disorder Society Task Force guidelines. *Movement Disorders*, *27*(3), 349-356.

107. Lyoo, C. H., Jeong, Y., Ryu, Y. H., Rinne, J. O., & Lee, M. S. (2010). Cerebral glucose metabolism of Parkinson's disease patients with mild cognitive impairment. *European neurology*, *64*(2), 65-73.

108. Ma, L., Wang, B., Chen, X., & Xiong, J. (2007). Detecting functional connectivity in the

resting brain: a comparison between ICA and CCA. *Magnetic resonance imaging*, *25*(1), 47-56.

109. Mak, E., Zhou, J., Tan, L. C., Au, W. L., Sitoh, Y. Y., & Kandiah, N. (2013). Cognitive deficits in mild Parkinson's disease are associated with distinct areas of grey matter atrophy. *Journal of Neurology, Neurosurgery & Psychiatry*, jnnp-2013.
110. Mamah, D., Conturo, T. E., Harms, M. P., Akbudak, E., Wang, L., McMichael, A. R., ... & Csernansky, J. G. (2010). Anterior thalamic radiation integrity in schizophrenia: a diffusion-tensor imaging study. *Psychiatry Research: Neuroimaging*, *183*(2), 144-150.
111. Marin, R. S., Biedrzycki, R. C., & Firinciogullari, S. (1991). Reliability and validity of the Apathy Evaluation Scale. *Psychiatry research*, *38*(2), 143-162.
112. Martin, W. R., Wieler, M., Gee, M., & Camicioli, R. (2009). Temporal lobe changes in early, untreated Parkinson's disease. *Movement Disorders*, *24*(13), 1949-1954.
113. Mascalchi, M., Toschi, N., Giannelli, M., Ginestroni, A., Della Nave, R., Nicolai, E., ... & Soricelli, A. (2015). Progression of microstructural damage in spinocerebellar ataxia type 2: A longitudinal DTI study. *American Journal of Neuroradiology*, *36*(6), 1096-1101.
114. McCann, H., Stevens, C. H., Cartwright, H., & Halliday, G. M. (2014). α-Synucleinopathy phenotypes. *Parkinsonism & related disorders*, *20*, S62-S67.
115. McKeown, M. J., & Sejnowski, T. J. (1998). Independent component analysis of fMRI data: examining the assumptions. *Human brain mapping*, *6*(5-6), 368-372.
116. Melzer, T. R., Watts, R., MacAskill, M. R., Pearson, J. F., Rüeger, S., Pitcher, T. L., ... & Alsop, D. C. (2011). Arterial spin labelling reveals an abnormal cerebral perfusion pattern in Parkinson’s disease. *Brain*, awq377.
117. Melzer, T. R., Watts, R., MacAskill, M. R., Pitcher, T. L., Livingston, L., Keenan, R. J., ... & Anderson, T. J. (2013). White matter microstructure deteriorates across cognitive stages in Parkinson disease. *Neurology*, *80*(20), 1841-1849.
118. Migliaccio, R., Agosta, F., Scola, E., Magnani, G., Cappa, S. F., Pagani, E., ... & Bartolomeo, P. (2012). Ventral and dorsal visual streams in posterior cortical atrophy: a DT MRI study. *Neurobiology of aging*, *33*(11), 2572-2584.
119. Mioshi, E., Dawson, K., Mitchell, J., Arnold, R., & Hodges, J. R. (2006). The Addenbrooke's Cognitive Examination Revised (ACE-R): a brief cognitive test battery for dementia screening. *International journal of geriatric psychiatry*, *21*(11), 1078-1085.
120. Morales, D. A., Vives-Gilabert, Y., Gómez-Ansón, B., Bengoetxea, E., Larrañaga, P., Bielza,

C., ... & Delfino, M. (2013). Predicting dementia development in Parkinson's disease using Bayesian network classifiers. *Psychiatry Research: NeuroImaging*, *213*(2), 92-98.

121. Moustafa, A. A., & Poletti, M. (2013). Neural and behavioral substrates of subtypes of Parkinson's disease.

122. Mukherjee, P., Berman, J. I., Chung, S. W., Hess, C. P., & Henry, R. G. (2008). Diffusion tensor MR imaging and fiber tractography: theoretic underpinnings. *American journal of neuroradiology*, *29*(4), 632-641.

123. Musiek, E. S., Chen, Y., Korczykowski, M., Saboury, B., Martinez, P. M., Reddin, J. S., ... & Newberg, A. B. (2012). Direct comparison of FDG-PET and ASL-MRI in Alzheimer's disease. *Alzheimer's & dementia: the journal of the Alzheimer's Association*, *8*(1), 51.

124. Muslimović, D., Post, B., Speelman, J. D., & Schmand, B. (2005). Cognitive profile of patients with newly diagnosed Parkinson disease. *Neurology*, *65*(8), 1239-1245.

125. Muslimović, D., Post, B., Speelman, J. D., & Schmand, B. (2007). Motor procedural learning in Parkinson's disease. *Brain*, *130*(11), 2887-2897.

126. Muslimović, D., Post, B., Speelman, J. D., Schmand, B., de Haan, R. J., & CARPA Study Group. (2008). Determinants of disability and quality of life in mild to moderate Parkinson disease. *Neurology*, *70*(23), 2241-2247.

127. Nasreddine, Z. S., Phillips, N. A., Bédirian, V., Charbonneau, S., Whitehead, V., Collin, I., ... & Chertkow, H. (2005). The Montreal Cognitive Assessment, MoCA: a brief screening tool for mild cognitive impairment. *Journal of the American Geriatrics Society*, *53*(4), 695-699.

128. Navon, D. (1977). Forest before trees: The precedence of global features in visual perception. *Cognitive psychology*, *9*(3), 353-383.

129. Nie, K., Zhang, Y., Huang, B., Wang, L., Zhao, J., Huang, Z., ... & Wang, L. (2013). Marked N-acetylaspartate and choline metabolite changes in Parkinson's disease patients with mild cognitive impairment. *Parkinsonism & related disorders*, *19*(3), 329-334.

130. Nobili, F., Abbruzzese, G., Morbelli, S., Marchese, R., Girtler, N., Dessi, B., ... & Rodriguez, G. (2009). Amnestic mild cognitive impairment in Parkinson's disease: a brain perfusion SPECT study. *Movement Disorders*, *24*(3), 414-421.

131. Nobili, F., Morbelli, S., Arnaldi, D., Ferrara, M., Campus, C., Brugnolo, A., ... & Rodriguez, G. (2011). Radionuclide brain imaging correlates of cognitive impairment in Parkinson's disease (PD). *Journal of the neurological sciences*, *310*(1), 31-35.

132. Nombela, C., Rowe, J. B., Winder-Rhodes, S. E., Hampshire, A., Owen, A. M., Breen, D. P.,

... & Chinnery, P. F. (2014). Genetic impact on cognition and brain function in newly diagnosed Parkinson's disease: ICICLE-PD study. *Brain*, *137*(10), 2743-2758.

133. Ogata, A., Tashiro, K., Nukuzuma, S., Nagashima, K., Hall, WW., A rat model of Parkinson's disease induced by Japanese encephalitis virus, Vol. 3, No. 2, Pages 141-147, 1997.

134. Pagonabarraga, J., Corcuera-Solano, I., Vives-Gilabert, Y., Llebaria, G., García-Sánchez, C., Pascual-Sedano, B., ... & Gómez-Ansón, B. (2013). Pattern of regional cortical thinning associated with cognitive deterioration in Parkinson's disease. *PLOS one*, *8*(1), e54980.

135. Pagonabarraga, J., Gómez-Ansón, B., Rotger, R., Llebaria, G., García-Sánchez, C., Pascual-Sedano, B., ... & Kulisevsky, J. (2012). Spectroscopic changes associated with mild cognitive impairment and dementia in Parkinson's disease. *Dementia and geriatric cognitive disorders*, *34*(5-6), 312-318.

136. Pappatà, S., Santangelo, G., Aarsland, D., Vicidomini, C., Longo, K., Bronnick, K., ... & Pellecchia, M. T. (2011). Mild cognitive impairment in drug-naive patients with PD is associated with cerebral hypometabolism. *Neurology*, *77*(14), 1357-1362.

137. Parkinson, J., An Essay on the Shaking Palsy. Originally published as a monograph by Sherwood, Neely, and Jones, 1817.

138. Pereira, J. B., Junqué, C., Martí, M. J., Ramirez-Ruiz, B., Bargalló, N., & Tolosa, E. (2009). Neuroanatomical substrate of visuospatial and visuoperceptual impairment in Parkinson's disease. *Movement Disorders*, *24*(8), 1193-1199.

139. Petersen, R. C., Parisi, J. E., Dickson, D. W., Johnson, K. A., Knopman, D. S., Boeve, B. F., ... & Braak, H. (2006). Neuropathologic features of amnestic mild cognitive impairment. *Archives of neurology*, *63*(5), 665-672.

140. Petersen, RC., Mild cognitive impairment as a diagnostic entity. J Intern Med. 256:183–194, 2004.

141. Petersen, RC., Roberts, RO., Knopman, DS., Mild cognitive impairment: ten years later. Arch Neurol. 66:1447–1455, 2009.

142. Pigott, K., Rick, J., Xie, S. X., Hurtig, H., Chen-Plotkin, A., Duda, J. E., ... & Siderowf, A. (2015). Longitudinal study of normal cognition in Parkinson disease. *Neurology*, *85*(15), 1276-1282.

143. Pringsheim, T., Jette, N., Frolkis, A., & Steeves, T. D. (2014). The prevalence of Parkinson's disease: A systematic review and meta-analysis. Movement disorders, 29(13), 1583-1590.

144. Provencher, S. W. (2001). Automatic quantitation of localized in vivo1H spectra with

LCModel. *NMR in Biomedicine*, *14*(4), 260-264.

145. Rachakonda, S., Egolf, E., Correa, N., & Calhoun, V. (2007). Group ICA of fMRI toolbox (GIFT) manual. *Dostupné z http://www. nitrc. org/docman/view. php/55/295/v1. 3d_ GIFTManual pdf [cit. 2011-11-5]*.

146. Raichle, M. E. (2011). The restless brain. *Brain connectivity*, *1*(1), 3-12.

147. Raichle, M. E. (2015). The brain's default mode network. *Annual review of neuroscience*, *38*, 433-447.

148. Rajput, AH., Uitti, RJ, Stern, W., Laverty, W. (1986). Early onset Parkinson`s disease in Saskatchewan: Environmental considerations for etiology. Can J Neurol Sci 13: 312-316.

149. Rektorova, I., Biundo, R., Marecek, R., Weis, L., Aarsland, D., & Antonini, A. (2014). Grey matter changes in cognitively impaired Parkinson's disease patients. *PloS one*, *9*(1), e85595.

150. Rektorova, I., Krajcovicova, L., Marecek, R., & Mikl, M. (2012). Default mode network and extrastriate visual resting state network in patients with Parkinson's disease dementia. *Neurodegenerative Diseases*, *10*(1-4), 232-237.

151. Schmahmann, J. D., Smith, E. E., Eichler, F. S., & Filley, C. M. (2008). Cerebral white matter. *Annals of the New York Academy of Sciences*, *1142*(1), 266-309.

152. Seeley, W. W., Crawford, R. K., Zhou, J., Miller, B. L., & Greicius, M. D. (2009). Neurodegenerative diseases target large-scale human brain networks. *Neuron*, *62*(1), 42-52.

153. Seibert, T. M., Murphy, E. A., Kaestner, E. J., & Brewer, J. B. (2012). Interregional correlations in Parkinson disease and Parkinson-related dementia with resting functional MR imaging. *Radiology*, *263*(1), 226-234.

154. Shin, J., Choi, S., Lee, J. E., Lee, H. S., Sohn, Y. H., & Lee, P. H. (2012). Subcortical white matter hyperintensities within the cholinergic pathways of Parkinson's disease patients according to cognitive status. *Journal of Neurology, Neurosurgery & Psychiatry*, *83*(3), 315-321.

155. Siegert, R. J., Weatherall, M., Taylor, K. D., & Abernethy, D. A. (2008). A meta-analysis of performance on simple span and more complex working memory tasks in Parkinson's disease.

156. Silbert, L. C., & Kaye, J. A. (2010). Neuroimaging and Cognition in Parkinson's Disease Dementia. *Brain Pathology (Zurich, Switzerland)*, *20*(3), 646–653.

http://doi.org/10.1111/j.1750-3639.2009.00368.x

157. Smith, A. (1968). The symbol-digit modalities test: a neuropsychologic test of learning and other cerebral disorders. *Learning disorders*, 83-91.

158. Smith, A. (1982). Symbol Digits Modalities Test. Los Angeles: Western Psychological Services.

159. Smith, S. M., Jenkinson, M., Woolrich, M. W., Beckmann, C. F., Behrens, T. E., Johansen-Berg, H., ... & Niazy, R. K. (2004). Advances in functional and structural MR image analysis and implementation as FSL. *Neuroimage*, *23*, S208-S219.

160. Smith, S. M., Miller, K. L., Moeller, S., Xu, J., Auerbach, E. J., Woolrich, M. W., ... & Van Essen, D. C. (2012). Temporally-independent functional modes of spontaneous brain activity. *Proceedings of the National Academy of Sciences*, *109*(8), 3131-3136.

161. Smith, S. M., Miller, K. L., Moeller, S., Xu, J., Auerbach, E. J., Woolrich, M. W., ... & Van Essen, D. C. (2012). Temporally-independent functional modes of spontaneous brain activity. *Proceedings of the National Academy of Sciences*, *109*(8), 3131-3136.

162. Smyser, C. D., Snyder, A. Z., Shimony, J. S., Blazey, T. M., Inder, T. E., & Neil, J. J. (2013). Effects of white matter injury on resting state fMRI measures in prematurely born infants. *PLoS One*, *8*(7), e68098.

163. Summerfield, C., Gómez-Ansón, B., Tolosa, E., Mercader, J. M., Martí, M. J., Pastor, P., & Junqué, C. (2002). Dementia in Parkinson disease: a proton magnetic resonance spectroscopy study. *Archives of neurology*, *59*(9), 1415-1420.

164. Sunwoo, M. K., Jeon, S., Ham, J. H., Hong, J. Y., Lee, J. E., Lee, J. M., ... & Lee, P. H. (2014). The burden of white matter hyperintensities is a predictor of progressive mild cognitive impairment in patients with Parkinson's disease. *European journal of neurology*, *21*(6), 922-e50.

165. Tanner, C.M., Langston., J.W. (1990). Do environmental toxins cause Parkinson`s disease? A critical review, Neurology 40: 17-31.

166. Taylor, C.A., Saint-Hilaire, M.H. (1999). Cupples, LA., Environmental, medical, and family history risk factors for Parkinson`s disease: A new England-based case control study, Am J Med Gent 88: 742-749.

167. Tessitore, A., Esposito, F., Vitale, C., Santangelo, G., Amboni, M., Russo, A., ... & Tedeschi, G. (2012). Default-mode network connectivity in cognitively unimpaired patients with Parkinson disease. *Neurology*, *79*(23), 2226-2232.

168.Thümler, R., Morbus Parkinson: ein Leitfaden für Klinik und Praxis. Springer-Verlag 2002

169.Uc, E. Y., Rizzo, M., Anderson, S. W., Sparks, J., Rodnitzky, R. L., & Dawson, J. D. (2006). Impaired visual search in drivers with Parkinson's disease. *Annals of neurology*, *60*(4), 407-413.

170.Uysal Cantürk, P. (2013). Parkinson hastalığı'nda "hafif kognitif bozukluk" tanı kriterlerinin detaylı nöropsikolojik testlerle validasyonu (The validation of diagnostic criteria for "mild cognitive impairment" in Parkinson's disease with detailed neuropsychological tests). PhD. Thesis, Istanbul University, Institute of Health Science, Department of Advanced Neuroscience, Istanbul, Turkey.

171.van Eimeren, T., Monchi, O., Ballanger, B., & Strafella, A. P. (2009). Dysfunction of the default mode network in Parkinson disease: a functional magnetic resonance imaging study. *Archives of neurology*, *66*(7), 877-883.

172.Veer, I. M., Beckmann, C., Van Tol, M. J., Ferrarini, L., Milles, J., Veltman, D., ... & Rombouts, S. A. (2010). Whole brain resting-state analysis reveals decreased functional connectivity in major depression. *Frontiers in systems neuroscience*, *4*, 41.

173.Watson, G., & Leverenz, J. B. (2010). Profile of cognitive impairment in Parkinson's disease. *Brain Pathology*, *20*(3), 640-645.

174.Watts, RL., Koller, WC., Movement disorders: Neurological Principles & Practice, Second Edition, McGraw-Hill, Medical Publishing, 2004.

175.Williams-Gray, C. H., Evans, J. R., Goris, A., Foltynie, T., Ban, M., Robbins, T. W., ... & Barker, R. A. (2009). The distinct cognitive syndromes of Parkinson's disease: 5 year follow-up of the CamPaIGN cohort. *Brain*, *132*(11), 2958-2969.

176.Williams-Gray, C. H., Foltynie, T., Brayne, C. E. G., Robbins, T. W., & Barker, R. A. (2007). Evolution of cognitive dysfunction in an incident Parkinson's disease cohort. *Brain*, *130*(7), 1787-1798.

177.Williams-Gray, C. H., Mason, S. L., Evans, J. R., Foltynie, T., Brayne, C., Robbins, T. W., & Barker, R. A. (2013). The CamPaIGN study of Parkinson's disease: 10-year outlook in an incident population-based cohort. *Journal of Neurology, Neurosurgery & Psychiatry*, *84*(11), 1258-1264.

178.Winder-Rhodes, S. E., Hampshire, A., Rowe, J. B., Peelle, J. E., Robbins, T. W., Owen, A. M., & Barker, R. A. (2015). Association between MAPT haplotype and memory function in patients with Parkinson's disease and healthy aging individuals. *Neurobiology of*

aging, *36*(3), 1519-1528.

179. Wolk, D. A., Price, J. C., Saxton, J. A., Snitz, B. E., James, J. A., Lopez, O. L., ... & Klunk, W. E. (2009). Amyloid imaging in mild cognitive impairment subtypes. *Annals of neurology*, *65*(5), 557-568.

180. Yarnall, A. J., Rochester, L., & Burn, D. J. (2013). Mild cognitive impairment in Parkinson's disease. *Age and ageing*, aft085.

181. Zhou, J., Greicius, M. D., Gennatas, E. D., Growdon, M. E., Jang, J. Y., Rabinovici, G. D., ... & Seeley, W. W. (2010). Divergent network connectivity changes in behavioural variant frontotemporal dementia and Alzheimer's disease. *Brain*, *133*(5), 1352-1367.

INTERNET REFERENCES

182. http://www.fil.ion.ucl.ac.uk (accessed 07.06.2017)

183. http://www.alivelearn.net/xjview (accessed 21.03.2017)

184. http://fmri.research.umich.edu/research/main_topics/asl.php (accessed 28.03.2017)

185. http://icatb.sourceforge.net/ (accessed 18.04.2017)

DECLARATION

I hereby declare that I have written the submitted dissertation by my own and that the thesis was produced without unauthorized third-party help. Furthermore, I confirm that no sources other than those specified have been used in the dissertation, and that the sources used have been marked as such. This work or parts of it should not be published without the writer's prior authorization or consent.

Emel Erdogdu, Bremen 20.06.2017